DESY 98-041
April 1998

Experimental Tests of Factorization in Charmless Non-Leptonic Two-Body B Decays

A. Ali
Deutsches Elektronen-Synchrotron DESY, 22607 Hamburg, Germany

G. Kramer[1] and Cai-Dian Lü[2]
II. Institut für Theoretische Physik, Universität Hamburg, 22761 Hamburg, Germany

Abstract

Using a theoretical framework based on the next-to-leading order QCD-improved effective Hamiltonian and a factorization Ansatz for the hadronic matrix elements of the four-quark operators, we reassess branching fractions in two-body non-leptonic decays $B \to PP, PV, VV$, involving the lowest lying light pseudoscalar (P) and vector (V) mesons in the standard model. We work out the parametric dependence of the decay rates making use of the currently available information on the weak mixing matrix elements, form factors, decay constants and quark masses. Using the sensitivity of the decay rates on the effective number of colors, N_c, as a criterion of theoretical predictivity, we classify all the current-current (tree) and penguin transitions in five different classes. The recently measured charmless two-body $B \to PP$ decays ($B^+ \to K^+\eta', B^0 \to K^0\eta', B^0 \to K^+\pi^-, B^+ \to \pi^+K^0$ and charge conjugates) are dominated by the N_c-stable QCD penguins (class-IV transitions) and their estimates are consistent with data. The measured charmless $B \to PV$ ($B^+ \to \omega K^+$, $B^+ \to \omega h^+$) and $B \to VV$ transition ($B \to \phi K^*$), on the other hand, belong to the penguin (class-V) and tree (class-III) transitions. The class-V penguin transitions are N_c-sensitive and/or involve large cancellations among competing amplitudes making their decay rates in general more difficult to predict. Some of these transitions may also receive significant contributions from annihilation and/or final state interactions. We propose a number of tests of the factorization framework in terms of the ratios of branching ratios for some selected $B \to h_1h_2$ decays involving light hadrons h_1 and h_2, which depend only moderately on the form factors. We also propose a set of measurements to determine the effective coefficients of the current-current and QCD penguin operators. The potential impact of $B \to h_1h_2$ decays on the CKM phenomenology is emphasized by analyzing a number of decay rates in the factorization framework.

[1]Supported by Bundesministerium für Bildung und Forschung, Bonn, under Contract 057HH92P(0) and EEC Program "Human Capital and Mobility" through Network "Physics at High Energy Colliders" under Contract CHRX-CT93-0357 (DG12COMA).

[2]Alexander von Humboldt Foundation Fellow.

1 Introduction

Recent measurements by the CLEO Collaboration [1,2] of a number of decays of the type $B \to h_1 h_2$, where h_1 and h_2 are light hadrons such as $h_1 h_2 = \pi\pi, \pi K, \eta' K, \omega K$, have triggered considerable theoretical interest in understanding two-body non-leptonic B decays. These decays involve the so-called tree (current-current) $b \to (u, c)$ and/or $b \to s$ (or $b \to d$) penguin amplitudes with, in general, both the QCD and electroweak penguins participating. The appropriate theoretical framework to study these decays is that of an effective theory based on the Wilson operator product expansion [3] obtained by integrating out the heavy degrees of freedom, which in the standard model (SM) are the top quark and $W^{\pm}$ bosons. This effective theory allows to separate the short- and long-distance physics and one can implement the perturbative QCD improvements systematically in this approach. Leading order corrections have been known for quite some time [4] and in many cases this program has been completed up to and including the next-to-leading order corrections [5]. Present QCD technology, however, does not allow to undertake a complete calculation of the exclusive non-leptonic decay rates from first principles, such as provided by the lattice-QCD approach, as this requires the knowledge of the hadronic matrix elements $< h_1 h_2 | \mathcal{H}_{eff} | B >$, where $\mathcal{H}_{eff}$ is an effective Hamiltonian consisting of the four-quark and magnetic moment operators. These are too complicated objects to be calculated with the current lattice-QCD methods. Hence, a certain amount of model building involving these hadronic matrix elements is at present unavoidable.

The approach which has often been employed in non-leptonic heavy hadron decays is based on factorization [6–8]. With the factorization Ansatz, the matrix elements $< h_1 h_2 | \mathcal{H}_{eff} | B >$ can be expressed as a product of two factors $< h_1 | J_1 | B >< h_2 | J_2 | 0 >$. The resulting matrix elements of the current operators J_i are theoretically more tractable and have been mostly calculated in well-defined theoretical frameworks, such as Lattice-QCD [9–11], QCD sum rules [12–15] and potential models [8],[16–18]; some are also available from data on semileptonic and leptonic decays [19]. One can then make quantitative predictions in this framework taking into account the theoretical and experimental dispersion in the input parameters in the decay rates. Factorization holds in the limit that one ignores soft non-perturbative effects. The rationale of this lies in the phenomenon of color-transparency [20], in which one expects intuitively that a pair of fast moving (energetic) quarks in a color-singlet state effectively decouples from long-wavelength gluons. In the decays $B \to h_1 h_2$, with typically $E_{h_{1,2}} \sim O(m_B/2)$, the energy of the quarks leaving the interaction is large and soft final state interactions should be small and hence factorization should be a good approximation. Final state interactions generated by hard gluon exchanges are, however, perturbatively calculable and can be included. Phenomenology of the factorization hypothesis in the decays $B \to D^{(*)}\pi(\rho)$, $B \to J/\psi K^{(*)}$ and related ones, involving the so-called current-current amplitudes, has been worked out and compared with the existing data with the tentative conclusion that data in these decays can be described in terms of two phenomenological parameters, a_1 and a_2 [8], whose values seem to be universal [18,21].

The decays $B \to h_1 h_2$ have been studied repeatedly in the factorization framework [22–26]. However, with the measurements of some of the $B \to h_1 h_2$ decays [1,2], theoretical interest in this field has resurged. In particular, NLO-improved perturbative framework with updated phenomenological input has been used in a number of recent papers [27–31] to study the CLEO data. We would like to take a closer look at the non-leptonic two-body decays $B \to h_1 h_2$, in

which QCD and/or electroweak penguins are expected to play a significant role.

There are several theoretical issues involved in $B \to h_1 h_2$ decays, which one does not encounter in the transitions $B \to H_1 h_2$, where H_1 is an open $(D^{(*)}, D_s^{(*)})$ or bound $(J/\psi, \eta_c, \chi_c)$ charmed hadron, or in decays such as $B \to D_s^{(*)} D^{(*)}$, which are governed by the current-current (tree) amplitudes. In the case of the induced $b \to s$ and $b \to d$ transitions, penguins play an important role. Of these penguin transitions, the ones involving the top-quark can be reliably calculated in perturbation theory as they represent genuine short-distance contributions. The rest of the penguins, which involve both the charm- and light-quarks, also have genuine short-distance contributions which can be calculated using perturbation theory. Their importance in the context of direct CP asymmetries has been emphasized repeatedly in the literature [32,33]. However, in principle, such penguin amplitudes may also involve significant non-perturbative (long-distance) contributions. Arguments for an enhanced role of non-perturbative penguin effects have been advanced in the literature [34]. In simpler cases, such as the electromagnetic decays $B \to X_s + \gamma$ and $B \to K^* + \gamma$, charm-penguins are likewise present and they introduce $1/m_c^2$ (and higher order) power corrections akin to the long-distance effects being discussed in non-leptonic decays. In these cases, one finds that the $1/m_c^2$ power corrections are negligible [35–37]. The same holds for the non-resonant $B \to X_s \ell^+ \ell^-$ decays [37]. The pattern of the $1/m_c^2$-corrections remains to be investigated systematically for non-leptonic $b \to (s,d) q\bar{q}$ decays. However, it is suggestive that the next-to-leading order QCD-improved framework based on factorization can explain most of the recent CLEO data without invoking a significant non-perturbative penguin contribution [27,28]. With improved measurements, this aspect will surely be scrutinized much more quantitatively.

A related issue is that of the current-current $b \to c\bar{c}s$ and $b \to c\bar{c}d$ transitions feeding into the $b \to sq\bar{q}$ and $b \to dq\bar{q}$ transitions, respectively, by (soft) final state interactions (FSI) [38–42]. While in the oft-studied case of $B \to K\pi$ decays, these effects are not found to be overwhelming for decay rates, yet, in general, it is not difficult to imagine situations where FSI may yield the dominant contribution to a decay width. There are three ways in which the amplitude for a decay in the factorization approach can become small: (i) the effective coefficients of the various operators entering into specific decays are small reflecting either their intrinsic (perturbative) values, implying they are small for $N_c = 3$, or their N_c-sensitivity meaning that they are small for some phenomenologically relevant value of N_c, (ii) due to CKM-suppression, (iii) due to delicate cancellations among various competing Feynman diagrams, resulting into an amplitude which is effectively small. Using N_c, the effective number of colors, as a variable parameter, it becomes immediately clear that some linear combinations of the effective coefficients entering in specific decays are particularly sensitive to N_c and they indeed become very small for certain values of $\xi = 1/N_c$. This then implies that other contributions such as the ones coming from FSI and/or annihilation may become important. A good case to illustrate this is the decay $B^\pm \to K^\pm K$, whose decay rate may be enhanced by an order of magnitude due to FSI [40] and/or annihilation [43] contributions.

In this paper, we undertake a comprehensive study, within the factorization framework, of all the two-body decay modes of the type $B \to PP$, $B \to PV$ and $B \to VV$ where $P(V)$ is a light pseudoscalar (vector) meson in the flavor $U(3)$ nonet. Concentrating on the lowest lying 0^- and 1^- mesons, there are some seventy-six (76) such decays (and an equal number involving the charge conjugate states). The branching ratios of these decays are found to vary over four orders of magnitude. We calculate their decay rates (branching ratios) and work out the most sensitive

parametric dependence of these quantities. In many cases the factorized amplitudes are small due to the reasons mentioned in the preceding paragraph. While this by itself does not imply an intrinsic inability to calculate, it becomes difficult to be confident if the rate is additionally unstable, requiring a good deal of theoretical fine tuning in the factorization approach. We list all such two-body decay modes here and caution about drawing too quantitative conclusions on their widths based on the factorized amplitudes alone. We think that the sensitivity of some of the effective coefficients a_i on N_c and the fine tuning required in some amplitudes can be used as a criterion of predictivity of $B \to h_1 h_2$ decay rates in the factorization approach. The pattern of color-suppression in current-current amplitudes has been previously used to classify the N_c-sensitivity of these decays into three classes [8]. We extend this to also include the penguin-dominated decays, which belong either to N_c-stable (class-IV) or N_c-sensitive (class-V) decays. In addition, penguin-dominated decay amplitudes involving large cancellations are also included in class-V. All penguin-dominated $B \to PP$ decays belong to class-IV. This class includes in particular the decays $B^0 \to K^+\pi^-$, $B^+ \to K^+\eta'$, $B^0 \to K^0\eta'$ and $B^+ \to \pi^+ K^0$, measured recently by the CLEO collaboration [1] (here and in what follows, charge conjugate decays are implied). On the other hand, the recently measured $B \to PV$ and $B \to VV$ decay modes by CLEO [2] are in class-V ($B^+ \to \omega K^+$ and $B \to K^*\phi$) or tree-dominated class-III ($B^+ \to \omega\pi^+$). Possibly some of these, and many more examples of class-V decays worked out by us here, indicate that the factorization-based approach is rather uncertain in these decays and one may have to develop more powerful methods to make theoretically stable predictions in this class. Factorization approach is expected to do a better job in accounting for class-IV decays - a claim which is pursued here and which is supported by present data.

We propose tests of factorization in $B \to h_1 h_2$ decays through measuring a number of ratios of the branching ratios which depend only on the form factors but are otherwise insensitive to other parameters, such as the effective coefficients a_i and hence N_c, quark masses, QCD-scale parameter and CKM matrix elements. The residual model dependence of these ratios on the form factors is worked out in two representative cases: (i) the Bauer-Stech-Wirbel (BSW) model [8] and (ii) a hybrid approach, based on Lattice-QCD/Light-cone QCD sum rules, specifically making use of the results obtained in the frameworks of lattice-QCD [10,11] and the Light-Cone QCD sum rules [12,15]. The proposed ratios will test factorization and determine the form factors.

A quantitative test of the factorization approach lies in a consistent determination of the effective coefficients a_i of this framework. The QCD perturbative contributions to a_i can be calculated in terms of the renormalized Wilson coefficients in the effective Hamiltonian governing the decays $B \to h_1 h_2$. Then, there are non-perturbative contributions which have to be determined phenomenologically. Of these a_1 and a_2 govern the current-current amplitudes and they should be determined in $B \to h_1 h_2$ decays without any *prior* prejudice. Four of the a_i's $(a_3, ..., a_6)$ govern the QCD-penguin amplitudes and four more $(a_7, ..., a_{10})$ govern the electroweak-penguin amplitudes. We propose measurements of selected branching ratios (and their ratios) to determine the effective coefficients a_1, a_2, a_4 and a_6 from the first six from data on $B \to h_1 h_2$ decays in the future. Since the Wilson coefficients of the electroweak penguin operators in the SM are rather small in magnitude (except for C_9), which in turn yield very small branching ratios for these decays, a determination of $a_7, ..., a_{10}$ is a formidable proposition. The coefficient a_9 can be determined and we propose several decays to measure this. We also list decay modes in which electroweak penguins (hence $a_7, ..., a_{10}$) do play a noticeable role,

and work out their corresponding branching ratios.

Finally, we explore the potential impact of the $B \to h_1 h_2$ decays on the phenomenology of the Cabibbo-Kobayashi-Maskawa (CKM) matrix [44]. Here, we discuss relations of the type put forward by Fleischer and Mannel [45] (see, also [46]) involving the decay rates of $B^0 \to K^+\pi^-$ and $B^+ \to K^0\pi^+$, which can be used to determine $\cos\gamma$, where γ is one of the angles of the CKM unitarity triangle, in terms of the ratio of the tree-to-penguin amplitudes $z \equiv T/P$ and δ, the strong phase shift difference involving these amplitudes. A bound on $\sin^2\gamma$ can be obtained, assuming that there are just the tree and QCD-penguin amplitudes:

$$R \equiv \frac{\Gamma(B^0 \to \pi^\mp K^\pm)}{\Gamma(B^\pm \to \pi^\pm K^0)} = 1 - 2\,z\cos\gamma\cos\delta + z^2 \geq \sin^2\gamma\ . \tag{1}$$

From this, constraints on γ of the form

$$0^\circ \leq \gamma \leq \gamma_0 \quad \vee \quad 180^\circ - \gamma_0 \leq \gamma \leq 180^\circ \tag{2}$$

follow, where γ_0 is the maximum value of γ, which are complementary to the ones from the CKM unitarity fits [47,48]. There are similar relations involving the decays $B \to PV$ and $B \to VV$, where $P = \pi, K$ and $V = \rho, K^*$. A determination of the angle γ, however, requires the knowledge of z_i and δ_i in these processes. Also, the effect of the electroweak penguins has to be included. Having a definite model, whose consistency can be checked in a number of decays, one could determine (within a certain range) the values of z_i and δ_i. Given data, this would allow us in turn to determine γ in a number of two-body non-leptonic B decays. We draw inferences on the angle γ based on existing data on R, and in line with [27], we show that the allowed values of γ (or the CKM-Wolfenstein [49] parameters ρ and η) from this analysis are consistent with the ones following from the CKM unitarity fits. Similar analysis can be carried out for the decays $B \to PP, PV, VV$, where now $P = \pi^0, \pi^\pm$ and $V = \rho^0, \rho^\pm$. Measurements of these decays and their ratios would allow to draw inferences on the angle α. We illustrate this in the context of our model. The other kind of relations discussed by us involve ratios of the decay rates dominated by the $b \to s$ and $b \to d$ penguins, respectively. As pointed out in ref. [50], these ratios can be used to determine the ratio of the CKM matrix elements $|V_{td}/V_{ts}|$. Since this CKM-ratio will, in principle, be measured also in B^0 - $\overline{B^0}$ mixings and radiative and semileptonic rare B decays [47,51], one could check the consistency of such determinations to reach quantitative conclusions about the QCD dynamics at work in non-leptonic decays. However, it is conceivable that some of the non-leptonic decays may already provide interesting information on V_{td} before the other mentioned processes are actually measured. While not competitive in terms of eventual theoretical precision, non-leptonic decays are nevertheless quite instructive in this respect for the current CKM phenomenology.

This paper is organized as follows: In section 2, we discuss the effective Hamiltonian together with the quark level matrix elements and the numerical values of the Wilson coefficients C_i^{eff} in the effective Hamiltonian approach. In section 3, we introduce the factorization Ansatz, define the relevant matrix elements and discuss their evaluation in the BSW model and in the hybrid lattice QCD/QCD sum rule approach. The matrix elements for the three classes $B \to PP$, $B \to PV$ and $B \to VV$, obtained in the factorization approach, are relegated to Appendix A, B and C, respectively. Section 4 contains a discussion of the various input parameters (CKM matrix elements, quark masses, hadronic form factors and mesonic constants). The numerical input we use in the estimates of branching ratios are collected in various tables. In section 5,

we tabulate the values of the phenomenological parameters a_i for three values of the effective number of colors ($N_c = 2, 3, \infty$) for the four cases of interest $b \to s$, $\bar{b} \to \bar{s}$, $b \to d$ and $\bar{b} \to \bar{d}$. This serves to show both the relative magnitude of the effective coefficients of the various operators in $B \to h_1 h_2$ decays in the factorization approach and also the stability of these coefficients against N_c. The classification of the $B \to h_1 h_2$ decays is also discussed here. We also discuss the contribution of the annihilation amplitudes and list some decays of potential interest. Section 6 contains the numerical results for the branching ratios which we tabulate for three specific values of the effective number of colors $N_c = 2, 3, \infty$. The parametric dependence on $\xi = 1/N_c$ is shown for some representative cases in various figures and compared with data, whenever available. In section 7, we list a number of ratios of branching ratios to test the hypothesis of factorization and give their values for the two sets of form factors (in the BSW and the hybrid Lattice-QCD/QCD sum rule approaches). We also discuss the determination of the effective coefficients $a_1, ..., a_6$ here through a number of relations. We estimate these ratios and make comparisons with data, whenever available. Potential impact of the $B \to h_1 h_2$ decay rates on CKM phenomenology are also discussed here. Finally, we conclude in section 8 with a summary and outlook.

2 The Effective Hamiltonian

2.1 Short-distance QCD corrections

We write the effective Hamiltonian H_{eff} for the $\Delta B = 1$ transitions as

$$\mathcal{H}_{eff} = \frac{G_F}{\sqrt{2}} \left[V_{ub} V_{uq}^* \left(C_1 O_1^u + C_2 O_2^u \right) + V_{cb} V_{cq}^* \left(C_1 O_1^c + C_2 O_2^c \right) - V_{tb} V_{tq}^* \left(\sum_{i=3}^{10} C_i \, O_i + C_g O_g \right) \right] \quad , \tag{3}$$

where $q = d, s$ and C_i are the Wilson coefficients evaluated at the renormalization scale μ. We specify below the operators in $\mathcal{H}_{eff}$ for $b \to s$ transitions (for $b \to d$ transitions, one has to make the replacement $s \to d$):

$$\begin{aligned}
O_1^u &= \bar{s}_\alpha \gamma^\mu L u_\alpha \cdot \bar{u}_\beta \gamma_\mu L b_\beta \ , & O_2^u &= \bar{s}_\alpha \gamma^\mu L u_\beta \cdot \bar{u}_\beta \gamma_\mu L b_\alpha \ , \\
O_1^c &= \bar{s}_\alpha \gamma^\mu L c_\alpha \cdot \bar{c}_\beta \gamma_\mu L b_\beta \ , & O_2^c &= \bar{s}_\alpha \gamma^\mu L c_\beta \cdot \bar{c}_\beta \gamma_\mu L b_\alpha \ , \\
O_3 &= \bar{s}_\alpha \gamma^\mu L b_\alpha \cdot \textstyle\sum_{q'} \bar{q}'_\beta \gamma_\mu L q'_\beta \ , & O_4 &= \bar{s}_\alpha \gamma^\mu L b_\beta \cdot \textstyle\sum_{q'} \bar{q}'_\beta \gamma_\mu L q'_\alpha \ , \\
O_5 &= \bar{s}_\alpha \gamma^\mu L b_\alpha \cdot \textstyle\sum_{q'} \bar{q}'_\beta \gamma_\mu R q'_\beta \ , & O_6 &= \bar{s}_\alpha \gamma^\mu L b_\beta \cdot \textstyle\sum_{q'} \bar{q}'_\beta \gamma_\mu R q'_\alpha \ , \\
O_7 &= \tfrac{3}{2} \bar{s}_\alpha \gamma^\mu L b_\alpha \cdot \textstyle\sum_{q'} e_{q'} \bar{q}'_\beta \gamma_\mu R q'_\beta \ , & O_8 &= \tfrac{3}{2} \bar{s}_\alpha \gamma^\mu L b_\beta \cdot \textstyle\sum_{q'} e_{q'} \bar{q}'_\beta \gamma_\mu R q'_\alpha \ , \\
O_9 &= \tfrac{3}{2} \bar{s}_\alpha \gamma^\mu L b_\alpha \cdot \textstyle\sum_{q'} e_{q'} \bar{q}'_\beta \gamma_\mu L q'_\beta \ , & O_{10} &= \tfrac{3}{2} \bar{s}_\alpha \gamma^\mu L b_\beta \cdot \textstyle\sum_{q'} e_{q'} \bar{q}'_\beta \gamma_\mu L q'_\alpha \ , \\
O_g &= (g_s / 8\pi^2) \, m_b \, \bar{s}_\alpha \, \sigma^{\mu\nu} \, R \, (\lambda^A_{\alpha\beta}/2) \, b_\beta \ G^A_{\mu\nu} \ .
\end{aligned} \tag{4}$$

Here α and β are the $SU(3)$ color indices and $\lambda^A_{\alpha\beta}$, $A = 1, ..., 8$ are the Gell-Mann matrices; L and R are the left- and right-handed projection operators with $L(R) = 1 - \gamma_5$ $(1 + \gamma_5)$, and $G^A_{\mu\nu}$ denotes the gluonic field strength tensor. The sum over q' runs over the quark fields that are active at the scale $\mu = O(m_b)$, i.e., $(q' \epsilon \{u, d, s, c, b\})$. The usual tree-level W-exchange contribution in the effective theory corresponds to O_1 (with $C_1(M_W) = 1 + O(\alpha_s)$) and O_2 emerges due to the QCD corrections. The operators $O_3, \ldots, O_6$ arise from the QCD-penguin diagrams which contribute in order α_s through the initial values of the Wilson coefficients at $\mu \approx M_W$ [52] and operator mixing due to the QCD corrections [53]. Similarly, the operators

$O_7, \ldots, O_{10}$ arise from the electroweak-penguin diagrams. Note that we neglect the effects of the electromagnetic penguin operator which we did not list explicitly. The effect of the weak annihilation and exchange diagrams will be discussed later.

The renormalization group evolution from $\mu \approx M_W$ to $\mu \approx m_b$ has been evaluated in leading order in the electromagnetic coupling and in the NLL precision in the strong coupling α_s [54]. Working consistently to the NLL precision, the coefficients $C_1, ..., C_{10}$ are needed in NLL precision, while it is sufficient to use the LL value for C_g. These coefficients depend on the renormalization scheme used. To obtain numerical values for the C_i we must specify the input parameters. We fix $\alpha_s(M_z) = 0.118$, $\alpha_{ew}(M_z) = 1/128$ and $\mu = 2.5\ GeV$. Then in the naive dimensional regularization (NDR) scheme, we have:

$$\begin{array}{llllll} C_1 & = & 1.117\ , & C_2 & = & -0.257\ , \\ C_3 & = & 0.017\ , & C_4 & = & -0.044\ , \\ C_5 & = & 0.011\ , & C_6 & = & -0.056\ , \\ C_7 & = & -1 \times 10^{-5}\ , & C_8 & = & 5 \times 10^{-4}\ , \\ C_9 & = & -0.010\ , & C_{10} & = & 0.002\ , \\ C_g^{eff} & = & -0.158\ . & & & \end{array} \tag{5}$$

Here, $C_g^{eff} = C_g + C_5$. From the electroweak coefficients $C_7, ..., C_{10}$, only C_9 has a sizable value compared to the coefficients of the QCD penguins; its major contribution arises from the Z penguin. Note that the scale (μ) and scheme-dependence of the Wilson coefficients will cancel against the corresponding dependences in the matrix elements of the operators in $\mathcal{H}_{eff}$, as shown explicitly in [54]. Since, the matrix elements given below are obtained in the NDR-scheme, we have listed the values of the Wilson coefficients C_i also in this scheme.

2.2 Quark-level Matrix Elements

In the NLL precision, the matrix elements of $\mathcal{H}_{eff}$ are to be treated at the one-loop level. The one-loop matrix elements can be rewritten in terms of the tree-level matrix elements of the effective operators

$$\langle sq'\bar{q}'|\mathcal{H}_{eff}|b\rangle = \sum_{i,j} C_i^{eff}(\mu)\langle sq'\bar{q}'|O_j|b\rangle^{\rm tree}. \tag{6}$$

In the NDR renormalization scheme and for $SU(3)_C$, the effective coefficients multiplying the matrix elements $< sq'\bar{q}'|O_j^{(q)}|b >^{\rm tree}$ become (r_V^T and γ_V^T are the transpose of the matrices given below)

$$\begin{aligned} C_1^{eff} &= C_1 + \frac{\alpha_s}{4\pi}\left(r_V^T + \gamma_V^T \log\frac{m_b}{\mu}\right)_{1j} C_j + \cdots, \\ C_2^{eff} &= C_2 + \frac{\alpha_s}{4\pi}\left(r_V^T + \gamma_V^T \log\frac{m_b}{\mu}\right)_{2j} C_j + \cdots, \\ C_3^{eff} &= C_3 - \frac{1}{6}\frac{\alpha_s}{4\pi}(C_t + C_p + C_g) + \frac{\alpha_s}{4\pi}\left(r_V^T + \gamma_V^T \log\frac{m_b}{\mu}\right)_{3j} C_j + \cdots, \\ C_4^{eff} &= C_4 + \frac{1}{2}\frac{\alpha_s}{4\pi}(C_t + C_p + C_g) + \frac{\alpha_s}{4\pi}\left(r_V^T + \gamma_V^T \log\frac{m_b}{\mu}\right)_{4j} C_j + \cdots, \end{aligned}$$

$$
\begin{aligned}
C_5^{eff} &= C_5 - \frac{1}{6}\frac{\alpha_s}{4\pi}\left(C_t + C_p + C_g\right) + \frac{\alpha_s}{4\pi}\left(r_V^T + \gamma_V^T \log\frac{m_b}{\mu}\right)_{5j} C_j + \cdots , \\
C_6^{eff} &= C_6 + \frac{1}{2}\frac{\alpha_s}{4\pi}\left(C_t + C_p + C_g\right) + \frac{\alpha_s}{4\pi}\left(r_V^T + \gamma_V^T \log\frac{m_b}{\mu}\right)_{6j} C_j + \cdots , \\
C_7^{\rm eff} &= C_7 + \frac{\alpha_{ew}}{8\pi} C_e \ , \\
C_8^{\rm eff} &= C_8 \ , \\
C_9^{\rm eff} &= C_9 + \frac{\alpha_{ew}}{8\pi} C_e \ , \\
C_{10}^{\rm eff} &= C_{10} \ . \qquad (7)
\end{aligned}
$$

We have separated the contributions C_t, C_p, and C_g arising from the penguin-type diagrams of the current-current operators $O_{1,2}$, the penguin-type diagrams of the operators O_3-O_6, and the tree-level diagram of the dipole operator O_g, respectively. Note also that we follow the procedure of ref. [27] of including the tree-level diagrams $b \to sg \to sq'\bar{q}'$ associated with the operator O_g into the contribution C_g appearing in the expressions for C_i^{eff}. So, we have the hadronic matrix elements of four-quark operators only. The process-independent contributions from the vertex-type diagrams are contained in the matrices r_V and γ_V. Here γ_V is that part of the anomalous matrix which is due to the vertex (and self-energy) corrections. This part can be easily extracted from $\hat{\gamma}^{(0)}$ in ref. [54]:

$$
\gamma_V = \begin{pmatrix}
-2 & 6 & 0 & 0 & 0 & 0 \\
6 & -2 & 0 & 0 & 0 & 0 \\
0 & 0 & -2 & 6 & 0 & 0 \\
0 & 0 & 6 & -2 & 0 & 0 \\
0 & 0 & 0 & 0 & 2 & -6 \\
0 & 0 & 0 & 0 & 0 & -16
\end{pmatrix} \quad . \qquad (8)
$$

The matrix r_V contains constant, i.e., momentum-independent, parts associated with the vertex diagrams. This matrix can be extracted from the matrix $\hat{r}$ defined in eqn. (2.12) (and given explicitly in eqn. (4.6)) by Buras et al. in ref. [54]:

$$
r_V = \begin{pmatrix}
\frac{7}{3} & -7 & 0 & 0 & 0 & 0 \\
-7 & \frac{7}{3} & 0 & 0 & 0 & 0 \\
0 & 0 & \frac{63}{27} & -7 & 0 & 0 \\
0 & 0 & -7 & \frac{7}{3} & 0 & 0 \\
0 & 0 & 0 & 0 & -\frac{1}{3} & 1 \\
0 & 0 & 0 & 0 & -3 & \frac{35}{3}
\end{pmatrix} \quad . \qquad (9)
$$

Note that the μ dependence and the scheme dependence of the vertex correction diagrams are fully taken into account in eqn. (7) by the terms involving the matrices γ_V and r_V, respectively. There are, however, still scheme-independent, process-specific terms omitted as indicated by the ellipses, and we refer to [27] for a discussion of these omitted terms in exclusive two-body B decays.

The quantities C_t, C_p, and C_g are given in the NDR scheme (after $\overline{MS}$ renormalization) by

$$
C_t = -\sum_{q'=u,c} \frac{V_{q'b}V_{q'q}^*}{V_{tb}V_{tq}^*}\left[\frac{2}{3} + \frac{2}{3}\log\frac{m_{q'}^2}{\mu^2} - \Delta F_1\left(\frac{k^2}{m_{q'}^2}\right)\right] C_1 \quad , \qquad (10)
$$

$$C_p = C_3 \left[\frac{4}{3} + \frac{2}{3}\log\frac{m_s^2}{\mu^2} + \frac{2}{3}\log\frac{m_b^2}{\mu^2} - \Delta F_1\left(\frac{k^2}{m_s^2}\right) - \Delta F_1\left(\frac{k^2}{m_b^2}\right)\right] + (C_4 + C_6)\sum_{i=u,d,s,c,b}\left[\frac{2}{3}\log\frac{m_i^2}{\mu^2} - \Delta F_1\left(\frac{k^2}{m_i^2}\right)\right] \quad . \tag{11}$$

$$C_g = -\frac{2m_b}{\sqrt{< k^2 >}}\, C_g^{eff} \quad , \tag{12}$$

with $C_g^{eff} = C_g + C_5$. The function $\Delta F_1(z)$ is defined as

$$\Delta F_1(z) = -4\int_0^1 dx\, x(1-x)\,\log\left[1 - z\,x(1-x) - i\epsilon\right] \quad . \tag{13}$$

The corresponding electroweak coefficient C_e is given by

$$C_e = -\frac{8}{9}(3C_2 + C_1)\sum_{q'=u,c}\frac{V_{q'b}V_{q'q}^*}{V_{tb}V_{tq}^*}\left(\frac{2}{3} + \frac{2}{3}\ln\frac{m_{q'}^2}{\mu^2} - \Delta F_1\left(\frac{k^2}{m_{q'}^2}\right)\right). \tag{14}$$

Note that the quantities C_t and C_e depend on the CKM matrix elements. In addition, the coefficients $C_i^{\rm eff}$ depend on k^2, where k is the momentum transferred by the gluon, photon or Z to the quark-antiquark pair $q'\overline{q'}$ in $b \to qq'\overline{q'}$. In two-body decays any information on k^2 is lost in the factorization assumption. However, given a specific model for the momentum distributions of the quark-antiquark pair inside the hadron, the partonic distributions calculated here can be folded with this distribution, as, for example, has been done in [55]. Since, we are interested here in the decays $B \to h_1 h_2$, where h_1, h_2 are light mesons, it is not unreasonable to assume that this smearing will be very similar in all the decays being considered. In particular, $\langle k^2\rangle$ is expected to be comparable in these decays. However, the actual value of $\langle k^2\rangle$ is model dependent. From simple two-body kinematics [56] or from the investigations in ref. [55] one expects k^2 to be typically in the range

$$\frac{m_b^2}{4} \lesssim k^2 \lesssim \frac{m_b^2}{2} \; . \tag{15}$$

As we shall see later, branching ratios considered here are not sensitive to the value of k^2 if it is varied in a reasonable range.

3 Factorization Ansatz for the hadronic matrix elements of the four-quark operators

We have now to calculate the hadronic matrix elements of the type $\langle h_1 h_2|O_i|B\rangle$, where O_i are the four-quark operators listed in the preceding section. These will be calculated in the factorization assumption, which in the present context has been explained in a number of papers (see, for example, ref. [27]). To recapitulate briefly, the hadronic matrix elements involving four-quark operators are split into a product of two matrix elements of the generic type $\langle h_1|\bar{q}b|B\rangle$ and $\langle h_2|\bar{q}'q'|0\rangle$, where Fierz transformation is used so that the flavor quantum numbers of the quark currents match those of the hadrons. Since fierzing yields operators which are in the color singlet-singlet and octet-octet forms, this procedure results in general in matrix elements which

have the right flavor quantum numbers but involve both the singlet-singlet and octet-octet operators. No direct experimental information is available on the latter. In the factorization approximation, one discards the color octet-octet piece and compensates this by introducing a phenomenological parameter which determines the strength of the singlet-singlet contribution, renormalizing it from its perturbative value. The hadronic matrix elements resulting from the factorization are calculated in a model or determined from data, if available.

To set our notation and introduce some auxiliary quantities which we shall need for numerical calculations, we illustrate the salient features of our framework below. When a pseudoscalar meson is a decay product, such as in the decay $B \to PP$, there are additional contributions from the $(V+A)$ penguin operator O_6 and O_8. After Fierz reordering and factorization they contribute terms which involve a matrix element of the quark-density operators between a pseudoscalar meson and the vacuum. For O_6 involving $b \to s$ transition (in $b \to d$ transition s is replaced by d), for example, this is given by

$$< P_1 P_2 | O_6 | B >= -2 \sum_q \Big(< P_1 | \bar{s} R q | 0 >< P_2 | \bar{q} L b | B > + [P_1 \leftrightarrow P_2] \Big) \ . \tag{16}$$

Using the Dirac equation, the matrix elements entering here can be rewritten in terms of those involving the usual $(V-A)$ currents,

$$< P_1 P_2 | O_6 | B >= R[P_1, P_2] < P_1 P_2 | O_4 | B > + [P_1 \leftrightarrow P_2] \ , \tag{17}$$

with

$$R[P_1, P_2] \equiv \frac{2 M_{P_1}^2}{(m_q + m_s)(m_b - m_q)} \ . \tag{18}$$

Here, m_s and m_q are the current masses of the quarks in the mesons P_1 and P_2. The same relations work for O_8. Finally, one arrives at the form

$$\begin{aligned} < P_1 \, P_2 | \mathcal{H}_{eff} | B > \ &= \ Z_1 < P_1 | j^\mu | 0 >< P_2 | j_\mu | B > \\ &+ \ Z_2 < P_2 | j'^\mu | 0 >< P_1 | j'_\mu | B > \ , \end{aligned} \tag{19}$$

where j_μ and j'_μ are the corresponding (neutral or charged) $V-A$ currents. The quantities Z_1 and Z_2 involve the effective coefficients, CKM factors and G_F. The $0^- \to 0^-$ form factors are defined as follows:

$$\langle P_1(p_1) | \bar{q} \gamma_\mu L b | B(p_B) \rangle = \left[(p_B + p_1)_\mu - \frac{m_B^2 - m_1^2}{q^2} q_\mu \right] F_1(q^2) + \frac{m_B^2 - m_1^2}{q^2} q_\mu F_0(q^2), \tag{20}$$

where $q = p_B - p_1$. In order to cancel the poles at $q^2 = 0$, we must impose the condition

$$F_1(0) = F_0(0).$$

The pseudoscalar decay constants are defined as:

$$\langle P(p) | \bar{q} \gamma^\mu L q' | 0 \rangle = i f_P \ p^\mu. \tag{21}$$

With this, we can write the required matrix element in its factorized form

$$\langle P_1 P_2 | \mathcal{H}_{eff} | B \rangle = i \frac{G_F}{\sqrt{2}} V_{qb} V_{qq'}^* \left(\frac{1}{N_c} C_i + C_j \right) f_{P_2} (m_B^2 - m_1^2) F_0^{B \to P_1}(m_2^2) + (1 \leftrightarrow 2). \tag{22}$$

The dynamical details are coded in the quantities a_i, which we define as

$$a_i \equiv C_i^{eff} + \frac{1}{N_c} C_{i+1}^{eff} \quad (i = \text{odd}); \quad a_i \equiv C_i^{eff} + \frac{1}{N_c} C_{i-1}^{eff} \quad (i = \text{even}), \tag{23}$$

where i runs from $i = 1, ..., 10$. Thus, we see that there are ten such quantities. They depend on the SM-input parameters, including the CKM matrix elements. The non-factorizing contributions in the matrix elements $\langle h_1 h_2 | O_i | B \rangle$ are modeled by treating N_c as a phenomenological parameter. Note, that this is the only place where N_c is treated as a phenomenological parameter. In particular, in the calculation of C_i^{eff}, we have used the QCD value $N_c = 3$. Insisting that there are no non-factorization effects present amounts to setting $N_c = 3$ in calculating a_i. This is also referred to as "naive factorization' and is known not to work in decays such as $B \to (D, D^*)(\pi, \rho), J/\psi K^{(*)}$ [18,21]. In these decays only the coefficients a_1 and a_2 are determined. Note that QCD does not demand the equality of a_1 and a_2 from these decays and from the ones $B \to h_1 h_2$, though their values may come out to be close to each other. Hence, all the ten quantities a_i should be treated as phenomenological parameters and fitted from data on $B \to h_1 h_2$ decays.

Returning to the discussion of the hadronic matrix elements, we recall that when a vector meson is involved in a decay, such as in $B \to PV$ and $B \to VV$ decays, we need also the $B \to V$ form factors, which are defined as follows:

$$\begin{aligned}
\langle V(p_V)|V_\mu - A_\mu|\bar{B}^0(p_B)\rangle &= -\epsilon_{\mu\nu\alpha\beta}\epsilon^{\nu *} p_B^\alpha p_V^\beta \frac{2V(q^2)}{(m_B + m_V)} \\
&- i\left(\epsilon_\mu^* - \frac{\epsilon^* \cdot q}{q^2} q_\mu\right)(m_B + m_V) A_1(q^2) \\
&+ i\left((p_B + p_V)_\mu - \frac{(m_B^2 - m_V^2)}{q^2} q_\mu\right)(\epsilon^* \cdot q)\frac{A_2(q^2)}{m_B + m_V} \\
&- i\frac{2m_V(\epsilon^* \cdot q)}{q^2} q_\mu A_0(q^2),
\end{aligned} \tag{24}$$

where $q = p_B - p_V$, and ϵ^* is the polarization vector of V. To cancel the poles at $q^2 = 0$, we must have

$$2m_V A_0(0) = (m_B + m_V)A_1(0) - (m_B - m_V)A_2(0). \tag{25}$$

The decay constants of the vector mesons are defined as follows:

$$< V|\bar{q}\gamma_\mu q|0 >= f_V \; m_V \epsilon_\mu. \tag{26}$$

This completes the discussion of the factorization Ansatz. The various input parameters needed to do numerical calculations, including the form factors and meson decay constants, are discussed in the next section.

4 Input parameters

The matrix elements for the decay $B \to h_1 h_2$ derived in the preceding section depend on the effective coefficients $a_1, ..., a_{10}$, quark masses, various form factors, decay constants, the CKM

parameters, the renormalization scale μ and the QCD scale parameter $\Lambda_{\overline{\rm MS}}$. We have fixed $\Lambda_{\overline{\rm MS}}$ using the central value of the present world average $\alpha_s(M_Z) = 0.118 \pm 0.003$ [57]. The scale μ is varied between $\mu = m_b$ and $\mu = m_b/2$, but due to the inclusion of the NLL expressions the dependence of the decay rates on μ is small and hence not pursued any further. To be specific, we use $\mu = 2.5$ GeV in the following. The dependence on the rest of the parameters is more pronounced and we discuss them below giving the present status of these quantities.

4.1 CKM Matrix Elements

The CKM matrix will be expressed in terms of the Wolfenstein parameters [49], A, λ, ρ and η.

$$V_{CKM} \simeq \begin{pmatrix} 1-\frac{1}{2}\lambda^2 & \lambda & A\lambda^3(\rho - i\eta) \\ -\lambda & 1-\frac{1}{2}\lambda^2 & A\lambda^2 \\ A\lambda^3(1-\rho-i\eta) & -A\lambda^2 & 1 \end{pmatrix} \tag{27}$$

Since the first two are well-determined with $A = 0.81 \pm 0.06$, $\lambda = \sin\theta_C = 0.2205 \pm 0.0018$ [19], we fix them to their central values. The other two are correlated and are found to lie (at 95% C.L.) in the range $0.25 \leq \eta \leq 0.52$ and $-0.2 \leq \rho \leq 0.35$ from the CKM unitarity fits [47]. We shall show the dependence of the decay rates on the parameters ρ and η in the allowed domain. However, for illustrative purposes and if not stated otherwise, we shall use $\rho = 0.12, \eta = 0.34$, which are the "best-fit" values from the CKM unitarity fits [47][3].

4.2 Quark masses

The quark masses enter our analysis in two different ways. First, they arise from the contributions of the penguin loops in connection with the function $\Delta F_1(k^2/m_i^2)$. We treat the internal quark masses in these loops as constituent masses rather than current masses. For them we use the following (renormalization scale-independent) values:

$$m_b = 4.88 \text{ GeV}, \quad m_c = 1.5 \text{ GeV}, \quad m_s = 0.5 \text{ GeV}, \quad m_u = m_d = 0.2 \text{ GeV} . \tag{28}$$

Variation in a reasonable range of these parameters does not change the numerical results of the branching ratios in question, as also investigated in [27]. The value of m_b is fixed to be the current quark mass value $\overline{m_b}(\mu = 2.5 \text{ GeV}) = 4.88$ GeV, given below. Second, the quark masses m_b, m_s, m_d and m_u appear through the equations of motion when working out the (factorized) hadronic matrix elements. In this case, the quark masses should be interpreted as current masses. It is worthwhile to discuss the spread in the quark masses, as determined from various calculational techniques and experiment. The top quark mass is now known rather precisely $\overline{m_t}(m_t) = 168 \pm 6$ GeV. Typical uncertainty on the b-quark mass $\delta(\overline{m_b}(\mu = 2.5 \text{ GeV})) = \pm 0.2$ GeV [58,59] is also small. Likewise, the mass difference $m_b - m_c = (3.39 \pm 0.06)$ GeV [59] is well determined, which can be used to determine m_c reasonably accurately for the calculations being done here. Hence, to the accuracy of the present framework, the uncertainties in the decay rates related to δm_t, δm_b and δm_c are small and ignored.

Light quark mass ratios have been investigated in chiral perturbation theory [60] and updated in [61], yielding: $m_u/m_d = 0.553 \pm 0.043$, $m_s/m_d = 18.9 \pm 0.9$, $m_s/m_u = 34.4 \pm 3.7$.

[3] The corresponding "best-fit" values obtained in [48] $\rho \simeq 0.15$ and $\eta \simeq 0.34$ are very close to the ones being used here.

Table 1: Input values in numerical calculations.

names	Values
$\alpha_s(m_Z)$	0.118
μ	2.5 GeV
A	0.81
λ	0.2205
$\tau(B^+)$	1.62 ps
$\tau(B^0)$	1.56 ps
$m_t(m_t)$	168 GeV
$m_b(2.5GeV)$	4.88 GeV
$m_c(2.5GeV)$	1.5 GeV
$m_s(2.5GeV)$	122 MeV
$m_d(2.5GeV)$	7.6 MeV
$m_u(2.5GeV)$	4.2 MeV

These ratios were converted into the quark masses by using the QCD sum rule estimates of the s-quark mass of the somewhat older vintage [62]: $\overline{m_s}(1\ \mathrm{GeV}) = 175 \pm 25$ MeV, yielding $\overline{m_u}(1\ \mathrm{GeV}) = 5.1 \pm 0.9$ MeV, $\overline{m_d}(1\ \mathrm{GeV}) = 9.3 \pm 1.4$ MeV [61]. Improved estimates based on QCD sum rules have been reported during the last year, which include $O(\alpha_s^3)$-perturbative improvements [63], improved estimates of $\Lambda^{(3)}_{\overline{\mathrm{MS}}}$ yielding $\Lambda^{(3)}_{\overline{\mathrm{MS}}} \simeq 380$ MeV, and improvements in the estimates of the spectral functions [64,65] lowering the s-quark mass. A contemporary representative values of the $s-$quark mass in the QCD sum rule approach is: $\overline{m_s}(1\ \mathrm{GeV}) = 150 \pm 30$ MeV [65].

The corresponding estimates in the quenched lattice-QCD approach have been recently reported in a number of papers [66–68]. The lattice community likes to quote the light quark masses at the scale $\mu = 2$ GeV, and in comparing them with the QCD-sum rule results, quoted above for 1 GeV, one should multiply the lattice numbers by a factor 1.3. Representative lattice-QCD values are: $\overline{m_s}(2\ \mathrm{GeV}) = 100 \pm 12$ MeV [66], $\overline{m_s}(2\ \mathrm{GeV}) = 130 \pm 2 \pm 18$ MeV [67], and $\overline{m_s}(2\ \mathrm{GeV}) = 110 \pm 20 \pm 11$ MeV [68]. The error due to unquenching is largely unknown and for a discussion of the given lattice-specific errors, we refer to the original literature. Taking the last of these values as fairly representative, one now has the central value $\overline{m_s}(1\ \mathrm{GeV}) \simeq 140$ MeV with a typical error of ± 25 MeV – in reasonably good agreement with the QCD sum rule estimates. Using $\overline{m_b}(\mu = m_b) = 4.45$ GeV from the central value in [58] and

$$\overline{m_s}(1\ \mathrm{GeV}) = 150\ MeV \quad , \quad \overline{m_d}(1\ \mathrm{GeV}) = 9.3\ MeV \quad , \quad \overline{m_u}(1\ \mathrm{GeV}) = 5.1\ MeV \quad , \qquad (29)$$

from the discussion above, the corresponding values at the scale $\mu = 2.5$ GeV used in our calculations are given in Table 1.

Varying the light quark masses by $\pm 20\%$ yields variation of up to $\pm 25\%$ in some selected decay rates (such as in $B^\pm \to \eta' K^\pm$ and $B^0 \to \eta' K^0$, as also noted in [28]). While this dependence should be kept in mind in fitting the quantities a_i from precise data, this is clearly not warranted by present data. Also, fitting the values of the quantities a_i is not the aim of this paper. Hence, we shall fix all the current quark masses to their values in Table 1.

Table 2: Form factors at zero momentum transfer in the BSW model [8].

Decay	$F_1 = F_0$	V	A_1	A_2	A_0
$B \to \pi$	0.33				
$B \to K$	0.38				
$B \to \eta$	0.145				
$B \to \eta'$	0.135				
$B \to \rho$		0.33	0.28	0.28	0.28
$B \to K^*$		0.37	0.33	0.33	0.32
$B \to \omega$		0.33	0.28	0.28	0.28

Table 3: Values of pole masses in GeV.

Current	m(0^-)	m(1^-)	m(1^+)	m(0^+)
$\bar{u}b$	5.2789	5.3248	5.37	5.73
$\bar{d}b$	5.2792	5.3248	5.37	5.73
$\bar{s}b$	5.3693	5.41	5.82	5.89

4.3 Form factors and hadronic coupling constants

Finally, we discuss the numerical values of the form factors and coupling constants introduced in the previous section. Concerning the form factors, we shall use two different theoretical approaches. The first is based on the quark model due to Bauer, Stech and Wirbel [8], which has been found to be rather successful in accommodating data on a number of exclusive decays. In the BSW model, the meson-meson matrix elements of the currents are evaluated from the overlap integrals of the corresponding wave functions. The dependence of the form factors on the momentum transfer squared Q^2 (which in $B \to h_1 h_2$ decays equals the mass squared of the light meson) is modeled by a single-pole Ansatz. The values of the form factors in the transitions $B \to \pi$, $B \to K$, $B \to \eta$, $B \to \eta'$, $B \to \rho$, $B \to K^*$ and $B \to \omega$, evaluated at $Q^2 = 0$ are given in Table 2. We assume ideal mixing for the (ω, ϕ) complex. This amounts to using in the quark language $\phi = s\bar{s}$ and $\omega = \frac{1}{\sqrt{2}}(u\bar{u} + d\bar{d})$. Note, that to implement the η-η' mixing, we shall use the two-mixing-angle formalism proposed recently in [69,70], in which one has:

$$|\eta\rangle = \cos\theta_8 |\eta_8\rangle - \sin\theta_0 |\eta_0\rangle \ , \quad |\eta'\rangle = \sin\theta_8 |\eta_8\rangle + \cos\theta_0 |\eta_0\rangle \ . \tag{30}$$

Here, η_8 and η_0 are, respectively, the flavor $SU(3)$-octet and -singlet components. The relations for the pseudoscalar decay constants in this mixing formalism involving the axial-vector currents A_μ^8 and A_μ^0 are:

$$\begin{aligned} \langle 0|A_\mu^8|\eta(p)\rangle &= i f_\eta^8 p_\mu, \quad \langle 0|A_\mu^8|\eta'(p)\rangle = i f_{\eta'}^8 p_\mu, \\ \langle 0|A_\mu^0|\eta(p)\rangle &= i f_\eta^0 p_\mu, \quad \langle 0|A_\mu^0|\eta'(p)\rangle = i f_{\eta'}^0 p_\mu \ . \end{aligned} \tag{31}$$

The best-fit values of the (η-η') mixing parameters from [71] yields: $\theta_8 = -22.2^\circ$, $\theta_0 = -9.1^\circ$, $f_8 = 168$ MeV, and $f_0 = 157$ MeV, which are used to calculate the decay rates in which η

Table 4: Form factors at zero momentum transfer from Lattice QCD and Light-cone QCD sum rules.

Decay	$F_1 = F_0$	V	A_1	A_2	A_0
$B \to \pi$ [15]	0.30 ± 0.04				
$B \to K$[15]	0.35 ± 0.05				
$B \to \eta$ (see text)	0.13 ± 0.02				
$B \to \eta'$ (see text)	0.12 ± 0.02				
$B \to \rho$ [11]		0.35 ± 0.05	0.27 ± 0.04	0.26 ± 0.04	0.30 ± 0.05
$B \to K^*$ [12]		0.48 ± 0.09	0.35 ± 0.07	0.34 ± 0.06	0.39 ± 0.10
$B \to \omega$ ([11] & SU(3))		0.35 ± 0.05	0.27 ± 0.04	0.26 ± 0.04	0.30 ± 0.05

and/or η' are involved. In deriving the expressions for the decays involving η and η', we include the anomaly term in $\partial_\mu A^\mu$ and the contributions of $b \to sgg \to s(\eta, \eta')$ as calculated in [28]. Definitions of the various matrix elements can be seen in the appendix and we refer to [27,28] for further discussions. The values of the input pole masses used in calculating the form factors are given in Table 3. However, in the decays $B \to h_1 h_2$, only small extrapolations from $Q^2 = 0$ are involved, hence the error due to the assumed Q^2-dependence and/or the specific values for the pole masses is small.

The second and more modern approach to calculating decay form factors is a hybrid approach, in which often lattice-QCD estimates in the so-called $heavy \to light$ mesons, calculated at high-Q^2, are combined with the Q^2-dependence following from the light-cone QCD sum rule analysis [12,13]. We refer to [10] for detailed discussions, compilation of the lattice-QCD analysis and references to the literature, and quote here the results from the UKQCD analysis [11]. For the $B \to \pi$ form factor: $F_1(0) = F_0(0) = 0.27 \pm 0.11$; for $B \to \rho$ form factors: $V(0) = 0.35^{+0.06}_{-0.05}$, $A_1(0) = 0.27^{+0.05}_{-0.04}$, $A_2(0) = 0.26^{+0.05}_{-0.03}$, and $A_0(0) = 0.30^{+0.06}_{-0.04}$. The results from an improved light-cone QCD sum rule calculation [15] for $F_1(B \to \pi) = F_0(B \to \pi)$ and $F_1(B \to K) = F_0(B \to K)$ are given in Table 4. The results for $F_1(B \to \eta) = F_0(B \to \eta)$ and $F_1(B \to \eta') = F_0(B \to \eta')$ are calculated from the $B \to \pi$ form factors from [15] taking into account additionally the (η, η') mixing, as discussed earlier and further detailed in Appendix A. The results for the $B \to K^*$ form factors have been obtained in the light-cone QCD sum rule in ref. [12], which yield:

$$\begin{aligned} \frac{A_1(0)^{B\to\rho}}{A_1(0)^{B\to K^*}} &= 0.76 \pm 0.05 \ , \\ \frac{V(0)^{B\to\rho}}{V(0)^{B\to K^*}} &= 0.73 \pm 0.05 \ , \end{aligned} \tag{32}$$

which, in turn, lead to the estimates $A_1(0)^{B\to K^*} = 0.35 \pm 0.07$ and $V(0)^{B\to K^*} = 0.48 \pm 0.09$. Assuming similar $SU(3)$-breaking in the remaining two form factors, and using the estimates for the corresponding form factors in $B \to \rho$ quoted above, one gets: $A_2(0)^{B\to K^*} = 0.34 \pm 0.06$ and $A_0(0)^{B\to K^*} = 0.39 \pm 0.10$. The values from this hybrid approach are collected in Table 4. As for the form factors in the BSW model, we use a simple pole approximation for calculating the form factors at Q^2 different from $Q^2 = 0$. However, for the decays of interest, this extrapolation

Table 5: Values of decay constants in MeV.

f_π	f_K	f_8	f_0	f_η^c	$f_{\eta'}^c$	f_ρ	f_{K^*}	f_ω	f_ϕ
133	158	168	157	-0.9	-2.3	210	214	195	233

is small and one does not expect any significant error from this source. For example, for the $B \to P$ form factors, using the parameterization of $F_{0,1}(Q^2)$ given in eq. (12) of ref. [15], the resulting difference in the form factors is found to be less than 2%.

The values for the pseudoscalar and vector decay constants are given in Table 5. The values for f_ω, f_K, f_{K^*} and f_π coincide with the central values quoted in [18] extracted from data on the electromagnetic decays of ω and τ decays, respectively [19]. The decay constants $f_{\eta'}^u$, $f_{\eta'}^s$, f_η^u and f_η^s defined in the appendix A are obtained from the values for f_0 and f_8, θ_8 and θ_0 for the (η, η') mixing, given earlier. The errors on the decay constants in Table 5 are small (typically $(1-3)\%$), except on $f_{\eta'}^{(c)}$ and $f_\eta^{(c)}$ for which we use here the estimates from [28] obtained using the QCD-anomaly method. These quantities have also been determined from the $\eta_c - \eta' - \eta$-mixing formalism and radiative decays $J/\psi \to (\eta_c, \eta', \eta)\gamma$ and the two-photon decay widths $(\eta_c, \eta', \eta) \to \gamma\gamma$ in ref. [27] with results similar to the corresponding values obtained using the QCD-anomaly method [28]. For some recent determinations of these quantities, see also [72,73].

5 Effective coefficients a_i and a classification of $B \to h_1 h_2$ decays

5.1 Effective coefficients a_i

The effective coefficients a_i, which are specific to the factorization approach, are the quantities of principal phenomenological interest. Note that there are four types of transitions that one encounters in the current-current and penguin-induced decays $B \to h_1 h_2$: $b \to s$ $[\bar{b} \to \bar{s}]$, and $b \to d$ $[\bar{b} \to \bar{d}]$. Numerical values of a_i $(i = 1, ..., 10)$ for representative values of the phenomenological parameter N_c are displayed in Table 6 and Table 7 for the $b \to s$ $[\bar{b} \to \bar{s}]$ and $b \to d$ $[\bar{b} \to \bar{d}]$ cases, respectively. A number of remarks on the entries in these tables is helpful for a discussion of the branching ratios worked out later.

- The determination of a_1 and a_2 in the $b \to c$ current-current transitions has received a lot of attention. It remains an open and interesting question if a_1 and a_2 in the $b \to u$ transitions are close to their $b \to c$ counterparts, which have the phenomenological values $a_1 \simeq 1$ and $a_2 \simeq 0.2$ [18,21]. These values correspond to the parameter $\xi \equiv 1/N_c$ having a value around 0.4. The decays $B \to \pi\pi$, $B \to \rho\pi$ and $B \to \omega\pi$ are well suited to determine these coefficients.

- The coefficients a_3 and a_5 in the QCD-penguin sector are smaller compared to a_4 and a_6. In particular, the combination $a_3 + a_5$ has a perturbative value of 3×10^{-4}, i.e., for $N_c = 3$, in all four cases resulting from large cancellations between a_3 and a_5. This coefficient also shows extreme sensitivity to the parameter N_c, which in the present model is a measure

Table 6: Numerical values of effective coefficients a_i for $b \to s$ [$\bar{b} \to \bar{s}$] at $N_c = 2, 3, \infty$, where $N_c = \infty$ corresponds to C_i^{eff}. The penguin coefficients $C_3^{eff}, ..., C_7^{eff}$ and C_9^{eff} are calculated for the Wolfenstein parameters $\rho = 0.12$ and $\eta = 0.34$. Note that the entries for a_3,...,a_{10} have to be multiplied with 10^{-4}.

	$N_c = 2$	$N_c = 3$	$N_c = \infty$
a_1	0.99 [0.99]	1.05 [1.05]	1.16 [1.16]
a_2	0.25 [0.25]	0.053 [0.053]	-0.33 [-0.33]
a_3	$-37 - 14i$ [$-36 - 14i$]	48 [48]	$218 + 29i$ [$215 + 29i$]
a_4	$-402 - 72i$ [$-395 - 72i$]	$-439 - 77i$ [$-431 - 77i$]	$-511 - 87i$ [$-503 - 87i$]
a_5	$-150 - 14i$ [$-149 - 14i$]	-45 [-45]	$165 + 29i$ [$162 + 29i$]
a_6	$-547 - 72i$ [$-541 - 72i$]	$-575 - 77i$ [$-568 - 77i$]	$-630 - 87i$ [$-622 - 87i$]
a_7	$1.3 - 1.3i$ [$1.4 - 1.3i$]	$0.5 - 1.3i$ [$0.5 - 1.3i$]	$-1.2 - 1.3i$ [$-1.1 - 1.3i$]
a_8	$4.4 - 0.7i$ [$4.4 - 0.7i$]	$4.6 - 0.4i$ [$4.6 - 0.4i$]	5.0 [5.0]
a_9	$-91 - 1.3i$ [$-91 - 1.3i$]	$-94 - 1.3i$ [$-94 - 1.3i$]	$-101 - 1.3i$ [$-101 - 1.3i$]
a_{10}	$-31 - 0.7i$ [$-31 - 0.7i$]	$-14 - 0.4i$ [$-14 - 0.4i$]	20 [20]

of non-factorizing effects. Hence, for decays whose decay widths depend dominantly on these coefficients, the factorization framework is not reliable. The reason is simply that the neglected contributions, such as the weak annihilation diagrams and/or feed down from final state interactions to these channels, could easily overwhelm the perturbative factorizable contributions.

- Concerning the effective coefficients of the electroweak operators, we note that a_7, a_8 and a_{10} are numerically very small. This again reflects their perturbative magnitudes, i.e. the coefficients C_i^{eff}, as can be seen in the columns for $N_c = 3$. Varying N_c, one sees no noticeable enhancement in these coefficients (except for a_{10} but it remains phenomenologically small to have any measurable effect). Hence, electroweak penguins enter dominantly through the operator O_9, barring rather drastic enhancements (of $O(100)$) in the matrix elements of the operators O_7, O_8 and O_{10}, which we discount. No attempts will be made to determine these coefficients here. In fact, in the context of the SM one could as well work with a much reduced basis in the effective theory in which the coefficients a_7, a_8 and a_{10} are set to zero.

- The dominant coefficients are then a_1, a_2 (current-current amplitudes), a_4, a_6 (QCD penguins) and a_9 (electroweak penguin), which can be eventually determined from experiments and we discuss this programmatically later. Of these a_1, a_2 (and to a very high accuracy also a_9) do not depend on the CKM matrix elements. The dependence of a_4 and a_6 (likewise, the smaller parameters a_3 and a_5) on the CKM factors enters through the function C_t. The numbers given in the tables for a_i are obtained for the CKM parameters having the values $\rho = 0.12$ and $\eta = 0.34$. Note that a_2 depends strongly on N_c.

This sets the stage for discussing the various branching ratios numerically and comparison with the available data.

Table 7: Numerical values of effective coefficients a_i for $b \to d$ [$\bar{b} \to \bar{d}$] at $N_c = 2, 3, \infty$, where $N_c = \infty$ corresponds to C_i^{eff}. The penguin coefficients $C_3^{eff}, ..., C_7^{eff}$ and C_9^{eff} are calculated for the Wolfenstein parameters $\rho = 0.12$ and $\eta = 0.34$. Note that the entries for a_3,...,a_{10} have to be multiplied with 10^{-4}.

	$N_c = 2$	$N_c = 3$	$N_c = \infty$
a_1	0.99 [0.99]	1.05 [1.05]	1.16 [1.16]
a_2	0.25 [0.25]	0.053 [0.053]	-0.33 [-0.33]
a_3	$-33 - 7i$ [$-42 - 23i$]	48 [48]	$208 + 14i$ [$226 + 47i$]
a_4	$-377 - 34i$ [$-423 - 116i$]	$-412 - 36i$ [$-461 - 124i$]	$-481 - 41i$ [$-536 - 140i$]
a_5	$-145 - 14i$ [$-154 - 14i$]	-45 [-45]	$155 + 14i$ [$173 + 47i$]
a_6	$-523 - 34i$ [$-568 - 116i$]	$-548 - 36i$ [$-597 - 124i$]	$-600 - 41i$ [$-655 - 140i$]
a_7	$1.5 - 1.0i$ [$1.1 - 1.8i$]	$0.7 - 1.0i$ [$0.3 - 1.8i$]	$-1.0 - 1.0i$ [$-1.4 - 1.8i$]
a_8	$4.5 - 0.5i$ [$4.3 - 0.9i$]	$4.7 - 0.3i$ [$4.5 - 0.6i$]	5.0 [5.0]
a_9	$-91 - 1.0i$ [$-91 - 1.8i$]	$-94 - 1.0i$ [$-95 - 1.8i$]	$-101 - 1.0i$ [$-101 - 1.8i$]
a_{10}	$-30 - 0.5i$ [$-31 - 0.9i$]	$-14 - 0.3i$ [$-14 - 0.6i$]	20 [20]

Before discussing the numerical results and their detailed comparison with experiment and existing results in the literature, it is worthwhile to organize the decays $B \to h_1 h_2$ in terms of their sensitivity on N_c and anticipated contributions due to the annihilation diagrams in some of these decays.

5.2 Classification of factorized amplitudes

In the context of the tree (T) decays, a classification was introduced in [8], which is used widely in the literature in the analysis of B decays involving charmed hadrons. These classes, concentrating now on the $B \to h_1 h_2$ decays, are the following

- Class-I decays, involving those decays in which only a charged meson can be generated directly from a singlet current, as in $B^0 \to \pi^+\pi^-$, and the relevant coefficient for these decays is a_1. This coefficient is stable against variation of N_c (see Tables 6 and 7). There are just five class-I decays: $B^0 \to \pi^-\pi^+$, $B^0 \to \rho^-\pi^+$, $B^0 \to \rho^+\pi^-$, $B^0 \to \rho^-\rho^+$, and exceptionally also $B^0 \to \rho^- K^+$.

- Class-II decays, involving those transitions in which the meson generated directly from the current is a neutral meson, like $B^0 \to \pi^0\pi^0$, and the relevant coefficient for these decays is a_2, which shows a strong N_c-dependence (see Tables 6 and 7). There are twelve such decays $B^0 \to h_1^0 h_2^0$, where h_1^0 and h_2^0 are mesons from the set $\pi^0, \eta, \eta', \rho^0$ and ω. The decays $B^0 \to \pi^0\eta^{(\prime)}$ exceptionally do not belong to this class, as their decay amplitudes proportional to a_2 almost cancel due to the destructive interference in two tree diagrams having to do with the configuration $\pi^0 \sim u\bar{u} - d\bar{d}$ and $\eta^{(\prime)} \sim (u\bar{u} + d\bar{d}) + ...$ Note that as a_2 has the smallest value at $N_c = 3$, all class-II decays have their lowest values at $N_c = 3$.

- Class-III decays, involving the interference of class-I and Class-II decays, as in this case both a charged and a neutral meson is present both of which can be generated through the

currents involved in H_{eff}. An example of these decays is $B^+ \to \pi^+\pi^0$, and the relevant coefficient is $a_1 + ra_2$, where r is process-dependent (but calculable in terms of the ratios of the form factors and decay constants). For $r \leq 1$, the N_c-dependence of the class-III amplitudes is below $\pm 20\%$ w.r.t. the perturbative value. As we shall see, the quantity r may considerably enhance the N_c-dependence if r is well in excess of 1. This, in particular, is the case in $B^+ \to \rho^0\pi^+$ and $B^+ \to \omega\pi^+$ decays, where $r \simeq 2$; hence these Class-III decays show marked N_c-dependence. However, one should note that the decay rates for this class do not have their minima at $N_c = 3$, but rather at $N_c = \infty$, reflecting the behavior of $a_1 + a_2$. There are eleven such decays involving $B^+ \to (\pi^+, \rho^+)(\pi^0, \eta, \eta', \rho^0, \omega)$ and exceptionally also the decay $B^+ \to K^{*+}\eta'$, in which case the penguin amplitudes interfere destructively. Its decay rate is, however, rather stable w.r.t. the variation in N_c but small due to the CKM suppression.

However, when QCD (P) and electroweak penguins ($P_{\rm EW}$) are also present, as is the case in the decays $B \to h_1 h_2$ being considered, in general, the above classification has to be extended. In this case, the generic decay amplitude depends on $T + P + P_{\rm EW}$. If the amplitude is still dominated by the tree amplitude, the BSW-classification given above can be applied as before. For those decays which are dominated by penguin amplitudes, i.e., $T + P + P_{\rm EW} \simeq P + P_{\rm EW}$, the above classification used for the tree amplitude is no longer applicable.

For the penguin-dominated decays, we introduce two new classes:

- Class-IV decays, consisting of decays whose amplitudes involve one (or more) of the dominant penguin coefficients a_4, a_6 and a_9, with constructive interference among them. They are stable against variation in N_c (see tables 6 and 7) and have the generic form:

$$\begin{aligned} \mathcal{M}(B^0 \to h_1^\pm h_2^\mp) &\simeq \alpha_1 a_1 + \sum_{i=4,6,9} \alpha_i a_i \ + ..., \\ \mathcal{M}(B^0 \to h_1^0 h_2^0) &\simeq \alpha_2 a_2 + \sum_{i=4,6,9} \alpha_i a_i \ + ..., \\ \mathcal{M}(B^\pm \to h_1^\pm h_2^0) &\simeq \alpha_1 (a_1 + r a_2) + \sum_{i=4,6,9} \alpha_i a_i \ + ..., \end{aligned} \tag{33}$$

  with the second $(P + P_{\rm EW})$ term dominant in each of the three amplitudes. The ellipses indicate possible contributions from the coefficients a_3, a_5, a_7, a_8 and a_{10} which can be neglected for this class of decays. The coefficients α_j are process-dependent and contain the CKM matrix elements, form factors etc. The decays where α_1 and α_2 are zero are pure penguin processes and are obviously included here. The tree-dominated decays, discussed earlier, also have a generic amplitude of the type shown above. However, in this case the penguin-related coefficients α_j are numerically small due to the CKM factors (specifically due to $V_{td} \ll V_{ts}$).

Examples of Class-IV decays are quite abundant. In our classification, all twelve $B \to PP$ decays dominated by penguin amplitudes are class-IV decays. They include decays such as $B^+ \to K^+\pi^0$, $B^+ \to K^+\eta^{(\prime)}$, which involve $a_1 + ra_2$ as the tree amplitude, and $B^0 \to K^0\pi^0$, and $B^0 \to K^0\eta^{(\prime)}$, which involve a_2 from the tree amplitude. Finally, the pure-penguin decays, such as $B^+ \to \pi^+ K^0$, $B^+ \to K^+\bar{K}^0$ and $B^0 \to K^0\bar{K}^0$ naturally belong here. There are altogether twenty nine such decays. The decay $B^0 \to K^{*0}\eta'$, in contrast to its B^+-counterpart,

is not a class-IV decay due to the destructive interference in the QCD-penguin amplitude. The variation in the decay rates belonging to class-IV decays is less than $\pm 30\%$ compared to their perturbative ($N_c = 3$) value.

- Class-V decays, involve penguins with strong N_c-dependent coefficients a_3, a_5, a_7 and a_{10}, interfering significantly with one of the dominant penguin coefficients a_4, a_6 and a_9 (analogous to the class-III decays $a_1 + ra_2$ dominated by tree amplitudes). Then, there are decays in which the dominant penguin coefficients (a_4, a_6, a_9) interfere destructively. Their amplitudes can be written much like the ones in eq. (33), except that the sum in the second term now goes over all eight penguin coefficients. Since these amplitudes involve large and delicate cancellations, they are generally not stable against N_c.

Examples of this class are present in $B \to PV$ and $B \to VV$ decays, such as $B^\pm \to \pi^\pm\phi$, $B^0 \to \pi^0\phi$, $B^0 \to \eta^{(\prime)}\phi$, $B^0 \to \omega\phi$, $B^\pm \to \rho^\pm\phi$, $B^0 \to \rho^0\phi$, etc. In all these cases, the amplitudes are proportional to the linear combination $[a_3 + a_5 - 1/2(a_7 + a_9)]$ (see Appendix B and C). Examples of those where the amplitudes proportional to the dominant penguin coefficients interfere destructively are: $B^+ \to K^+\phi$, $B^0 \to K^0\phi$ etc. The above five classes exhaust all cases, though clearly there are some amplitudes where comparable T and penguin $(P + P_{\rm EW})$ contributions are present. They can be assigned to one of the classes depending on their tree and/or penguin coefficients, the criterion being the N_c-dependence of the decay rates.

Summarizing the classification, Class-I and Class-IV decays are relatively large, unless suppressed by the CKM factors, and stable against variation of N_c, which is a measure of non-factorizing effects in the present model. Class-III decays are mostly stable, except for the already mentioned $B \to PV$ decays. Many Class-II and Class-V decays are rather unstable against variation of N_c either due the dependence on the N_c-sensitive coefficients or due to delicate cancellations. Many decays in Class-II and Class-V may receive significant contribution from the annihilation diagrams which we discuss now.

5.3 Contribution of annihilation amplitudes

Annihilation (by which are meant here both $W^\pm$-exchange and $W^\pm$-annihilation) contributions are present in almost all decays of the type $B \to h_1 h_2$ being considered here. However, their contribution should be understood as power corrections in inverse powers of m_b (equivalently in $1/m_B$) in B decays. In inclusive B decays, their contribution to the decay width relative to that of the parton model is determined by the factor

$$4\pi^2 \frac{f_B^2 m_B}{m_b^3} \simeq \left(\frac{2\pi f_B}{m_b}\right)^2 \simeq 5\%, \tag{34}$$

where $f_B \simeq 200$ MeV is the B-meson decay constant. The near equality of the lifetimes of $B^\pm$, $\bar{B}^0(B^0)$ and $\bar{B}_s^0(B_s^0)$ mesons shows that the above crude estimate is largely correct, and that annihilation contributions are sufficiently power-suppressed in B-meson decays. For more sophisticated but in their spirit essentially similar calculations, see, for example, [74].

However, in exclusive two-body B-decays, the contribution to a particular channel depends on the CKM factors and the dynamical quantities a_i, and in some cases the non-annihilation contribution is enormously suppressed. In these channels, the annihilation diagrams, despite

being power suppressed in $1/m_b^2$, may yield the dominant contributions to the decay and must therefore be included in the rate estimates and CP-asymmetries. Instead of working out the annihilation contribution in all the channels discussed here, which necessarily introduces unknown hadronic quantities, we do a classification of annihilation diagrams and list only those decays in which they are anticipated to be important.

For the decays $B \to h_1 h_2$, we need to consider the following annihilation amplitudes:

- $W^\pm$-Exchange: $\mathcal{M}(\bar{b}d \to \bar{u}u) \Longrightarrow \mathcal{M}(B^0 \to (\bar{u}q)(\bar{q}u)) \propto a_2\lambda^3$,
- $W^\pm$-Annihilation: $\mathcal{M}(\bar{b}u \to \bar{d}u) \Longrightarrow \mathcal{M}(B^+ \to (\bar{d}q)(\bar{q}u)) \propto a_1\lambda^3$,
- $W^\pm$-Annihilation: $\mathcal{M}(\bar{b}u \to \bar{s}u) \Longrightarrow \mathcal{M}(B^+ \to (\bar{s}q)(\bar{q}u)) \propto a_1\lambda^4$,

where $\lambda = \sin\theta_C$. Here, $q\bar{q}$ is a light quark-antiquark pair. These amplitudes can be termed as the tree-annihilation contributions. In addition, there are also the penguin-annihilation contributions which are important for certain decays. For example, they feed dominantly to the decay $B^0 \to \phi\phi$.

There are yet more decays which can be reached via annihilation followed by rearrangement of the quark-antiquark pairs in the final state. Representative of these are the decays $B^\pm \to \phi\pi^\pm$, $B^\pm \to \phi\rho^\pm$ and $B^0(\bar{B}^0) \to \phi\pi^0$, $B^0(\bar{B}^0) \to \phi\eta^{(\prime)}$, $B^0(\bar{B}^0) \to \phi\omega$ and $B^0(\bar{B}^0) \to \phi\rho^0$. However, these rescattering effects (final state interactions) are expected to suffer from suppression due to the color-transparency argument used in defense of the factorization Ansatz. Since we have neglected these rescattering contributions in the factorization amplitudes worked out in this paper, it is only consistent that we also drop the annihilation contributions which feed into other channels through rescattering.

We specify below those two-body B decays which are accessible directly in annihilation processes and hence may have significant annihilation contributions:

- $B \to PP$ decays: $B^0 \to \pi^0\eta^{(\prime)}$, $B^0 \to \eta\eta'$.
- $B \to PV$ decays: $B^0 \to \rho^0\pi^0$, $B^0 \to \rho^0\eta^{(\prime)}$, $B^0 \to \omega\pi^0$, $B^0 \to \omega\eta^{(\prime)}$, $B^+ \to K^{*+}\bar{K}^0$, $B^+ \to K^+\phi$, $B^0 \to K^{*+}K^-$, $B^0 \to K^+K^{*-}$.
- $B \to VV$ decays: $B^0 \to \rho^0\rho^0$, $B^0 \to \rho^0\omega$, $B^0 \to \omega\omega$, $B^0 \to \phi\phi$, $B^+ \to K^{*+}\bar{K}^{*0}$, $B^+ \to K^{*+}\phi$, $B^0 \to K^{*+}K^{*-}$.

Note, that in addition to the decay modes listed above, there are quite a few others in the Class-I, Class-III and Class-IV decays given in the tables, which also have annihilation contributions but in view of the large T and/or $P + P_{\rm EW}$ contributions in these decays, the annihilation contributions are not expected to alter the decay rates in these channels significantly and hence we have not listed them.

The annihilation amplitude can be written as

$$< h_1h_2|\mathcal{H}_{eff}|B >_a = Z < h_1h_2|j^\mu|0 >< 0|j_\mu|B > . \tag{35}$$

If h_1 and h_2 are two pseudoscalars, the annihilation form factors are defined as

$$< P_1P_2|j^\mu|0 >= \left[(p_1 - p_2)^\mu - \frac{m_1^2 - m_2^2}{Q^2}Q^\mu\right] F_1^{P_1P_2}(Q^2) + \frac{m_1^2 - m_2^2}{Q^2}Q^\mu F_0^{P_1P_2}(Q^2), \tag{36}$$

where $Q = p_1 + p_2$. With this, we can write the required matrix element from the annihilation contribution (denoted here by a subscript) in its factorized form

$$< P_1P_2|\mathcal{H}_{eff}|B >_a = i\frac{G_F}{\sqrt{2}}V_{qb}V^*_{qq'}a_i f_B(m_1^2 - m_2^2)F_0^{P_1P_2}(m_B^2) \ , \tag{37}$$

where a_i, $i = 1, 2$. Note that the annihilation amplitude in the decay $B \to P_1P_2$ is proportional to the mass difference of the two mesons in the final state. Hence, in the present framework, there is no annihilation contribution to the decays such as $B^0 \to \pi^0\pi^0$, $B^0 \to K^+K^-$ etc. Comparing this amplitude with the non-annihilation contributions given in eqn (22), one finds that the annihilation amplitude in $B \to P_1P_2$ decays is indeed suppressed by a hefty factor

$$\frac{(m_1^2 - m_2^2)F_0^{P_1P_2}(m_B^2)}{(m_B^2 - m_1^2)F_0^{B\to P_1}(m_2^2)}. \tag{38}$$

The annihilation form factors are difficult to relate directly to experimental measurements but they can be modeled. We expect $F_0^{P_1P_2}(0)$ to have a similar magnitude as the the corresponding form factors $F_0^{B\to P_1}(0)$, to which they are related by crossing, and which we have listed in Tables 2 and 4. Based on this, the annihilation form factors appearing in eqs. (37) and (38) are suppressed due to large momentum transfer at $q^2 = m_B^2$, at which they have to be evaluated. The total suppression factor in $B \to PP$ decays is then $\mathcal{O}(m_{1,2}^4/m_B^4)$. However, the effective coefficients a_i, $i = 1, 2$ entering in the annihilation amplitude are much larger than a_j, $j = 3, ..., 10$ governing the penguin-amplitudes. So, a part of the power suppression is offset by the favorable effective coefficients.

In the decays $B \to PV$ and $B \to VV$, we do not anticipate the annihilation suppression as severe as in the decay $B \to PP$. Concentrating on the decays $B \to PV$, the annihilation form factors are

$$\begin{aligned} < PV|j^\mu|0 > \ &= \ \epsilon_{\mu\nu\alpha\beta}\epsilon^{*\nu}p_P^\alpha p_V^\beta \frac{2V(Q^2)}{m_P + m_V} \\ &\quad -i\left[\epsilon_\mu^* - \frac{(\epsilon^*\cdot Q)}{Q^2}Q_\mu\right](m_P + m_V)A_1(Q^2) \\ &\quad +i\left[(p_P - p_V)_\mu - \frac{m_P^2 - m_V^2}{Q^2}Q_\mu\right](\epsilon^*\cdot Q)\frac{A_2(Q^2)}{m_P + m_V} \\ &\quad -i\frac{2m_V}{Q^2}Q_\mu(\epsilon^*\cdot Q)A_0(Q^2). \end{aligned} \tag{39}$$

The annihilation matrix element in the factorization approximation can now be written as follows:

$$< PV|\mathcal{H}_{eff}|B >_a = i\sqrt{2}G_F V_{qb}V^*_{qq'}a_i f_B m_V(\epsilon^*\cdot p_B)A_0(m_B^2). \tag{40}$$

From this, it is easy to see that for this class of decays the suppression factor is only due to the large momentum transfer involved in the form factors $A_0(m_B^2)$. Hence, the annihilation diagrams can contribute more significantly in the decay amplitude. For some of the channels for which the non-annihilation contributions are highly suppressed, the annihilation diagram can be easily dominant. For example, the annihilation amplitude to the decay $B^+ \to K^{*+}\bar{K}^0$ is

$$< K^{*+}\bar{K}^0|\mathcal{H}_{eff}|B^+ >_a = i\sqrt{2}G_F V^*_{ub}V_{ud}a_1 f_B m_{K^*}(\epsilon^*\cdot p_B)A_0(m_B^2). \tag{41}$$

If we take $A_0(0) = 0.4$, $f_B = 200$ MeV, the annihilation branching ratio is of the order 10^{-8} which is an order of magnitude higher than the branching ratio calculated with the penguin contribution alone. Other channels where the annihilation channel may play a significant role have been listed above.

For $B \to VV$ decays, the conclusion is quite similar to the one for the $B \to PV$ decays. However, as these decays involve yet more untested form factors, their numerical estimates require a model for these form factors. The suspected channels in $B \to VV$ decays sensitive to annihilation contribution have been listed above. We conclude that the decays most sensitive to the annihilation channel are indeed the Class-II and Class-V decays, mostly involving $\bar{B}^0(B^0)$ decays.

6 Branching Ratios and Comparison with Data

Table 8: $B \to PP$ Branching Ratios (in units of 10^{-6}) using the BSW [Lattice QCD/QCD sum rule] form factors, with $k^2 = m_b^2/2$, $\rho = 0.12$, $\eta = 0.34$, and $N_c = 2, 3, \infty$ in the factorization approach. The last column contains measured branching ratios and upper limits (90% C.L.) [1].

Channel	Class	$N_c = 2$	$N_c = 3$	$N_c = \infty$	Exp.
$B^0 \to \pi^+\pi^-$	I	9.0 [11]	10.0 [12]	12 [15]	< 15
$B^0 \to \pi^0\pi^0$	II	0.35 [0.42]	0.12 [0.14]	0.63 [0.75]	< 9.3
$B^0 \to \eta'\eta'$	II	0.05 [0.07]	0.02 [0.02]	0.09 [0.10]	< 47
$B^0 \to \eta\eta'$	II	0.19 [0.22]	0.08 [0.10]	0.29 [0.34]	< 27
$B^0 \to \eta\eta$	II	0.17 [0.20]	0.10 [0.11]	0.24 [0.29]	< 18
$B^+ \to \pi^+\pi^0$	III	6.8 [8.1]	5.4 [6.4]	3.0 [3.6]	< 20
$B^+ \to \pi^+\eta'$	III	2.7 [3.2]	2.1 [2.5]	1.1 [1.4]	< 31
$B^+ \to \pi^+\eta$	III	3.9 [4.7]	3.1 [3.7]	1.9 [2.2]	< 15
$B^0 \to \pi^0\eta'$	IV	0.06 [0.07]	0.07 [0.09]	0.11 [0.13]	< 11
$B^0 \to \pi^0\eta$	IV	0.20 [0.24]	0.23 [0.27]	0.30 [0.36]	< 8
$B^+ \to K^+\pi^0$	IV	9.4 [11]	10 [12]	12 [15]	< 16
$B^0 \to K^+\pi^-$	IV	14 [16]	15 [18]	18 [21]	$15^{+5}_{-4} \pm 1$
$B^0 \to K^0\pi^0$	IV	5.0 [5.9]	5.7 [6.8]	7.4 [8.9]	< 41
$B^+ \to K^+\eta'$	IV	21 [25]	25 [29]	35 [41]	$65^{+15}_{-14} \pm 9$
$B^0 \to K^0\eta'$	IV	20 [24]	25 [29]	35 [41]	$47^{+27}_{-20} \pm 9$
$B^+ \to K^+\eta$	IV	2.0 [2.3]	2.4 [2.7]	3.4 [3.9]	< 14
$B^0 \to K^0\eta$	IV	1.7 [1.9]	2.0 [2.2]	2.6 [3.0]	< 33
$B^+ \to \pi^+K^0$	IV	14 [17]	16 [20]	22 [26]	$23^{+11}_{-10} \pm 4$
$B^+ \to K^+\bar{K}^0$	IV	0.82 [0.95]	0.96 [1.1]	1.3 [1.5]	< 21
$B^0 \to K^0\bar{K}^0$	IV	0.79 [0.92]	0.92 [1.1]	1.2 [1.4]	< 17

The decay branching ratios are shown in Tables 8 - 11 for the decays $B \to PP$, $B \to PV$ (involving $b \to d$ transitions), $B \to PV$ (involving $b \to s$ transitions) and $B \to VV$, respectively, for the two sets of form factors given in Tables 2 and 4. The numbers shown

for the hybrid Lattice-QCD/QCD sum rules correspond to using $F_{1,0}^{B\to\pi} = 0.36$, $F_{1,0}^{B\to K} = 0.41$, $F_{1,0}^{B\to\eta} = 0.16$ and $F_{1,0}^{B\to\eta'} = 0.145$. The first two are slightly above the range determined in [15] but within the (larger) range as determined from the lattice-QCD calculations [11]. This choice is dictated by data, as discussed in detail below. The k^2-dependence of the branching ratios in the range $k^2 = m_b^2/2 \pm 2$ GeV^2 is small and hence the numbers in these tables are shown only for the case $k^2 = m_b^2/2$. The CKM parameters are fixed at their "best-fit" values: $\rho = 0.12, \eta = 0.34$. All other parameters have their central values, discussed in the preceding section. In these tables we give the averages of the branching fractions of $\bar{B}^0$ and B^0, and of B^+ and B^-, respectively. Hence, when we refer to branching fractions in the following sections we always mean the averages over the B and anti-B decays. The CP-asymmetries are, however, in general quite sensitive to k^2 [33,32]. We shall discuss this point in a forthcoming paper on CP asymmetries [75].

A number of observations are in order:

- There are so far five measured $B \to h_1 h_2$ decay modes in well-identified final states: $B^0 \to K^+\pi^-$, $B^+ \to K^+\eta'$, $B^0 \to K^0\eta'$, $B^+ \to \pi^+ K^0$, and $B^+ \to \omega K^+$, with their branching ratios (averaged over the charge conjugate modes) given in Tables 8 and 10. In addition, the decay modes $B^+ \to \pi^0 h^+ (h^+ = \pi^+, K^+)$ with a branching ratio $\mathcal{B}(B^+ \to \pi^0 h^+) = (1.6^{+0.6}_{-0.5} \pm 0.4) \times 10^{-5}$ [1], the decay mode $B^+ \to \omega h^+ (h^+ = \pi^+, K^+)$ with a branching ratio $\mathcal{B}(B^+ \to \omega h^+) = (2.5^{+0.8}_{-0.7} \pm 0.3) \times 10^{-5}$ [2] and the decay modes $B \to K^*\phi$, averaged over B^+ and B^0 decays with a branching ratio $\mathcal{B}(B \to K^*\phi) = (1.1^{+0.6}_{-0.5} \pm 0.2) \times 10^{-5}$ [2], have also been measured.

- The branching ratios for $B^0 \to K^+\pi^-$ and $B^+ \to \pi^+ K^0$ are in good agreement with the CLEO data. Moreover, being class-IV decays, they show only a small sensitivity on ξ. The estimated branching ratios for $B^+ \to \pi^+\pi^0$ and $B^+ \to K^+\pi^0$ are in agreement with the respective upper bounds. The latter being a class-IV decay is again stable w.r.t. the variation of N_c; the former (a class-III decay) varies by approximately a factor 2.3 as N_c is varied. The branching ratio for the sum $B^+ \to \pi^0 h^+$ is plotted as a function of $\xi = 1/N_c$ in Fig. 1 for the BSW model form factors (dashed-dotted curve) and two different sets, corresponding to the central values of the hybrid Lattice QCD/QCD-SR form factors (dashed curve) and for values which are closer to their theoretical range given in Table 4 (dotted curve). We see that data for this mode is well explained.

- We estimate the branching ratio for $B^0 \to \pi^+\pi^-$ to be around 1×10^{-5} for the central values of the CKM parameters, which could go down to about 5×10^{-6} for $V_{ub}/V_{cb} = 0.06$. The present CLEO upper limit is in comfortable accord with our estimates but we expect that this decay mode should be measured soon. However, the decay $B^0 \to \pi^0\pi^0$ is not expected to go above 10^{-6}, which makes it at least a factor 10 below the present experimental sensitivity.

- We show the dependence of the branching ratios on the input form factors and the parameter $\xi = 1/N_c$ for the decays $B^+ \to K^+\eta'$ and $B^0 \to K^0\eta'$ in Figs. 2 and 3, respectively. As can be seen in these figures, data tends to prefer somewhat larger values for the form factors $F_{1,0}$ than the central values given by the Lattice-QCD/QCD sum rules in Table 4. However, the experimentally preferred values of the form factors all lie within the range allowed by the present theoretical estimates. Likewise, the branching ratio increases as

Table 9: $B \to PV$ Branching Ratios (in units of 10^{-6}) involving $b \to d$ (or $\Delta S = 0$) transitions using the BSW [Lattice QCD/QCD sum rule] form factors, with $k^2 = m_b^2/2$, $\rho = 0.12$, $\eta = 0.34$, and $N_c = 2, 3, \infty$ in the factorization approach. The last column contains upper limits (90% C.L.) from [1]. The upper limit on the branching ratio for $B^+ \to \rho^+\pi^0$ is taken from the PDG tables [19].

Channel	Class	$N_c = 2$	$N_c = 3$	$N_c = \infty$	Exp.
$B^0 \to \rho^-\pi^+$	I	5.7 [6.6]	6.4 [7.3]	7.8 [9.0]	$\} < 88$
$B^0 \to \rho^+\pi^-$	I	21 [25]	23 [28]	28 [34]	
$B^0 \to \rho^0\pi^0$	II	0.75 [0.88]	0.07 [0.08]	1.4 [1.7]	< 18
$B^0 \to \omega\pi^0$	II	0.28 [0.33]	0.08 [0.10]	0.10 [0.12]	< 14
$B^0 \to \rho^0\eta$	II	0.02 [0.03]	0.02 [0.02]	0.06 [0.07]	< 13
$B^0 \to \rho^0\eta'$	II	0.01 [0.01]	0.001 [0.001]	0.03 [0.04]	< 23
$B^0 \to \omega\eta$	II	0.46 [0.54]	0.05 [0.06]	0.63 [0.74]	< 12
$B^0 \to \omega\eta'$	II	0.29 [0.34]	0.02 [0.02]	0.46 [0.54]	< 60
$B^+ \to \rho^0\pi^+$	III	6.3 [7.3]	3.9 [4.5]	0.89 [0.98]	< 58
$B^+ \to \rho^+\pi^0$	III	14 [16]	13 [15]	11 [13]	< 77
$B^+ \to \omega\pi^+$	III	6.8 [7.9]	4.2 [4.9]	1.0 [1.1]	< 23
$B^+ \to \rho^+\eta$	III	6.3 [7.4]	5.5 [6.5]	4.2 [5.0]	< 32
$B^+ \to \rho^+\eta'$	III	4.5 [5.3]	4.0 [4.7]	3.0 [3.7]	< 47
$B^0 \to \bar{K}^{*0}K^0$	IV	0.31 [0.36]	0.38 [0.44]	0.55 [0.64]	–
$B^+ \to \bar{K}^{*0}K^+$	IV	0.32 [0.37]	0.40 [0.46]	0.57 [0.67]	–
$B^+ \to K^{*+}\bar{K}^0$	V	0.001 [0.002]	0.0005 [0.0007]	0.002 [0.002]	–
$B^+ \to \phi\pi^+$	V	0.040 [0.047]	0.005 [0.005]	0.36 [0.43]	< 5.0
$B^0 \to \phi\pi^0$	V	0.019 [0.023]	0.002 [0.003]	0.17 [0.21]	< 5.0
$B^0 \to \phi\eta$	V	0.008 [0.010]	0.0009 [0.001]	0.073 [0.087]	< 9
$B^0 \to \phi\eta'$	V	0.006 [0.007]	0.0007 [0.0008]	0.053 [0.064]	< 3.1
$B^0 \to K^{*0}\bar{K}^0$	V	0.001 [0.002]	0.0004 [0.0006]	0.002 [0.002]	–

the s-quark mass decreases, as already noted in [27,28]. Thus, for m_s (μ = 2.5 GeV) = 100 MeV, and $F_{1,0}^{B\to\eta'} = 0.15$, there is no problem to accommodate the CLEO data within the measured $\pm 1\sigma$ range. As already discussed at length in refs. [27,28], these decay modes are dominated by the QCD penguin, and while the contributions of the anomaly terms are included in the rate estimates, their role numerically is subleading. The decay modes $B^+ \to K^+\eta'$ and $B^0 \to K^0\eta'$ show some preference for smaller values of ξ, though this is correlated with other input parameters and at this stage one can not draw completely quantitative conclusions. Summarizing the $B \to PP$ decays, we stress that the factorization-based estimates described here are consistent with the measured decay modes. All other estimated branching ratios are consistently below their present experimental limits. However, we do expect the modes $B^0 \to \pi^+\pi^-$, $B^+ \to \pi^+\pi^0$, and $B^+ \to K^+\pi^0$ to be measured soon.

- The two observed $B \to PV$ decays, $B^+ \to \omega K^+$ and $B^+ \to \omega h^+$, $h^+ = \pi^+, K^+$, show strong N_c-dependence as anticipated. The decay $B^+ \to \omega\pi^+$, a class-III decay, has not

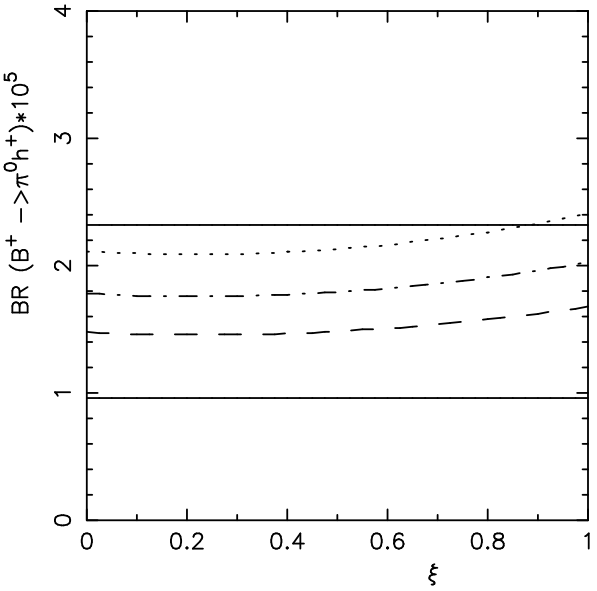

Figure 1: Branching ratio for the decays $B^+ \to \pi^0 h^+$ ($h^+ = \pi^+, K^+$) as a function of ξ for three different sets of form factors: BSW Model (dashed-dotted curve), Lattice-QCD/QCD-sum rules with central values in Table 4 (dashed curve), with the values $F_{0,1}^{B\to\pi} = 0.36$ and $F_{0,1}^{B\to K} = 0.41$ (dotted curve). The horizontal solid lines are the $\pm 1\sigma$ measurements from experiment [1].

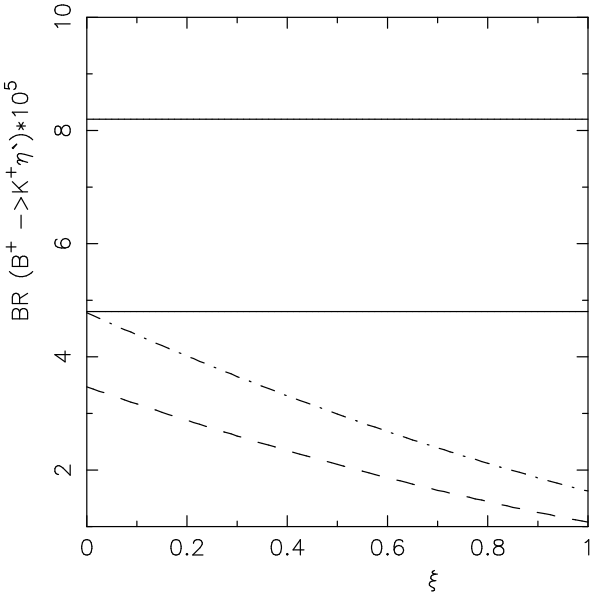

Figure 2: Branching ratio for $B^+ \to K^+\eta'$ as a function of $\xi = 1/N_c$. The dash-dotted and dashed curves correspond to the choice $F_1^{B\to\eta'}(0) = F_0^{B\to\eta'}(0) = 0.15$, $m_s(\mu = 2.5\ \text{GeV}) = 100$ MeV, and $F_1^{B\to\eta'}(0) = F_0^{B\to\eta'}(0) = 0.135$, $m_s(\mu = 2.5\ \text{GeV}) = 122$ MeV, respectively. The horizontal solid lines are the $\pm 1\sigma$ measurements from experiment [1].

Table 10: $B \to PV$ Branching Ratios (in units of 10^{-6}) involving $b \to s$ (or $|\Delta S| = 1$) transitions using the BSW [Lattice QCD/QCD sum rule] form factors, with $k^2 = m_b^2/2$, $\rho = 0.12$, $\eta = 0.34$, and $N_c = 2, 3, \infty$ in the factorization approach. The last column contains the measured branching ratio and upper limits (90% C.L.) [1].

Channel	Class	$N_c = 2$	$N_c = 3$	$N_c = \infty$	Exp.
$B^0 \to \rho^- K^+$	I	0.40 [0.46]	0.45 [0.52]	0.56 [0.64]	< 33
$B^+ \to K^{*+}\eta'$	III	0.28 [0.39]	0.24 [0.29]	0.33 [0.33]	< 130
$B^0 \to K^{*+}\pi^-$	IV	6.0 [7.2]	6.6 [7.8]	7.8 [9.3]	< 67
$B^0 \to K^{*0}\pi^0$	IV	1.8 [2.0]	2.2 [2.5]	3.2 [3.6]	< 20
$B^0 \to \rho^0 K^0$	IV	0.50 [0.58]	0.49 [0.57]	0.62 [0.73]	< 30
$B^+ \to K^{*+}\pi^0$	IV	4.4 [5.4]	4.7 [5.9]	5.6 [6.9]	< 80
$B^+ \to \rho^0 K^+$	IV	0.58[0.67]	0.50[0.58]	0.47[0.55]	< 14
$B^+ \to K^{*+}\eta$	IV	2.2 [2.8]	2.2 [2.7]	2.0 [2.4]	< 30
$B^0 \to K^{*0}\eta$	IV	2.0 [2.5]	2.1 [2.7]	2.6 [3.1]	< 30
$B^+ \to K^{*0}\pi^+$	IV	5.6 [6.7]	6.9 [8.3]	10 [12]	< 39
$B^+ \to \rho^+ K^0$	IV	0.03 [0.03]	0.01 [0.01]	0.01 [0.02]	< 64
$B^0 \to K^{*0}\eta'$	V	0.06 [0.12]	0.07 [0.07]	0.41 [0.39]	< 39
$B^+ \to \phi K^+$	V	16 [18]	8.3 [9.6]	0.45 [0.53]	< 5.0
$B^0 \to \phi K^0$	V	15 [18]	8.0 [9.3]	0.44 [0.51]	< 31
$B^0 \to \omega K^0$	V	2.8 [3.3]	0.02 [0.02]	8.9 [10]	< 57
$B^+ \to \omega K^+$	V	3.2 [3.7]	0.25 [0.28]	11 [13]	$15^{+7}_{-6} \pm 2$

yet been measured and the mode $B^+ \to K^+\omega$ (a class-V decay) has a 3.9σ experimental significance. The branching ratios of $B^+ \to \omega K^+$ and $B^+ \to \omega\pi^+$ are plotted as functions of ξ in Figs. 4 and 5, respectively, showing the variations on other parameters (form factors and CKM matrix elements) as well. Taking the CLEO measurement $\mathcal{B}(B^+ \to \omega K^+) = (1.5^{+0.7}_{-0.6} \pm 0.2) \times 10^{-5}$ on face value, this mode suggests that $\xi \leq 0.1$ or $\xi \geq 0.6$. The present CLEO upper limit $\mathcal{B}(B^+ \to \omega\pi^+) < 2.3 \times 10^{-5}$ is not yet restrictive enough. The branching ratio for the combined decay $B^+ \to \omega h^+ (h^+ = \pi^+, K^+)$ is shown in Fig 6 as a function of ξ for two values of the form factors $F_1^{B\to K}$ and $F_1^{B\to\pi}$ and two sets of values for the CKM parameters ρ and η. The values of these form factors correspond to the BSW model and the upper limit in Table 4 to the Lattice-QCD/QCD sum rule case. Again, one sees that there is a tendency in the data to prefer larger values of the form factors. We note that both small values $\xi \simeq 0$ and $\xi \geq 0.5$ are compatible with data in this decay, with the theoretical branching ratio rising above 1×10^{-5}. The value corresponding to the naive factorization, $N_c = 3$ (or $\xi = 0.33$) is definitely too low compared to the data on the two measured $B \to PV$ decays. This is in line with earlier observations in the literature [27,29,31].

- No other $B \to PV$ decays have been measured yet. However, an interesting upper bound $\mathcal{B}(B^+ \to K^+\phi) < 0.5 \times 10^{-5}$ (at 90% C.L.) has been put by the CLEO collaboration [2]. This and the related decay $B^0 \to K^0\phi$ are both penguin dominated and their decay rates are expected to be almost equal. The only worthwhile CKM-dependence is on the

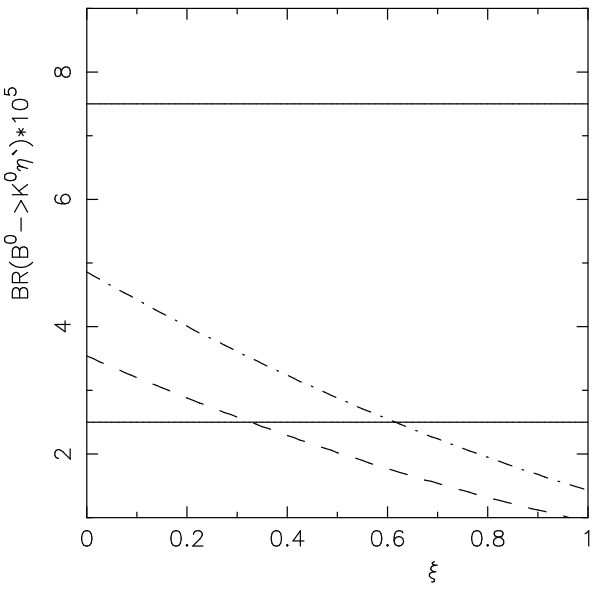

Figure 3: Branching ratio for $B^0 \to K^0\eta'$ as a function of ξ. The legends are the same as in Figure 2.

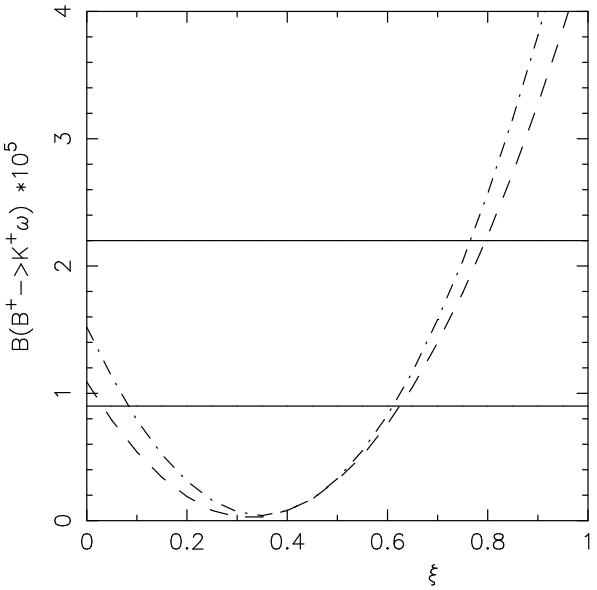

Figure 4: Branching ratio for $B^+ \to K^+\omega$ and as a function of ξ. The legends are as follows: $\rho = 0.30, \eta = 0.42, F_1^{B\to K} = 0.44$ (dashed-dotted curve), $\rho = 0.12, \eta = 0.34, F_1^{B\to K} = 0.38$ (dashed curve). The horizontal solid lines are the $\pm 1\sigma$ measurements from experiment [2].

Table 11: $B \to VV$ Branching Ratios (in units of 10^{-6}) using the BSW [Lattice QCD/QCD sum rule] form factors, with $k^2 = m_b^2/2$, $\rho = 0.12$, $\eta = 0.34$, and $N_c = 2, 3, \infty$ in the factorization approach. The last column contains upper limits (90% C.L.) mostly from [1] except for the branching ratios for $B^0 \to \rho^+\rho^-$, $B^0 \to \rho^0\rho^0$, $B^+ \to \rho^+\rho^0$, $B^0 \to K^{*0}\rho^0$ and $B^+ \to K^{*+}\rho^0$, which are taken from the PDG tables [19].

Channel	Class	$N_c = 2$	$N_c = 3$	$N_c = \infty$	Expt.
$B^0 \to \rho^+\rho^-$	I	18 [20]	20 [22]	24 [27]	< 2200
$B^0 \to \rho^0\rho^0$	II	1.3 [1.3]	0.59 [0.59]	2.5 [2.5]	< 280
$B^0 \to \omega\omega$	II	0.87 [0.96]	0.15 [0.17]	0.86 [0.96]	< 19
$B^+ \to \rho^+\rho^0$	III	14 [15]	11 [12]	6.1 [6.8]	< 1000
$B^+ \to \rho^+\omega$	III	15 [16]	12 [13]	6.6 [7.3]	< 67
$B^0 \to K^{*+}\rho^-$	IV	5.4 [6.0]	5.9 [6.6]	7.0 [7.8]	–
$B^0 \to K^{*0}\rho^0$	IV	1.1 [1.2]	1.3 [1.4]	1.9 [1.9]	< 460
$B^+ \to K^{*+}\rho^0$	IV	5.0 [5.8]	5.5 [6.3]	6.6 [7.6]	< 900
$B^+ \to \rho^+K^{*0}$	IV	5.1 [5.6]	6.3 [6.9]	9.1 [10]	–
$B^+ \to K^{*+}\bar{K}^{*0}$	IV	0.29 [0.38]	0.37 [0.47]	0.53 [0.68]	–
$B^0 \to K^{*0}\bar{K}^{*0}$	IV	0.28 [0.36]	0.35 [0.45]	0.51 [0.65]	–
$B^0 \to \rho^0\omega$	V	0.018 [0.020]	0.005 [0.006]	0.23 [0.26]	< 11
$B^0 \to K^{*0}\omega$	V	10 [12]	3.6 [4.0]	0.63 [1.1]	< 23
$B^+ \to K^{*+}\omega$	V	11 [13]	3.7 [4.1]	1.7 [2.4]	< 87
$B^+ \to K^{*+}\phi$	V	16 [20]	8.2 [10]	0.45 [0.57]	< 41
$B^0 \to K^{*0}\phi$	V	15 [19]	7.9 [10]	0.43 [0.55]	< 21
$B^+ \to \rho^+\phi$	V	0.039 [0.043]	0.004 [0.005]	0.35 [0.38]	< 16
$B^0 \to \rho^0\phi$	V	0.019 [0.021]	0.002 [0.002]	0.17 [0.18]	< 13
$B^0 \to \omega\phi$	V	0.019 [0.020]	0.002 [0.002]	0.17 [0.18]	< 21

Wolfenstein parameter A (hence weak). However, being class-V decays, their branching ratios depend strongly on ξ, with both having their lowest values at $\xi = 0$. The branching ratio $\mathcal{B}(B^+ \to K^+\phi)$ is shown as a function of ξ in Fig. 7 for $A = 0.81$ (dashed curve) and $A = 0.75$ (dashed-dotted curve) and the CLEO 90% C.L. upper bound is also indicated. This shows that values $\xi \geq 0.4$ are disfavored by the present data. In fact, taken the data on their face value the measured branching ratios for the decays $B^+ \to \omega h^+ (h^+ = \pi^+, K^+)$ and $B^+ \to \omega K^+$, as well as the upper bounds on the branching ratios for $B^+ \to K^+\phi$ and $B^+ \to \omega\pi^+$ can be accommodated for a value of ξ, close to $\xi = 0$. All other decay modes in Tables 9 and 10 (for the $B \to PV$ case) are consistent with their respective upper limits. However, we do expect that the decay modes $B^+ \to \rho^+\eta$, $B^+ \to \rho^+\eta'$, $B^0 \to K^{*0}\pi^0$, $B^+ \to K^{*0}\pi^+$ and $B^+ \to \rho^+\omega$ should be observed in the next round of experiments at CLEO and at B factories.

- There is one $B \to VV$ decay mode $B \to \phi K^*$, for which some experimental evidence exists, and an averaged branching ratio $\mathcal{B}(B \to \phi K^*) = (1.1^{+0.6}_{-0.5} \pm 0.2) \times 10^{-5}$ has been posted by the CLEO collaboration [2]. The decay modes $B^+ \to \phi K^{*+}$ and $B^0 \to \phi K^{*0}$ are dominated by penguins and are expected to be almost equal (see Table 11). They also

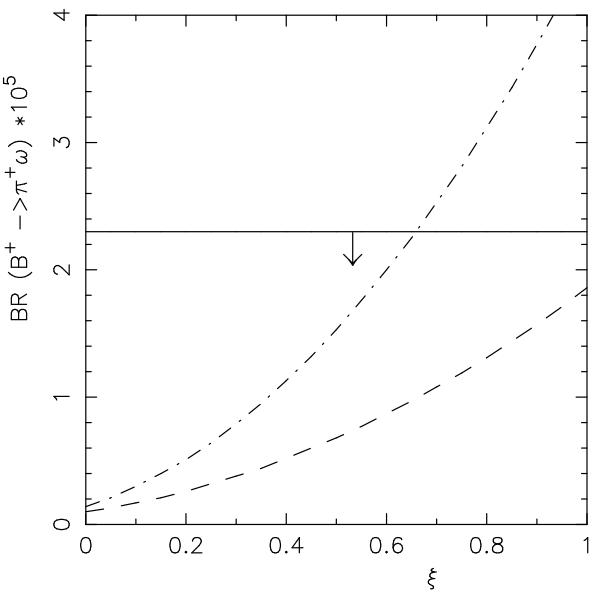

Figure 5: Branching ratio for $B^+ \to \pi^+\omega$ as a function of ξ. The legends are as follows: $\rho = 0.30, \eta = 0.42, F_1^{B\to\pi} = 0.38$ (dashed-dotted curve), $\rho = 0.12, \eta = 0.34, F_1^{B\to K} = 0.34$ (dashed curve). The horizontal solid line is the 90% C.L. upper limit from experiment [2].

belong to class-V decays, showing very strong ξ-dependence (almost a factor 35!), with the branching ratios having their smallest values at $\xi = 0$. A comparison of data and factorization-based estimates is shown in Fig. 8. In this case, data favors $0.4 \leq \xi \leq 0.6$, apparently different from the values of ξ suggested by the $B \to PV$ decays discussed earlier. In fact, the branching ratios of the decays $B^+ \to \phi K^+$, $B^0 \to \phi K^0$, $B^+ \to \phi K^{*+}$ and $B^0 \to \phi K^{*0}$ are almost equal in the factorization approach and they all belong to class-V. Hence, their measurements will be rather crucial in testing this framework.

- Based on the present measurements of the $B \to PV$ and $B \to VV$ decay modes, we summarize that all of them belong to the class-V (and one to class-III) decays, for which the factorization-based estimates show strong sensitivity to ξ. This implies that they are harder to predict. The classification given above, however, does not imply that the class-V decays are necessarily small. In fact for $N_c = 2$, the measured class-IV decays and a number of class-V $B \to PV$ and $B \to VV$ decays such as the ones mentioned above are comparable in rates (within a factor 2). For the class-V decays, the amplitudes can become very small in some range of ξ, implying large non-perturbative renormalizations which are harder to quantify in this framework. Also, many class-V penguin decays may have significant contributions from annihilation and/or FSI, as the factorization-based amplitudes, depending on ξ, may not dominate the decay rates. This is generally not foreseen for the class-I (tree-dominated) and class-IV (penguin-dominated) decays and most of the class-III decays. Hence, these decays can be predicted with greater certainty.

- Concerning comparison of our results with the earlier ones in [27,28], we note that we have made use of the theoretical work presented in these papers. We reproduce all the numerical results for the same values of the input parameters. Our decay amplitudes agree with the ones presented in [31], though our estimates of the matrix elements of pseudoscalar densities $\langle 0|\bar{u}\gamma_5 u|\eta^{(\prime)}\rangle$ and $\langle 0|\bar{d}\gamma_5 d|\eta^{(\prime)}\rangle$ differ from the ones used in [31]. Our

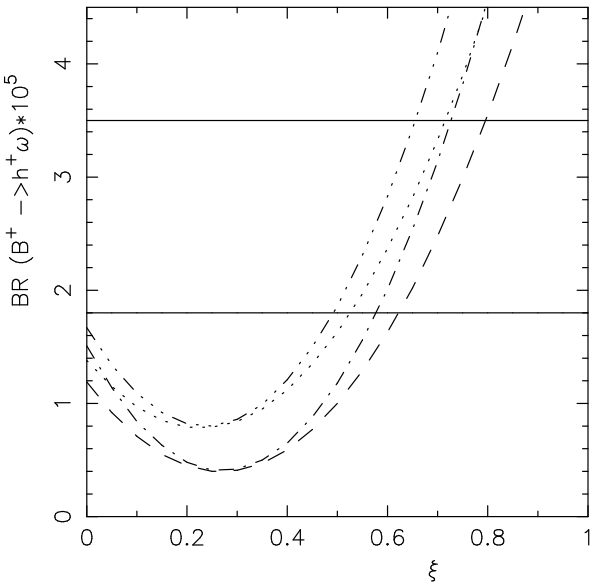

Figure 6: Branching ratio for $B^+ \to h^+\omega$ as a function of ξ. The legends are as follows: $\rho = 0.30, \eta = 0.42, F_1^{B\to\pi} = 0.38, F_1^{B\to K} = 0.44$ (dashed-triple dotted curve), $\rho = 0.30, \eta = 0.42, F_1^{B\to\pi} = 0.33, F_1^{B\to K} = 0.38$ (dotted curve), $\rho = 0.12, \eta = 0.34, F_1^{B\to\pi} = 0.38, F_1^{B\to K} = 0.44$ (dashed-dotted curve), $\rho = 0.12, \eta = 0.34, F_1^{B\to\pi} = 0.33, F_1^{B\to K} = 0.38$ (dashed curve). The horizontal solid lines are the $\pm 1\sigma$ measurements from experiment [1].

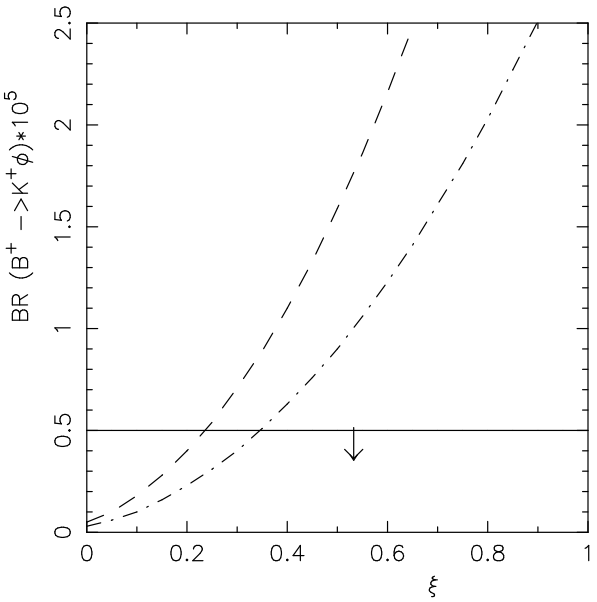

Figure 7: Branching ratio for $B^+ \to K^+\phi$ as a function of ξ. The legends are as follows: Upper curve: Wolfenstein parameter $A = 0.81$, $F_1^{B\to K} = 0.38$. Lower curve: Wolfenstein parameter $A = 0.75$, $F_1^{B\to K} = 0.31$. The horizontal solid line is the 90% C.L. upper limit from experiment [1].

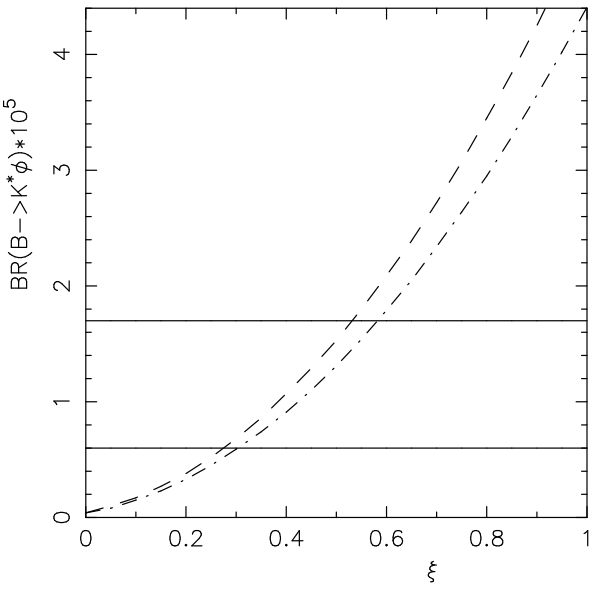

Figure 8: Branching ratio for $B \to K^*\phi$ as a function of ξ, after averaging over the B^+ and B^0 decay rates. The legends are as follows: Upper curve: Wolfenstein parameter $A = 0.81$. Lower curve: Wolfenstein parameter $A = 0.75$. For the form factors, we use the BSW model. The horizontal solid lines represent the CLEO measurement with $\pm 1\sigma$ errors. [1].

expressions are given explicitly in Appendix A. The disagreement in the decay rates for $B^0 \to \rho^0\eta$ and $B^0 \to \rho^0\eta'$ between our results and the ones given in [31] has now been resolved [4]. However, we do not subscribe to the notion that $N_c(V+A)$ induced by the $(V-A)(V+A)$ penguin operators is different from the $N_c(V-A)$ arising from the $(V-A)(V-A)$ operators, advocated in [31] and continue to use the same N_c irrespective of the chiral structure of the four-quark operators. We have discussed at length the difficulties in predicting class-V decays some of which, in our opinion, may require annihilation and/or FSI effects.

Comparison of our numerical results in the branching ratios for the $B \to PV$ modes with the ones presented in [29] requires a more detailed comment. First of all, our input parameters are significantly different from those of [29]. For the same values of input parameters, our results in charged $B^+ \to (PV)^+$ decays are in reasonable accord. However, significant differences exist in the neutral $B^0 \to (PV)^0$ decay rates, which persist also if we adopt the input values used in [29]. In particular, in this case we find for $N_c = \infty$: $\mathcal{B}(B^0 \to \rho^0\eta) = 2.7 \times 10^{-7}$ compared to 6.7×10^{-6} [29], $\mathcal{B}(B^0 \to \rho^0\eta') = 1.2 \times 10^{-7}$ compared to 3.6×10^{-6} [29], $\mathcal{B}(B^0 \to \omega\eta) = 6.9 \times 10^{-7}$ compared to 7.1×10^{-6} [29], and $\mathcal{B}(B^0 \to \omega\eta') = 1.3 \times 10^{-7}$ compared to 3.6×10^{-6} [29]. For our input values, the differences in branching ratios are even more drastic, as can be seen by comparing our results with the ones in [29] for these decays. We have given sufficient details in our paper to enable a comparison of the formulae, including matrix elements of the pseudoscalar densities, and hence it should not be too difficult to figure out the source of the present discrepancy. Such details are not given in [29].

[4] We thank Hai-Yang Cheng for a correspondence on this point.

- Within the present framework, we have calculated the relative importance of electroweak penguins in all the $B \to PP$, $B \to PV$ and $B \to VV$ decays studied in this paper. The decay modes where the electroweak penguins may make a significant contribution are shown in Table 12 where we give the ratio

$$R_{\rm W} \equiv \frac{\mathcal{B}(B \to h_1 h_2)(\text{with } a_7, ..., a_{10} = 0)}{\mathcal{B}(B \to h_1 h_2)} \ . \tag{42}$$

In the $B \to PP$ case, there are five such decays whose rates show moderate dependence on the electroweak penguins. The decay $B^0 \to \pi^0\pi^0$ receives significant electroweak penguin contribution for $N_c = 3$. In the class-IV $B \to PP$ decays, three decays, namely $B^0 \to K^0\pi^0$, $B^0 \to K^0\eta$ and $B^+ \to K^+\eta$ (all having branching ratios in excess of 10^{-6}) have significant electroweak contributions. The presence of electroweak penguins in these decays reduces the decay rate by about $\sim 20\%$ to $\sim 40\%$.

In the $B \to PV$ decays, the three class-II decays which may have significant electroweak penguin amplitudes are $B^0 \to \rho^0\pi^0$ and $B^0 \to \rho^0\eta^{(\prime)}$. Most striking among the class-IV decays is $B^0 \to \rho^0 K^0$, which is completely dominated by the electroweak penguins for all values of N_c. This decay is estimated to have a branching ratio of $O(10^{-6})$. Measurement of this decay mode will enable us to determine the largest electroweak-penguin coefficient a_9. In the $B \to VV$ decays, the class-II decay $B^0 \to \rho^0\rho^0$ is sensitive to the electroweak penguins. Likewise, the two class-IV decays, $B^0 \to \rho^0 K^{*0}$ and $B^+ \to \rho^0 K^{*+}$ are sensitive to electroweak penguins. All of them are expected to have branching ratios of $O(10^{-6})$ or larger, and can in principle all be used to determine the coefficients of the electroweak penguins. Once again, a large number of class-V decays show extreme sensitivity to the electroweak penguins, as can be seen in Table 12.

7 Stringent tests of the factorization approach and determination of form factors

In the preceding section, we have compared available data with estimates based on the factorization approach and have already commented on the tendency of data to favor somewhat higher values of the form factors $F_{0,1}^{B\to P}$, than, for example, the central values given in Table 4. However, as the decay rates depend on a number of parameters and the various parametric dependences are correlated, it is worthwhile, in our opinion, to measure some ratios of branching ratios in which many of the parameters endemic to the factorization framework cancel. In line with this, we propose three different types of ratios which can be helpful in a quantitative test of the present framework:

- Ratios which do not depend on the effective coefficients a_i, and which will allow to determine the form factors more precisely in the factorization framework.

- Ratios which depend on the parameters a_i, and whose measurements will determine these effective coefficients.

- Ratios whose measurements will impact on the CKM phenomenology, i.e., they will help determine the CKM parameters ρ and η (equivalently $\sin\alpha$, $\sin\beta$ and $\sin\gamma$).

Table 12: Ratios of branching ratios $R_{\rm W}$ defined in eq. (42) for $N_c = 2, 3, \infty$ for the form factors in the BSW model [Lattice-QCD/QCD sum rule method]. The horizontal lines demarcate the decays $B \to PP$, $B \to PV$ and $B \to VV$.

Channel	Class	$N_c = 2$	$N_c = 3$	$N_c = \infty$
$B^0 \to \pi^0\pi^0$	II	1.2 [1.2]	1.5 [1.5]	1.1 [1.1]
$B^0 \to \pi^0\eta'$	II	1.3 [1.3]	1.3 [1.3]	1.4 [1.4]
$B^0 \to K^0\pi^0$	IV	1.5 [1.4]	1.4 [1.4]	1.3 [1.3]
$B^0 \to K^0\eta$	IV	1.5 [1.5]	1.5 [1.5]	1.4 [1.4]
$B^+ \to K^+\eta$	IV	1.6 [1.6]	1.5 [1.5]	1.3 [1.3]
$B^0 \to \rho^0\pi^0$	II	1.0 [1.0]	1.9 [1.9]	1.1 [1.1]
$B^0 \to \rho^0\eta$	II	1.4 [1.4]	1.5 [1.5]	1.1 [1.1]
$B^0 \to \rho^0\eta'$	II	1.1 [1.2]	4.7 [4.9]	1.3 [1.2]
$B^0 \to K^{*0}\pi^0$	IV	1.7 [1.8]	1.6 [1.7]	1.4 [1.5]
$B^0 \to \rho^0 K^0$	IV	0.077 [0.077]	0.008 [0.008]	0.11 [0.11]
$B^0 \to K^{*0}\eta$	IV	0.69 [0.66]	0.70 [0.67]	0.71 [0.69]
$B^+ \to K^{*+}\pi^0$	IV	0.63 [0.61]	0.68 [0.66]	0.78 [0.75]
$B^+ \to \rho^0 K^+$	IV	0.83 [0.83]	0.59 [0.59]	0.13 [0.13]
$B^+ \to K^{*+}\eta$	IV	0.60 [0.58]	0.66 [0.63]	0.78 [0.76]
$B^+ \to \rho^+ K^0$	IV	0.45 [0.45]	0.60 [0.60]	0.66 [0.66]
$B^0 \to K^{*0}\eta'$	V	0.97 [0.54]	1.8 [1.6]	1.1 [1.2]
$B^0 \to \omega K^0$	V	0.83 [0.83]	0.42 [0.42]	1.2 [1.2]
$B^0 \to \phi\pi^0$	V	1.7 [1.7]	0.002 [0.002]	0.78 [0.78]
$B^0 \to \phi\eta$	V	1.7 [1.7]	0.002 [0.002]	0.78 [0.78]
$B^0 \to \phi\eta'$	V	1.7 [1.7]	0.002 [0.002]	0.78 [0.78]
$B^0 \to \phi K^0$	V	1.2 [1.2]	1.3 [1.3]	2.1 [2.1]
$B^0 \to K^{*0}\bar{K}^0$	V	0.46 [0.46]	0.84 [0.84]	0.73 [0.73]
$B^+ \to K^{*+}\bar{K}^0$	V	0.46 [0.46]	0.84 [0.84]	0.73 [0.73]
$B^+ \to \phi\pi^+$	V	1.7 [1.7]	0.002 [0.002]	0.78 [0.78]
$B^+ \to \phi K^+$	V	1.2 [1.2]	1.3 [1.3]	2.1 [2.1]
$B^0 \to \rho^0\rho^0$	II	0.58 [0.58]	0.31 [0.31]	1.0 [1.0]
$B^0 \to \rho^0 K^{*0}$	IV	2.5 [2.7]	2.4 [2.6]	2.1 [2.2]
$B^+ \to \rho^0 K^{*+}$	IV	0.54 [0.52]	0.61 [0.58]	0.74 [0.72]
$B^0 \to \rho^0\omega$	V	1.9 [1.9]	0.08 [0.08]	0.77 [0.77]
$B^0 \to \rho\phi$	V	1.7 [1.7]	0.002 [0.002]	0.78 [0.78]
$B^0 \to \omega\phi$	V	1.7 [1.7]	0.002 [0.002]	0.78 [0.78]
$B^0 \to K^{*0}\omega$	V	0.93 [0.92]	0.84 [0.82]	1.7 [1.6]
$B^0 \to K^{*0}\phi$	V	1.2 [1.2]	1.3 [1.3]	2.1 [2.1]
$B^+ \to \rho^+\phi$	V	1.7 [1.7]	0.002 [0.002]	0.78 [0.78]
$B^+ \to K^{*+}\phi$	V	1.2 [1.2]	1.3 [1.3]	2.1 [2.1]

7.1 Ratios of branching ratios independent of the coefficients a_i

We start with the ratios of branching ratios in which the effective coefficients $a_1, ..., a_{10}$ cancel. In the present approach, these ratios depend on the form factors and hadronic coupling constants. Their measurements will allow us to discriminate among models, determine some of the hadronic quantities and improve the quality of theoretical predictions for a large number of other decays where these hadronic quantities enter.

In what follows, we shall illustrate this by giving complete expressions for the relative decay widths of the decay modes in question. These expressions can be derived in a straightforward way from the matrix elements given in the Appendices. Then, we shall present simple formulae, which are approximate but instructive, and highlight the particular form factors which play dominant roles in these decays. Finally, we shall compare the numerical results for these ratios obtained from the complete expressions, which have been used in calculating the entries in Tables 8 - 11, and the corresponding ones obtained from the simple formulae to judge the quality of the approximation in each case. As practically an almost endless number of ratios can be formed from the seventy six branching ratios given in Tables 8 - 11, some thought has gone into selecting the eleven ratios which we discuss below. Our criterion is based on the theoretical simplicity and experimental feasibility of these ratios. To be specific, these ratios involve those decays whose branching ratios are expected to be $O(10^{-6})$ or higher, with the ratios of branching ratios of order one so that a reasonable experimental accuracy could be achieved, and whose decay widths are dominated by a single form factor.

We start with the discussion of decay modes involving the final states $\pi\pi$, $\rho\pi$ and $\rho\rho$. These ratios are listed below:

$$\begin{aligned} P_1 &\equiv \frac{\mathcal{B}(B^0 \to \rho^+\pi^-)}{\mathcal{B}(B^0 \to \rho^+\rho^-)} \\ &= \frac{x^2 f(\pi,\rho)^3 |F_1^{B\to\pi}(m_\rho^2)|^2}{f(\rho,\rho)^3 \left[\frac{1}{4}(\frac{3x^4}{f(\rho,\rho)^2}+1)(1+x)^2 A_1^2 + \frac{f(\rho,\rho)^2 A_2^2}{(1+x)^2} + \frac{2x^4 V^2}{(1+x)^2} - (\frac{1}{2}-x^2)A_1 A_2\right]}, \end{aligned} \tag{43}$$

where $x = m_\rho/m_B$. The form factors A_1, A_2 and V involve the $B \to \rho$ transition. The function $f(a,b)$ is the momentum fraction carried by the final particles, $f(a,b) < 1/2$.

$$f(a,b) = \frac{\sqrt{(m_B^2 - m_a^2 - m_b^2)^2 - 4m_a^2 m_b^2}}{2m_B^2}.$$

Since $f(\pi,\rho) \simeq f(\rho,\rho) \simeq 1/2 - x^2$, and in almost all models one expects $A_1 \simeq A_2$, the expression given in eq. (43) gets considerably simplified. Neglecting the terms proportional to x^4 in the denominator, one has:

$$P_1 \simeq \frac{|F_1^{B\to\pi}(m_\rho^2)|^2}{(1+x)|A_1^{B\to\rho}(m_\rho^2)|^2}\ , \tag{44}$$

which is essentially determined by the ratios of the form factors $F_1^{B\to\pi}$ and $A_1^{B\to\rho}$. We show the values of the ratio P_1 in Table 13 for the BSW model and the lattice-QCD/QCD sum rules method for both the full widths and following from the approximate relation given in eq. (44).

Table 13: Values of P_i's calculated with the form factors from the BSW model and the hybrid lattice-QCD/QCD-sum rule method. The numbers in square brackets are calculated using the approximate formulae derived in the text.

Ratio	BSW model	Lattice-QCD/QCD-Sum rules
P_1	1.19 [1.21]	1.27 [1.55]
P_2	0.43 [0.39]	0.43 [0.39]
P_3	0.28 [0.28]	0.27 [0.27]
P_4	0.49 [0.47]	0.53 [0.61]
P_5	0.52 [0.47]	0.55 [0.61]
P_6	1.11 [1.21]	1.19 [1.55]
P_7	1.11 [1.21]	1.19 [1.55]
P_8	1.08 [1.14]	0.99 [1.18]
P_9	1.09 [1.14]	0.99 [1.18]
P_{10}	1.01 [1.15]	0.92 [1.19]
P_{11}	1.01 [1.15]	0.92 [1.19]

There are various other relations of a similar kind. For example, neglecting the small QCD penguin contribution and the very small difference in phase space, we get the relations:

$$P_2 \equiv \frac{\mathcal{B}(B^0 \to \pi^- \pi^+)}{\mathcal{B}(B^0 \to \rho^+ \pi^-)} \simeq \left(\frac{f_\pi F_0^{B\to\pi}(m_\pi^2)}{f_\rho F_1^{B\to\pi}(m_\rho^2)} \right)^2 , \tag{45}$$

$$P_3 \equiv \frac{\mathcal{B}(B^0 \to \pi^+ \rho^-)}{\mathcal{B}(B^0 \to \rho^+ \pi^-)} \simeq \left(\frac{f_\pi A_0^{B\to\rho}(m_\pi^2)}{f_\rho F_1^{B\to\pi}(m_\rho^2)} \right)^2 . \tag{46}$$

As can be seen in Table 13, both eqs. (45) and (46) are excellent approximations and, for the two models in question, we get an almost form-factor independent prediction, namely $P_2 \simeq 0.4$ and $P_3 \simeq 0.28$. It must be remarked here that one must disentangle B^0 decays from the $\overline{B^0}$ decays as both P_2 and P_3 are defined for the decays of B^0.

In the same vein, we define the ratios P_4 and P_5 involving the $\pi\pi$ and $\rho\rho$ modes:

$$P_4 \equiv \frac{\mathcal{B}(B^+ \to \pi^+ \pi^0)}{\mathcal{B}(B^+ \to \rho^+ \rho^0)}, \tag{47}$$

$$P_5 \equiv \frac{\mathcal{B}(B^0 \to \pi^- \pi^+)}{\mathcal{B}(B^0 \to \rho^- \rho^+)}. \tag{48}$$

Neglecting the QCD penguin contribution in P_4 and the EW penguin in P_5, which are excellent approximations (see Table 13), we can obtain these ratios as:

$$P_4 \simeq P_5 \simeq \left(\frac{f_\pi}{f_\rho} \right)^2 \frac{x^2(1 - m_\pi^2/m_B^2) f(\pi,\pi) |F_0^{B\to\pi}(m_\pi^2)|^2}{f(\rho,\rho)^3 \left[\frac{1}{4}(\frac{3x^4}{f(\rho,\rho)^2} + 1)(1+x)^2 A_1^2 + \frac{f(\rho,\rho)^2 A_2^2}{(1+x)^2} + \frac{2x^4 V^2}{(1+x)^2} - \frac{1}{2}(1-2x^2) A_1 A_2 \right]}. \tag{49}$$

Neglecting higher order terms in x, we get:

$$P_4 \simeq P_5 \simeq \left(\frac{f_\pi}{f_\rho}\right)^2 \frac{|F_1^{B\to\pi}(m_\pi^2)|^2}{(1+x)|A_1^{B\to\rho}(m_\rho^2)|^2}, \tag{50}$$

very similar to the relation for P_1, except for the ratio of the decay constants.

The next ratios are defined for the final states involving $K^*\pi$ and $K^*\rho$.

$$\begin{aligned} P_6 &\equiv \frac{\mathcal{B}(B^0 \to K^{*+}\pi^-)}{\mathcal{B}(B^0 \to K^{*+}\rho^-)} , \\ P_7 &\equiv \frac{\mathcal{B}(B^+ \to \pi^+ K^{*0})}{\mathcal{B}(B^+ \to \rho^+ K^{*0})} . \end{aligned} \tag{51}$$

One can express these ratios as:

$$\begin{aligned} P_6 &= P_7 \qquad (52) \\ &= \frac{x^2 f(\pi,K^*)^3 |F_1^{B\to\pi}(m_{K^*}^2)|^2}{f(\rho,K^*)^3\left[\frac{1}{4}(\frac{3x^2y^2}{f(\rho,K^*)^2}+1)(1+x)^2A_1^2 + \frac{f(\rho,K^*)^2A_2^2}{(1+x)^2} + \frac{2x^2y^2V^2}{(1+x)^2} - \frac{1}{2}(1-x^2-y^2)A_1A_2\right]}, \end{aligned}$$

where $y = m_{K^*}/m_B$, and we have neglected the small phase space difference. Similar to the expression for P_1, we can derive a simple formula by dropping higher powers in x

$$P_6 = P_7 \simeq \frac{|F_1^{B\to\pi}(m_{K^*}^2)|^2}{(1+x)|A_1^{B\to\rho}(m_{K^*}^2)|^2}. \tag{53}$$

Again, neglecting the small phase space factor and the extrapolations of the form factors between $q^2 = m_\rho^2$ and $q^2 = m_{K^*}^2$, the near equality $P_1 \simeq P_6 \simeq P_7$ holds in the factorization assumption.

The next ratios, called P_8 and P_9, involve the final states $K\bar{K}^*$ and $K^*\bar{K}^*$, respectively. Defining

$$\begin{aligned} P_8 &\equiv \frac{\mathcal{B}(B^+ \to K^+ \bar{K}^{*0})}{\mathcal{B}(B^+ \to K^{*+} \bar{K}^{*0})} , \\ P_9 &\equiv \frac{\mathcal{B}(B^0 \to K^0 \bar{K}^{*0})}{\mathcal{B}(B^0 \to K^{*0} \bar{K}^{*0})} , \end{aligned} \tag{54}$$

we now have

$$P_8 \simeq P_9 = \frac{y^2|F_1^{B\to K}(m_{K^*}^2)|^2 |f(K,K^*)/f(K^*,K^*)|^3}{\frac{1}{4}(\frac{3y^4}{f(K^*,K^*)^2}+1)(1+y)^2|A_1^{K^*}|^2 + \frac{f(K^*,K^*)^2|A_2^{K^*}|^2}{(1+y)^2} + \frac{2y^4|V^{K^*}|^2}{(1+y)^2} - \frac{1}{2}(1-2y^2)A_1^{K^*}A_2^{K^*}} . \tag{55}$$

The form factors $A_1^{K^*}$, $A_2^{K^*}$, V^{K^*} are abbreviations for $A_1^{B\to K^*}$ etc., and again small phase space differences have been neglected. Expanding in y and dropping higher order terms, we get:

$$P_8 \simeq P_9 \simeq \frac{|F_1^{B\to K}(m_{K^*}^2)|^2}{(1+y)|A_1^{B\to K^*}(m_{K^*}^2)|^2}, \tag{56}$$

which involves ratios of the form factors $F_1^{B\to K}$ and $A_1^{B\to K^*}$.

Finally, in this series we define the ratio P_{10} and P_{11} involving the states $K\phi$ and $K^*\phi$, respectively:

$$\begin{aligned} P_{10} &\equiv \frac{\mathcal{B}(B^+\to K^+\phi)}{\mathcal{B}(B^+\to K^{*+}\phi)}\ , \\ P_{11} &\equiv \frac{\mathcal{B}(B^0\to K^0\phi)}{\mathcal{B}(B^0\to K^{*0}\phi)}\ . \end{aligned} \tag{57}$$

Ignoring the small phase space difference, we get

$$P_{10}\simeq P_{11}=\frac{y^2|F_1^{B\to K}(m_\phi^2)|^2|f(K,\phi)/f(K^*,\phi)|^3}{\frac{1}{4}(\frac{3y^2z^2}{f(K^*,\phi)^2}+1)(1+y)^2|A_1^{K^*}|^2+\frac{f(K^*,\phi)^2|A_2^{K^*}|^2}{(1+y)^2}+\frac{2y^2z^2|V^{K^*}|^2}{(1+y)^2}-\frac{1}{2}(1-y^2-z^2)A_1^{K^*}A_2^{K^*}}, \tag{58}$$

where $z=m_\phi/m_B$. Expanding in y and z and again neglecting higher order terms in y and z, we get:

$$P_{10}\simeq P_{11}\simeq\frac{|F_1^{B\to K}(m_\phi^2)|^2}{(1+y)|A_1^{B\to K^*}(m_\phi^2)|^2}\ . \tag{59}$$

So, in the factorization approximation and ignoring the small extrapolation between $q^2=m_{K^*}^2$ and $q^2=m_\phi^2$, in the form factors, we have the near equality $P_8\simeq P_9\simeq P_{10}\simeq P_{11}$. These ratios are all proportional to the ratios of the form factors $F_1^{B\to K}$ and $A_1^{B\to K^*}$.

The ratios $P_1,...,P_{11}$ involve decays in which at least one of the 0^- mesons is replaced by the corresponding vector 1^- particle. If these particles in the decay $B\to h_1h_2$ were heavy, such as D, D^*, D_s, D_s^*, one could use the large energy $(1/E)$ expansion to derive the ratios P_i. We have not investigated this point and hence can not claim that these ratios are at the same theoretical footing as the corresponding relations involving the decays $B\to D(D^*)\pi(\rho)$, studied, for example, in [18]. However, as the energy released in $B\to h_1h_2$ decays is large, and no fine tuning among the various amplitudes is involved, which is the case in class-V decays, we think that the above relations are likely to hold. The ratios of branching ratios are also independent of the CKM matrix elements, therefore they constitute good test of the factorization hypotheses. In Table 13, we have presented the numerical values of the ratios P_i, $i=1,...,11$. This table shows that almost all the ratios are remarkably close for the two models used for the form factors. This, however, reflects our choice of the specific values of the form factors, which is influenced by the present CLEO data. In general, the ratios P_i are measures of the ratios of the form factors, which could vary quite significantly from model to model, and hence they can be used to distinguish between them. It can also be seen that in most cases, the simple formulae are good approximations and would enable us to draw quantitative conclusions about the ratios of dominant form factors in these decays.

7.2 Determination of the effective coefficients a_i

In this section, we aim at measuring the effective coefficients a_i of the factorization framework. To that end, we shall study some ratios of branching ratios which are largely free of hadronic form factors and decay constants. In general, these ratios depend on the effective coefficients a_i

and the CKM parameters in a rather entangled fashion. To disentangle this and gain some insight, we will have to make approximations, whose accuracy, however, we specify quantitatively within the present framework.

7.2.1 Determination of the tree coefficients a_1 and a_2

We start with a discussion of the decays $B^0 \to \pi^+\pi^-$ and $B^+ \to \pi^+\pi^0$, which are on the verge of measurements [1]. Neglecting the electroweak contributions, which we have checked is a very good approximation in these decays, we can derive from eqs. (78) and (80) the following relation:

$$S_1 \equiv \frac{\mathcal{B}(B^0 \to \pi^+\pi^-)}{2\mathcal{B}(B^+ \to \pi^+\pi^0)} \simeq \frac{\tau_{B^0}}{\tau_{B^+}} \left[\left(\frac{a_1}{a_1 + a_2} \right)^2 - 2 \frac{a_1}{a_1 + a_2} z_1 \cos\alpha \cos\delta_1 + z_1^2 \right], \tag{60}$$

where

$$z_1 = \left| \frac{V_{tb} V_{td}^*}{V_{ub} V_{ud}^*} \right| \left| \frac{a_4 + a_6 R_1}{a_1 + a_2} \right| .$$

Here, the quantities τ_{B^0} and τ_{B^+} are the lifetimes of the B^0 and B^+ mesons, which, within present experimental accuracy, are equal to each other. The implicit dependence on the CKM matrix elements in the quantity $a_4 + a_6 R_1$ is not very marked (see section 2). The explicit CKM factor is bounded from the unitarity fits in the range (at 95% C.L.): $1.4 < |V_{tb}V_{td}^*|/|V_{ub}V_{ud}^*| < 4.6$. Varying then N_c from $N_c = 2$ to $N_c = \infty$, we get $0.08 < z_1 < 0.50$. This would suggest that one might be able to determine the quantity $\cos\alpha$ from this ratio. However, the value of z_1 is strongly correlated with that of the product $y_1 \equiv \cos\delta_1 \cos\alpha$, as shown in Fig. 9 where the dependence of this product is shown as a function of z_1, indicating the allowed range of z_1 for assumed values of the ratio S_1. As a result of this correlation, which is specific to the factorization approach, the ratio $z_1 \cos\delta_1 \cos\alpha$ remains small in the entire allowed parameter space. The quantity $z_1 \cos\delta_1 \cos\alpha$ is bounded from above to lie below 0.16, which corresponds to using $N_c = 2$ and $|V_{ub}/V_{cb}| = 0.06$. This is then bad news for determining the quantity $\cos\alpha$ from the ratio S_1 but good news as far as the determination of the effective coefficients $a_1/(a_1 + a_2)$ from S_1 is concerned. Taking this as a generic case for other decays of interest, our best bet in the determination of the effective coefficients is to find ratios of branching ratios in which the quantity $z_i \cos\delta_i \cos\phi_i$ (here $\phi_i = \alpha, \beta$ or γ) as well as z_i^2 are both small. Within the factorization framework, and using the present constraints on the CKM parameters, this can be systematically studied. With this in mind, we shall present a number of approximate formulae for the ratios S_i, which are expected to hold in the limit: $z_i \cos\delta_i \cos\phi_i \ll 1$ and $z_i^2 \ll 1$. To quantify the quality of our approximation, we shall make detailed numerical comparisons between the numerical results for S_i, obtained with the complete expressions for the respective decay widths, and the ones following from our approximate formulae.

There are some ratios of branching ratios in which, within our theoretical framework, the factors $z_i \cos\delta_i \cos\phi_i$ are large, or else the CKM dependence of the ratios factorizes in a simple way. We shall use these ratios to determine the CKM parameters in non-leptonic two-body decays $B \to h_1 h_2$. This kind of analysis has already been suggested in the literature [45,27,50]. We add a number of interesting decay modes to the cases already studied in the literature and make quantitative predictions for them in the present model.

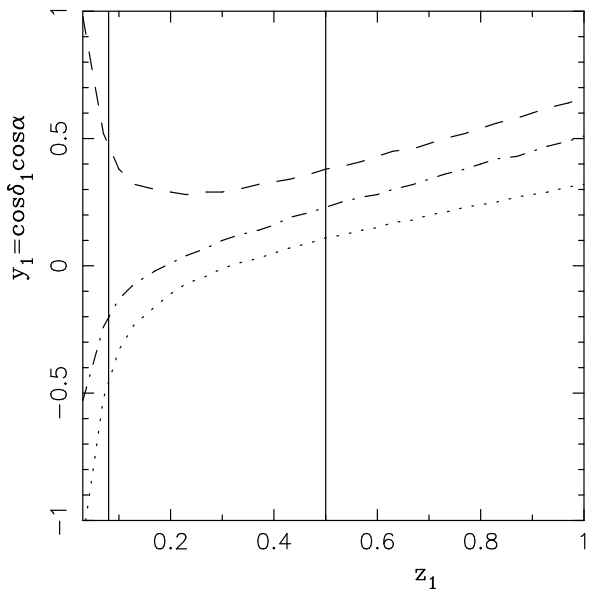

Figure 9: $y_1 = \cos\delta_1 \cos\alpha$ as a function of z_1 in the factorization approach. The dotted, dashed-dotted and dashed curves correspond to $N_c = \infty$ and $|V_{ub}/V_{cb}| = 0.11$, $N_c = 3$ and $|V_{ub}/V_{cb}| = 0.08$ and $N_c = 2$ and $|V_{ub}/V_{cb}| = 0.06$, yielding in the BSW model the values $S_1 = 2.07$, $S_1 = 0.94$ and $S_1 = 0.59$, respectively. The two vertical lines indicate the bounds on z_1 from our model and the CKM unitarity fits $0.08 < z_1 < 0.50$.

Returning to the determination of the coefficients a_i, we note that a ratio similar to S_1 can be defined with the $\rho\rho$ final states:

$$S_2 \equiv \frac{\mathcal{B}(B^0 \to \rho^+\rho^-)}{2\mathcal{B}(B^+ \to \rho^+\rho^0)} \simeq \frac{\tau_{B^0}}{\tau_{B^+}} \left[\left(\frac{a_1}{a_1 + a_2} \right)^2 - 2\frac{a_1}{a_1 + a_2} z_2 \cos\alpha \cos\delta_2 + z_2^2 \right], \tag{61}$$

where

$$z_2 = \left| \frac{V_{tb}V_{td}^*}{V_{ub}V_{ud}^*} \right| \left| \frac{a_4}{a_1 + a_2} \right| .$$

This is not expected to exceed its maximum value $z_2^{max} = 0.26$, the central value being around $z_2 \simeq 0.08$. Hence, one could use an approximate formulae for S_1 and S_2 by keeping the dominant term arising from the tree contributions (setting $\tau_{B^0} = \tau_{B^+}$):

$$S_1 \equiv \frac{\mathcal{B}(B^0 \to \pi^+\pi^-)}{2\mathcal{B}(B^+ \to \pi^+\pi^0)} \simeq \left(\frac{a_1}{a_1 + a_2} \right)^2 , \tag{62}$$

$$S_2 \equiv \frac{\mathcal{B}(B^0 \to \rho^+\rho^-)}{2\mathcal{B}(B^+ \to \rho^+\rho^0)} \simeq \left(\frac{a_1}{a_1 + a_2} \right)^2 . \tag{63}$$

Likewise, neglecting the penguin contributions, which give only several percent uncertainties, the value a_2/a_1 can also be measured from the following ratios,

$$S_3 \equiv \frac{2\mathcal{B}(B^+ \to \rho^+\pi^0)}{\mathcal{B}(B^0 \to \rho^+\pi^-)} \simeq \left(1 + \frac{1}{x}\frac{a_2}{a_1} \right)^2 , \tag{64}$$

$$S_4 \equiv \frac{2\mathcal{B}(B^+ \to \pi^+\rho^0)}{\mathcal{B}(B^0 \to \pi^+\rho^-)} \simeq \left(1 + x\frac{a_2}{a_1} \right)^2 , \tag{65}$$

where the quantity $x = (f_\rho F_1^{B\to\pi})/(f_\pi A_0^{B\to\rho})$ can be measured by measuring the ratio P_3.

Table 14: The ratios S_i calculated using the indicated values of N_c and different values of ρ and η. The values are calculated using the approximate formula (Approx.) derived in the text also.

	N_c	$N_c = 2$			$N_c = 3$			$N_c = \infty$		
	$\lvert V_{ub}/V_{cb}\rvert$	0.06	0.08	0.11	0.06	0.08	0.11	0.06	0.08	0.11
S_1	Exact	0.59	0.66	0.68	0.83	0.94	0.95	1.81	2.03	2.07
	Approx.	0.64	0.64	0.64	0.91	0.91	0.91	1.97	1.97	1.97
S_2	Exact	0.60	0.64	0.65	0.85	0.90	0.91	1.84	1.95	1.98
	Approx.	0.64	0.64	0.64	0.91	0.91	0.91	1.97	1.97	1.97
S_3	Exact	1.33	1.32	1.32	1.09	1.09	1.09	0.74	0.75	0.75
	Approx.	1.29	1.29	1.29	1.06	1.06	1.06	0.71	0.71	0.71
S_4	Exact	2.41	2.20	2.13	1.40	1.23	1.17	0.32	0.23	0.19
	Approx.	2.13	2.13	2.13	1.20	1.20	1.20	0.22	0.22	0.22
S_5	Exact	0.55	0.97	1.96	0.37	0.66	1.33	0.16	0.28	0.56
	Approx.	0.55	0.95	1.89	0.38	0.66	1.31	0.17	0.29	0.58
S_6	Exact	3.07	5.46	11.01	1.95	3.47	7.00	0.75	1.34	2.71
	Approx.	3.10	5.30	10.56	2.06	3.53	7.03	0.86	1.46	2.92
S_7	Exact	1.97	3.73	7.62	1.77	3.35	6.84	1.49	2.82	5.76
	Approx.	1.99	3.40	6.78	1.87	3.19	6.36	1.68	2.88	5.74
S_8	Exact	1.84	3.47	7.10	1.65	3.12	6.37	1.39	2.62	5.36
	Approx.	1.99	3.40	6.78	1.87	3.19	6.36	1.68	2.88	5.74
S_9	Exact	0.32	0.65	1.33	0.31	0.62	1.27	0.28	0.57	1.17
	Approx.	0.36	0.61	1.22	0.35	0.59	1.18	0.33	0.57	1.13
S_{10}	Exact	0.22	0.18	0.13	0.15	0.14	0.13	0.09	0.12	0.18
	Approx.	0.14	0.14	0.14	0.13	0.13	0.13	0.11	0.11	0.11
S_{11}	Exact	0.37	0.17	0.06	0.28	0.15	0.07	0.20	0.16	0.12
	Approx.	0.26	0.15	0.07	0.25	0.14	0.07	0.23	0.13	0.07

7.2.2 Determining the penguin coefficients

Concerning the coefficients $a_3, ..., a_6$, we recall that the dominant QCD penguin amplitudes are proportional to a_4 and a_6. The others (a_3 and a_5) enter either as small corrections in class-IV decays, or else enter in class-V decays, which in most cases are highly unstable due to large cancellations in the respective amplitudes, hence rendering this exercise not very trustworthy for determining the smaller coefficients. In view of this we concentrate on relations involving the QCD-penguin coefficients a_4 and a_6. For this purpose, quite a few class-IV decays listed in Tables 8 - 11 suggest themselves. Here, we take the ratios between some of the representative decays from this class and from class-I or class-III decays. These ratios and their approximate dependence on the coefficients of interest are as follows:

$$S_5 \equiv \frac{2\mathcal{B}(B^+ \to \pi^+\pi^0)}{\mathcal{B}(B^+ \to \pi^+ K^0)} \simeq \left(\frac{f_\pi}{f_K}\right)^2 \left|\frac{V_{ub}V_{ud}^*}{V_{tb}V_{ts}^*}\right|^2 \left|\frac{a_1 + a_2}{a_4 + a_6 R_5}\right|^2 , \tag{66}$$

$$S_6 \equiv \frac{2\mathcal{B}(B^+ \to \rho^+\rho^0)}{\mathcal{B}(B^+ \to \rho^+ K^{*0})} \simeq \left(\frac{f_\rho}{f_{K^*}}\right)^2 \left|\frac{V_{ub}V_{ud}^*}{V_{tb}V_{ts}^*}\right|^2 \left|\frac{a_1+a_2}{a_4}\right|^2 \ , \tag{67}$$

$$S_7 \equiv \frac{\mathcal{B}(B^0 \to \pi^-\rho^+)}{\mathcal{B}(B^+ \to \pi^+ K^{*0})} \simeq \left(\frac{f_\rho}{f_{K^*}}\right)^2 \left|\frac{V_{ub}V_{ud}^*}{V_{tb}V_{ts}^*}\right|^2 \left|\frac{a_1}{a_4}\right|^2 \ , \tag{68}$$

$$S_8 \equiv \frac{\mathcal{B}(B^0 \to \rho^-\rho^+)}{\mathcal{B}(B^+ \to \rho^+ K^{*0})} \simeq \left(\frac{f_\rho}{f_{K^*}}\right)^2 \left|\frac{V_{ub}V_{ud}^*}{V_{tb}V_{ts}^*}\right|^2 \left|\frac{a_1}{a_4}\right|^2 \ , \tag{69}$$

$$S_9 \equiv \frac{\mathcal{B}(B^0 \to \pi^+\pi^-)}{\mathcal{B}(B^+ \to \pi^+ K^0)} \simeq \left(\frac{f_\pi}{f_K}\right)^2 \left|\frac{V_{ub}V_{ud}^*}{V_{tb}V_{ts}^*}\right|^2 \left|\frac{a_1}{a_4+a_6R_5}\right|^2 \ . \tag{70}$$

Here, the quantity R_5 is defined as $R_5 \equiv 2m_{K^0}^2/(m_b-m_d)(m_d+m_s)$. As is obvious from the formulae given above, the determination of the effective coefficients through these ratios is correlated with the values of the CKM factors, which in all cases are given essentially by the ratio $|V_{ub}/V_{ts}| \simeq |V_{ub}/V_{cb}| \simeq 0.08 \pm 0.02$. We expect that the CKM matrix element $|V_{ub}/V_{cb}|$ will be very precisely measured in forthcoming experiments. Hence, a better use of these ratios is to determine the effective coefficients. To give a quantitative content to the approximations made in reaching the simple expressions for S_i, $i = 1, ..., 9$, we display in Table 14 the numerical values of these ratios, together with the ratios S_{10} and S_{11} discussed below, as a function of $|V_{ub}/V_{cb}|$, taking a rather generous error on this quantity in the range $0.06 \leq |V_{ub}/V_{cb}| \leq 0.11$, for three values of N_c. The rows labeled as "Exact" are the results obtained by using the complete amplitudes and the rows labeled as "Approx." are the results following from the simple relations given above for these ratios. As one can see, these formulae are quite accurate over a large parameter space, with the deviations mostly remaining well within 10%. One can also check that the ratios S_5 - S_9 for the complete result scale almost quadratically with V_{ub}/V_{cb}, as follows from the simple formulae, which shows that the CKM dependence displayed in the approximate formulae is actually quite accurate.

Concerning the measurements of the electroweak coefficients, $a_7, ..., a_{10}$, we recall that the dominant contribution of the electroweak penguin amplitudes is proportional to a_9. The rest of the electroweak coefficients are either small or they enter in combinations which render them very sensitive to the variation in N_c. It is instructive to consult Table 12, where the decays in which electroweak penguins may make a significant contribution to the branching ratios are listed. In line with our argument, we will concentrate only on class-IV penguin-decays, and pick up the decay mode $B^0 \to \rho^0 K^0$ as an illustrative example. To that end, we define the following two ratios involving a class-I and a class-IV processes, dominated by the tree and QCD-penguins, respectively.:

$$\begin{aligned} S_{10} &\equiv \frac{2\mathcal{B}(B^0 \to \rho^0 K^0)}{\mathcal{B}(B^+ \to \pi^+ K^{*0})} \simeq \frac{9}{4}\left|\frac{f_\rho F_1^{B\to K}(m_\rho^2)}{f_{K^*}F_1^{B\to\pi}(m_K^2)}\right|^2 \left|\frac{a_9}{a_4}\right|^2 \ , \\ S_{11} &\equiv \frac{2\mathcal{B}(B^0 \to \rho^0 K^0)}{\mathcal{B}(B^0 \to \rho^-\pi^+)} \simeq \frac{9}{4}\left|\frac{V_{tb}V_{ts}^*}{V_{ub}V_{ud}^*}\right|^2 \left|\frac{f_\rho F_1^{B\to K}(m_\rho^2)}{f_\pi A_0^{B\to\rho}(m_\pi^2)}\right|^2 \left|\frac{a_9}{a_1}\right|^2 \ . \end{aligned} \tag{71}$$

We show the numerical values of these ratios in Table 14 for the three indicated values of the ratio $|V_{ub}/V_{cb}|$, both for the exact and approximate cases. The approximate relations are reliable over most part of the parameter space. Other similar ratios can be written down in

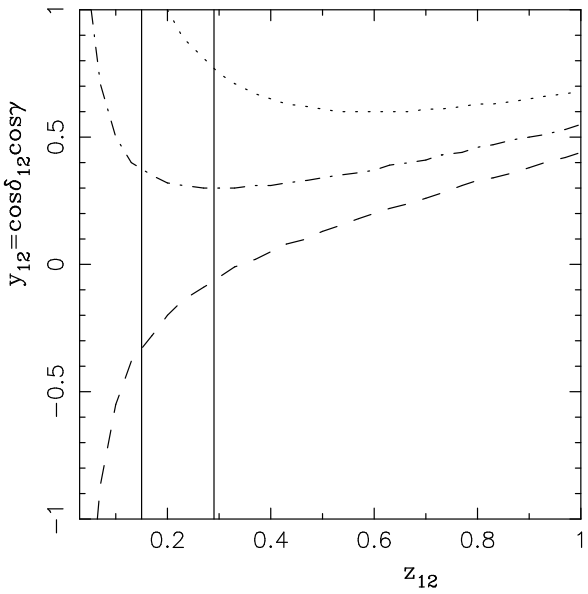

Figure 10: $y_{12} = \cos\delta_{12}\cos\gamma$ as a function of z_{12} in the factorization approach. The dotted, dashed-dotted and dashed curves correspond to $N_c = \infty$ and $|V_{ub}/V_{cb}| = 0.11$, $N_c = 3$ and $|V_{ub}/V_{cb}| = 0.08$, and $N_c = 2$ and $|V_{ub}/V_{cb}| = 0.06$, yielding in the BSW model the values $S_{12} = 0.46$, $S_{12} = 0.91$ and $S_{12} = 1.12$, respectively. The two vertical lines indicate the bounds on z_{12} from our model and the CKM factors discussed in the text, yielding $0.15 < z_{12} < 0.29$.

a straightforward way. Measurements of the ratios S_1 - S_{11} will overconstrain the coefficients a_4, a_6 and a_9, testing both the factorization hypothesis and determining these crucial penguin coefficients. Note that S_{10} depends only slightly on the CKM factors, compared to the others discussed above, and S_1 to S_4 do not depend on $|V_{ub}/V_{cb}|$ when we use the approximations in eqs. (62) - (65).

7.3 Potential impact of $B \to h_1 h_2$ decays on CKM phenomenology

(i) $B \to \pi K$ channels:

In this subsection, we consider the ratios of branching ratios which can be gainfully used to get information on the CKM parameters. The most celebrated one in this class is the ratio discussed by Fleischer and Mannel recently [45], involving the decays $B^0 \to K^+\pi^-$ and $B^+ \to K^0\pi^+$. Ignoring the electroweak penguin contribution, which is estimated to be small in our model, one can write this ratio as:

$$S_{12} \equiv \frac{\mathcal{B}(B^0 \to K^+\pi^-)}{\mathcal{B}(B^+ \to K^0\pi^+)} \simeq 1 - 2z_{12}\cos\delta_{12}\cos\gamma + z_{12}^2, \tag{72}$$

with

$$z_{12} = \frac{|T|}{|P|} = \left|\frac{V_{ub}V_{us}^*}{V_{tb}V_{ts}^*}\right| \left|\frac{a_1}{a_4 + a_6 R_5}\right|.$$

The branching ratios involved in S_{12} have been measured by the CLEO collaboration and

their values can be seen in Table 8. The ratio S_{12} itself has the following value:

$$S_{12} = 0.65 \pm 0.39 \quad . \tag{73}$$

For the central values of the CKM parameter ($\rho = 0.12, \eta = 0.34$), the value of S_{12} is found to be $0.80 \leq S_{12} \leq 1.0$ varying N_c and using the two form factor models displayed in Table 8. However, varying the CKM parameters in their presently allowed range, we find $0.46 \leq S_{12} \leq 1.12$, where the lower and upper values correspond to $|V_{ub}/V_{cb}| = 0.11$ and $|V_{ub}/V_{cb}| = 0.06$, respectively. The ratio S_{12} is, formally speaking, very similar to the one defined for the ratio S_1. However, the difference between S_1 and S_{12} is that the product $z_{12}\cos\delta_{12}\cos\gamma$, as opposed to the corresponding quantity $z_1\cos\delta_1\cos\alpha$ in S_1, is not small in the allowed region of z_{12}. The range $0.15 \leq z_{12} \leq 0.29$ is estimated in the factorization approach varying the CKM matrix element ratio in the range $0.013 < |V_{ub}V_{us}^*|/|V_{tb}V_{ts}^*| < 0.023$ and N_c. This is shown in Fig. 10. Hence, the ratio S_{12} and its kinds, discussed below, do provide, in principle, a constraint on $\cos\gamma$. This figure also shows that the ratio S_{12} is in quite good agreement with the measured ratio by CLEO.

In the context of the factorization models, the CLEO data was analyzed in [27] and it was shown that theoretical estimates in this framework are in agreement with data. The ratio S_{12} (called R_1 in [27]) provides a constraint on the CKM parameter ρ (equivalently $\cos\gamma$). Taking data at $\pm 1\sigma$ value, the CLEO data disfavored the negative-ρ region. The allowed values of this parameter resulting from the measurement of S_{12} were found to be in comfortable agreement with the ones allowed by the CKM unitarity fits. In addition, the dependence of S_{12} on the CKM parameter η was found to be weak. This overlap in the value of ρ following from the analysis of the ratio S_{12} in the factorization approach and from the CKM unitarity fits has also been confirmed recently in [48]. We show here the ratio S_{12} plotted as a function of $\cos\gamma$ for $N_c = 2, 3$ and ∞ and fixed value of the ratio $|V_{ub}/V_{cb}| = 0.08$ in Fig. 11. The form factor dependence of this ratio is rather weak (as can be seen in Table 8) and for the sake of definiteness we display the result for the BSW form factors. It is seen that for all values of N_c, the CLEO data provides a constraint on $\cos\gamma$, which is compatible with the one allowed by the CKM fits, yielding $32^\circ \leq \gamma \leq 122^\circ$ [47]. This is in line with what has already been reported in [27].

The ratio S_{12} given in eq. (72) is a generic example of the kind of relations that one can get from the ratios of branching ratios in which the quantity $z_i\cos\delta_i\cos\gamma$ is not small. We have argued, in line with [27], that the factorization model gives an adequate account of S_{12}. We discuss below some related ratios, which, once measured, could be used to determine $\cos\gamma$ as well as further test the consistency of the factorization approach.

(ii) Ratios for $B \to \pi K^*$ modes:

One can define analogous to eq. (72), the ratio S_{13}, involving the decays $B^0 \to \pi^- K^{*+}$ and $B^+ \to K^{*0}\pi^+$:

$$S_{13} \equiv \frac{\mathcal{B}(B^0 \to \pi^- K^{*+})}{\mathcal{B}(B^+ \to \pi^+ K^{*0})} \simeq 1 - 2z_{13}\cos\delta_{13}\cos\gamma + z_{13}^2, \tag{74}$$

with

$$z_{13} = \frac{|T|}{|P|} = \left|\frac{V_{ub}V_{us}^*}{V_{tb}V_{ts}^*}\right| \left|\frac{a_1}{a_4}\right|$$

Using $0.013 < |V_{ub}V_{us}^*|/|V_{tb}V_{ts}^*| < 0.023$, and from $N_c = 2$ to $N_c = \infty$, we get $0.30 < z_{13} < 0.60$, indicated in Fig.12. The ratio S_{13} is plotted in Fig. 13 as a function of $\cos\gamma$ for three different

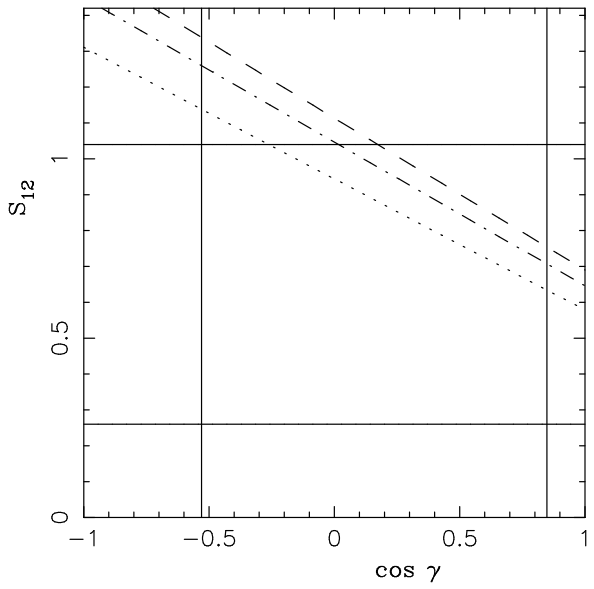

Figure 11: S_{12} as a function of $\cos\gamma$ in the factorization approach. The dotted, dashed-dotted and dashed curves correspond to $N_c = \infty$, $N_c = 3$ and $N_c = 2$, respectively. The horizontal lines are the CLEO ($\pm 1\sigma$) measurements of S_{12}. The two vertical lines correspond to $32° < \gamma < 122°$.

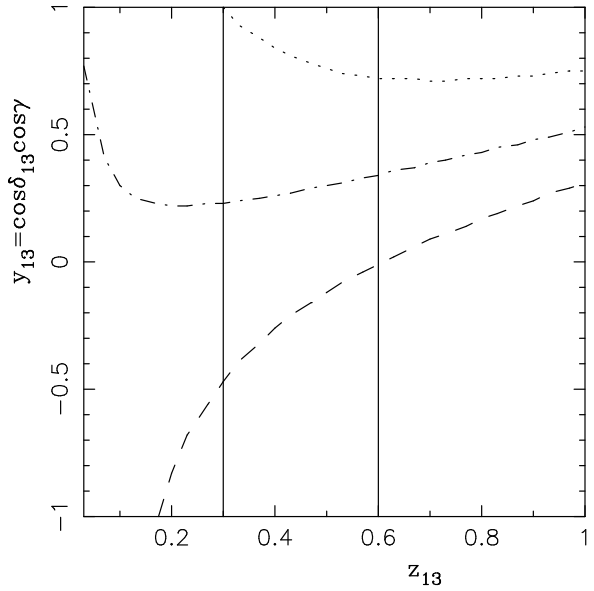

Figure 12: $y_{13} = \cos\delta_{13}\cos\gamma$ as a function of z_{13} in the factorization approach. The dotted, dashed-dotted and dashed curves correspond to $N_c = \infty$ and $|V_{ub}/V_{cb}| = 0.11$, $N_c = 3$ and $|V_{ub}/V_{cb}| = 0.08$, and $N_c = 2$ and $|V_{ub}/V_{cb}| = 0.06$, yielding in the BSW model the values $S_{13} = 0.49$, $S_{13} = 0.95$ and $S_{13} = 1.37$, respectively. The two vertical lines indicate the bounds on z_{13} from our model and the CKM factors $0.30 < z_{13} < 0.60$.

values of N_c and $|V_{ub}/V_{cb}|$. When measured, this ratio will provide a constraint on the phase $\cos\gamma$. Varying the CKM parameters and N_c in the indicated range, we find the ratio S_{13} to lie in the range $0.49 \le S_{13} \le 1.37$. The upper bound is larger than the one for S_{12} given earlier, reflecting that the QCD-penguin contributions in the two ratios are similar but not identical.

(iii) Ratios for $B \to \rho K$ modes

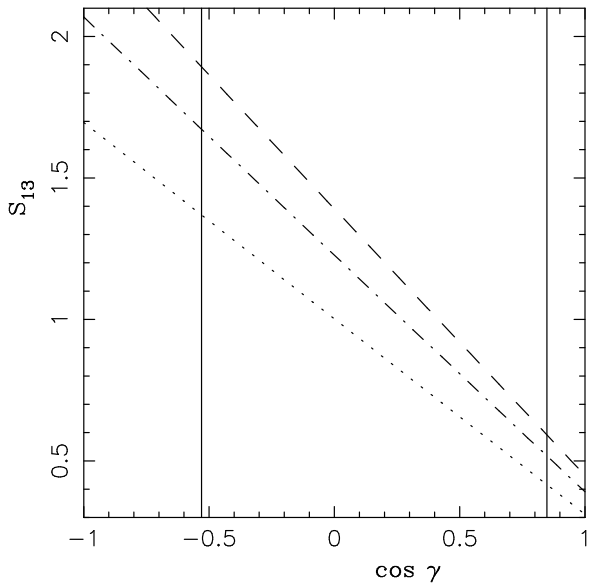

Figure 13: $S_{13} = S_{15}$ as a function of $\cos\gamma$. The dotted, dashed-dotted and dashed lines correspond to results with $N_c = \infty$, $N_c = 3$ and $N_c = 2$, respectively. The two vertical lines correspond to $32^\circ < \gamma < 122^\circ$.

$$S_{14} \equiv \frac{\mathcal{B}(B^0 \to \rho^- K^+)}{\mathcal{B}(B^+ \to \rho^+ K^0)} \simeq 1 - 2z_{14}\cos\delta_{14}\cos\gamma + z_{14}^2, \tag{75}$$

with

$$z_{14} = \frac{|T|}{|P|} = \left|\frac{V_{ub}V_{us}^*}{V_{tb}V_{ts}^*}\right| \left|\frac{a_1}{a_4 + a_6 Q_4}\right| .$$

The central value of the quantity z_{14} is $z_{14} \simeq 5.07$. However, being very large, the ratio S_{14} implies that the branching ratio in the denominator is appreciably smaller and perhaps lot more difficult to measure. In view of this, we are less sure of its utility of the ratio S_{14} in the foreseeable future.

(iv) Ratios for $B \to \rho K^*$ modes

Finally, we note that the ratio S_{15} defined below provides, within our model, a very similar constraint on $\cos\gamma$ as the one following from the ratio S_{13}:

$$S_{15} \equiv \frac{\mathcal{B}(B^0 \to \rho^- K^{*+})}{\mathcal{B}(B^+ \to \rho^+ K^{*0})} \simeq 1 - 2z_{15}\cos\delta_{15}\cos\gamma + z_{15}^2 , \tag{76}$$

where $z_{15} = z_{13}$ and $\delta_{15} = \delta_{13}$. This will be a further test of the factorization Ansatz.

Finally, in conclusion of this section, we mention that a method of measuring the CKM matrix element ratio $|V_{td}/V_{ts}|$ using exclusive non-leptonic B decays has been proposed in ref. [50]. Some of these ratios have modest theoretical uncertainties due to SU(3) breaking effects. These relations hold in the factorization framework as well, and we list a few of them below:

$$\begin{aligned} \frac{\mathcal{B}(B^+ \to K^+\bar{K}^0)}{\mathcal{B}(B^+ \to \pi^+ K^0)} &\simeq \frac{\mathcal{B}(B^+ \to K^+\bar{K}^{*0})}{\mathcal{B}(B^+ \to \pi^+ K^{*0})} \simeq \frac{\mathcal{B}(B^+ \to K^{*+}\bar{K}^0)}{\mathcal{B}(B^+ \to \rho^+ K^0)} \\ &\simeq \frac{\mathcal{B}(B^+ \to K^{*+}\bar{K}^{*0})}{\mathcal{B}(B^+ \to \rho^+\ K^{*0})} \simeq \left|\frac{V_{td}}{V_{ts}}\right|^2 . \end{aligned} \tag{77}$$

8 Summary and Conclusions

We have presented estimates of the decay rates in two-body non-leptonic decays $B \to h_1 h_2$ involving pseudoscalar and vector light hadrons in which QCD and electroweak penguins play a significant role. This work partly overlaps with studies done earlier along these lines on branching ratios, in particular in [27–31]. We make use of the theoretical framework detailed in [27,28] but we think that this is the most comprehensive study of its kind in the factorization framework.

Using the sensitivity on N_c as a criterion of theoretical stability, we have classified all the decays $B \to h_1 h_2$ into five different classes involving penguin and tree amplitudes. This extends the classification of tree amplitudes *en vogue* in the literature [8,18]. We hope that the detailed anatomy of the decays $B \to h_1 h_2$ presented here, in particular concerning the QCD and electroweak penguins, will serve to have a more critical view of what can be reasonably calculated in the factorization framework and what involves a good deal of theoretical fine tuning. Following the classification discussed here, we think that class-I and class-IV decays, and probably also class-III decays, can be calculated with a reasonable theoretical uncertainty, typically a factor 2. However, most class-II and class-V decays deserve a careful theoretical reappraisal to establish the extent of non-factorizing contributions. In particular, we have outlined the pattern of power suppression in annihilation contributions to two-body non-leptonic B decays. Being suppressed by m_h^4/m_B^4, the annihilation contributions are small in the decays $B \to PP$ but since this suppression is only m_h^2/m_B^2 in $B \to PV$ and $B \to VV$ decays, in specific cases this can be easily overcome by the favorable effective coefficients. Hence, annihilation contributions can be significant in some $B \to h_1 h_2$ decays involving vector mesons.

Our results can be summarized as follows.

- The recently measured decay modes $B^0 \to K^+\pi^-, B^+ \to K^+\eta', B^0 \to K^0\eta', B^+ \to \pi^+ K^0$, and $B^+ \to \omega K^+$ can be explained in the factorization framework. The first four of these belong to the QCD-penguin dominated class-IV decays, which we argue can be reliably calculated. The last belongs to the N_c-unstable class-V decays, which may receive significant FSI and/or annihilation contributions. Taken the present theory and data on face value, all measured decay modes are consistently accommodated, with some preference for $\xi = 1/N_c \leq 0.2$. Data on the combined decay modes $B \to \phi K^*$ prefers somewhat higher value for ξ. However, we caution against drawing too quantitative conclusions at this stage.

- A number of decays is tantalizingly close to the present experimental upper limits. We think that with $O(10^8)$ $B/\bar{B}$ hadrons, available in the next three to five years, a good fraction of the seventy six decay modes worked out here will be measured providing a detailed test of the factorization approach.

- To further quantify these tests, we have put forward numerous proposals which involve measurements of the ratios of branching ratios. Carefully selecting the decay modes, one could determine the effective coefficients a_1, a_2, a_4, a_6 and a_9 from data on $B \to h_1 h_2$ decays in the future. A consistent determination of these coefficients will greatly help in developing a completely quantitative theory of non-leptonic B decays. Leaving out a_2 from this list, which depends significantly on N_c, we do not expect that the rest

will be greatly modified by non-perturbative effects. It will be difficult to quantitatively determine the smaller penguin coefficients not listed explicitly.

- We have proposed a number of ratios involving the decays $B \to h_1 h_2$, relating the final states in which a pseudoscalar meson is replaced by a vector meson. They will help in determining the form factors for the various decays considered here. While these relations are derived in the factorization approach, perhaps their validity is more general.

- The current and impending interest in two-body non-leptonic decays for the CKM phenomenology is illustrated, arguing that they provide potentially non-trivial constraints on the CKM parameters. While ultimately not competitive to more precise determinations of the CKM parameters from B^0-$\overline{B^0}$ mixings and radiative and semileptonic B decays, they are of current phenomenological interest as the constraints following from them are already complementary to the ones from the CKM unitarity fits.

- Finally, within the factorization framework which gives an adequate account of the present data on decay rates, it will be instructive to study direct and indirect CP violation in all two-body non-leptonic B decays discussed here. We hope to return to this in a forthcoming publication [75].

Acknowledgments
We thank Christoph Greub and Jim Smith for helpful discussions on various aspects of theory and data discussed in this paper. We also thank Jim Smith for critically reading the manuscript.

A Matrix elements for B decays to two pseudo-scalar mesons

(1) $b \to d$ processes:

$$\begin{aligned} M(\bar{B}^0 \to \pi^- \pi^+) &= -i \frac{G_F}{\sqrt{2}} f_\pi F_0^{B\to\pi}(m_\pi^2)(m_B^2 - m_\pi^2) \\ &\times \left\{ V_{ub} V_{ud}^* a_1 - V_{tb} V_{td}^* [a_4 + a_{10} + (a_6 + a_8) R_1] \right\}, \end{aligned} \tag{78}$$

with $R_1 = \frac{2m_\pi^2}{(m_b - m_u)(m_u + m_d)}$.

$$\begin{aligned} M(\bar{B}^0 \to \pi^0 \pi^0) &= i \frac{G_F}{\sqrt{2}} f_\pi F_0^{B\to\pi}(m_\pi^2)(m_B^2 - m_\pi^2) \left\{ V_{ub} V_{ud}^* a_2 \right. \\ &\left. + V_{tb} V_{td}^* [a_4 - \frac{1}{2} a_{10} + \frac{3}{2} a_7 - \frac{3}{2} a_9 + (a_6 - \frac{1}{2} a_8) R_2] \right\}, \end{aligned} \tag{79}$$

with $R_2 = \frac{2m_{\pi^0}^2}{(m_b - m_d)(m_d + m_d)}$. After squaring of the matrix element, the decay rate should be divided by 2, for the symmetric factor of identical particles in the final states.

$$\begin{aligned} M(B^- \to \pi^- \pi^0) &= -i \frac{G_F}{2} f_\pi F_0^{B\to\pi}(m_\pi^2)(m_B^2 - m_\pi^2) \\ &\times \left\{ V_{ub} V_{ud}^* (a_1 + a_2) - V_{tb} V_{td}^* \times \frac{3}{2} [a_9 + a_{10} - a_7 + a_8 R_2] \right\}. \end{aligned} \tag{80}$$

$$
\begin{aligned}
M(B^- \to \pi^- \eta^{(\prime)}) &= -i\frac{G_F}{\sqrt{2}} f_\pi F_0^{B\to\eta^{(\prime)}}(m_\pi^2)(m_B^2 - m_{\eta^{(\prime)}}^2)\,\{V_{ub}V_{ud}^* a_1 \\
&\quad - V_{tb}V_{td}^*[a_4 + a_{10} + (a_6 + a_8)R_1]\} \qquad (81)\\
&- i\frac{G_F}{\sqrt{2}} f^u_{\eta^{(\prime)}} F_0^{B\to\pi}(m^2_{\eta^{(\prime)}})(m_B^2 - m_\pi^2)\left\{ V_{ub}V_{ud}^* a_2 + V_{cb}V_{cd}^* a_2 \frac{f^c_{\eta^{(\prime)}}}{f^u_{\eta^{(\prime)}}} \right. \\
&\quad - V_{tb}V_{td}^*\left[a_4 - \frac{1}{2}a_{10} + 2a_3 - 2a_5 + \frac{1}{2}(a_9 - a_7) + (a_6 - \frac{1}{2}a_8)R_3^{(\prime)}\left(1 - \frac{f^u_{\eta^{(\prime)}}}{f^s_{\eta^{(\prime)}}}\right)\right. \\
&\quad \left.\left. + (a_3 - a_5 + a_9 - a_7)\frac{f^c_{\eta^{(\prime)}}}{f^u_{\eta^{(\prime)}}} + \left(a_3 - a_5 - \frac{1}{2}(a_9 - a_7)\right)\frac{f^s_{\eta^{(\prime)}}}{f^u_{\eta^{(\prime)}}}\right]\right\},
\end{aligned}
$$

with $R_3^{(\prime)} = \frac{m^2_{\eta^{(\prime)}}}{(m_b - m_d)m_s}$. The definitions of the decay constants involving η and η' are as follows:

$$
\langle 0|\bar{u}\gamma_\mu\gamma_5 u|\eta^{(\prime)}(p)\rangle = i f^u_{\eta^{(\prime)}} p_\mu\ , \quad \langle 0|\bar{s}\gamma_\mu\gamma_5 s|\eta^{(\prime)}(p)\rangle = i f^s_{\eta^{(\prime)}} p_\mu\ , \quad \langle 0|\bar{c}\gamma_\mu\gamma_5 c|\eta^{(\prime)}(p)\rangle = i f^c_{\eta^{(\prime)}} p_\mu\ . \qquad (82)
$$

The quantities $f^u_{\eta^{(\prime)}}$ and $f^s_{\eta^{(\prime)}}$ in the two-angle mixing formalism are:

$$
f^u_{\eta'} = \frac{f_8}{\sqrt{6}}\sin\theta_8 + \frac{f_0}{\sqrt{3}}\cos\theta_0, \qquad f^s_{\eta'} = -2\frac{f_8}{\sqrt{6}}\sin\theta_8 + \frac{f_0}{\sqrt{3}}\cos\theta_0; \qquad (83)
$$

$$
f^u_{\eta} = \frac{f_8}{\sqrt{6}}\cos\theta_8 - \frac{f_0}{\sqrt{3}}\sin\theta_0, \qquad f^s_{\eta} = -2\frac{f_8}{\sqrt{6}}\cos\theta_8 - \frac{f_0}{\sqrt{3}}\sin\theta_0. \qquad (84)
$$

We shall also need the matrix elements of the pseudoscalar densities for which we use the following equations:

$$
\begin{aligned}
\frac{\langle 0|\bar{u}\gamma_5 u|\eta\rangle}{\langle 0|\bar{s}\gamma_5 s|\eta\rangle} &= \frac{f^u_\eta}{f^s_\eta}\ ,\\
\frac{\langle 0|\bar{u}\gamma_5 u|\eta'\rangle}{\langle 0|\bar{s}\gamma_5 s|\eta'\rangle} &= \frac{f^u_{\eta'}}{f^s_{\eta'}}\ , \qquad (85)
\end{aligned}
$$

which differ from the corresponding equations in [76], which have been sometimes used in the literature. In the approximation of setting $f_8 = f_0$, and $\theta_8 = \theta_0$, the relations given above, however, agree with the results derived in [77]. The results for the densities $\langle 0|\bar{s}\gamma_5 s|\eta'\rangle$ and $\langle 0|\bar{s}\gamma_5 s|\eta\rangle$ have been derived in [27] which we use here:

$$
\begin{aligned}
\langle 0|\bar{s}\gamma_5 s|\eta'\rangle &= -i\frac{(f^s_{\eta'} - f^u_{\eta'})m^2_{\eta'}}{2m_s}\ ,\\
\langle 0|\bar{s}\gamma_5 s|\eta\rangle &= -i\frac{(f^s_{\eta} - f^u_{\eta})m^2_{\eta}}{2m_s}\ . \qquad (86)
\end{aligned}
$$

We point out that the anomaly contributions have been taken into account in deriving these expressions. They are numerically important. The relevant form factors for the $B \to \eta'$ and $B \to \eta$ transitions are:

$$
F_{0,1}^{B\to\eta'} = F_{0,1}^{\pi}\left(\frac{\sin\theta_8}{\sqrt{6}} + \frac{\cos\theta_0}{\sqrt{3}}\right), \qquad F_{0,1}^{B\to\eta} = F_{0,1}^{\pi}\left(\frac{\cos\theta_8}{\sqrt{6}} - \frac{\sin\theta_0}{\sqrt{3}}\right). \qquad (87)
$$

The mixing angles that we have used in the numerical calculations are $\theta_8 = -22.2°$, $\theta_0 = -9.1°$ [71].

$$
\begin{aligned}
M(\bar{B}^0 \to \pi^0\eta^{(\prime)}) &= -i\frac{G_F}{2} f_\pi F_0^{B\to\eta^{(\prime)}}(m_\pi^2)(m_B^2 - m_{\eta^{(\prime)}}^2)\,\{V_{ub}V_{ud}^* a_2 \\
&\quad -V_{tb}V_{td}^*\left[-a_4 + \frac{1}{2}a_{10} + (-a_6 + \frac{1}{2}a_8)R_2 + \frac{3}{2}(a_9 - a_7)\right]\Big\} \qquad (88)\\
&+ i\frac{G_F}{2} f_{\eta^{(\prime)}}^u F_0^{B\to\pi}(m_{\eta^{(\prime)}}^2)(m_B^2 - m_\pi^2)\left\{V_{ub}V_{ud}^* a_2 + V_{cb}V_{cd}^* a_2 \frac{f_{\eta^{(\prime)}}^c}{f_{\eta^{(\prime)}}^u}\right. \\
&\quad -V_{tb}V_{td}^*\left[a_4 + 2a_3 - 2a_5 + \frac{1}{2}(a_9 - a_7 - a_{10}) + (a_6 - \frac{1}{2}a_8)R_3^{(\prime)}\left(1 - \frac{f_{\eta^{(\prime)}}^u}{f_{\eta^{(\prime)}}^s}\right)\right. \\
&\quad \left.\left. +(a_3 - a_5 + a_9 - a_7)\frac{f_{\eta^{(\prime)}}^c}{f_{\eta^{(\prime)}}^u} + \left(a_3 - a_5 - \frac{1}{2}(a_9 - a_7)\right)\frac{f_{\eta^{(\prime)}}^s}{f_{\eta^{(\prime)}}^u}\right]\right\}.
\end{aligned}
$$

$$
\begin{aligned}
M(\bar{B}^0 \to \eta\eta') &= -i\frac{G_F}{\sqrt{2}} f_\eta^u F_0^{B\to\eta'}(m_\eta^2)(m_B^2 - m_{\eta'}^2)\left\{V_{ub}V_{ud}^* a_2 + V_{cb}V_{cd}^* a_2 \frac{f_\eta^c}{f_\eta^u}\right. \qquad (89)\\
&\quad -V_{tb}V_{td}^*\left[a_4 + 2a_3 - 2a_5 + \frac{1}{2}(a_9 - a_7 - a_{10}) + (a_6 - \frac{1}{2}a_8)R_3\left(1 - \frac{f_\eta^u}{f_\eta^s}\right)\right. \\
&\quad \left.\left. +(a_3 - a_5 + a_9 - a_7)\frac{f_\eta^c}{f_\eta^u} + \left(a_3 - a_5 - \frac{1}{2}(a_9 - a_7)\right)\frac{f_\eta^s}{f_\eta^u}\right]\right\} \\
&- i\frac{G_F}{\sqrt{2}} f_{\eta'}^u F_0^{B\to\eta}(m_{\eta'}^2)(m_B^2 - m_\eta^2)\left\{V_{ub}V_{ud}^* a_2 + V_{cb}V_{cd}^* a_2 \frac{f_{\eta'}^c}{f_{\eta'}^u}\right. \\
&\quad -V_{tb}V_{td}^*\left[a_4 + 2a_3 - 2a_5 + \frac{1}{2}(a_9 - a_7 - a_{10}) + (a_6 - \frac{1}{2}a_8)R_3'\left(1 - \frac{f_{\eta'}^u}{f_{\eta'}^s}\right)\right. \\
&\quad \left.\left. +(a_3 - a_5 + a_9 - a_7)\frac{f_{\eta'}^c}{f_{\eta'}^u} + \left(a_3 - a_5 - \frac{1}{2}(a_9 - a_7)\right)\frac{f_{\eta'}^s}{f_{\eta'}^u}\right]\right\}.
\end{aligned}
$$

$$
\begin{aligned}
M(\bar{B}^0 \to \eta'\eta') &= -i\frac{2G_F}{\sqrt{2}} f_{\eta'}^u F_0^{B\to\eta'}(m_{\eta'}^2)(m_B^2 - m_{\eta'}^2)\left\{V_{ub}V_{ud}^* a_2 + V_{cb}V_{cd}^* a_2 \frac{f_{\eta'}^c}{f_{\eta'}^u}\right. \qquad (90)\\
&\quad - V_{tb}V_{td}^*\left[a_4 + 2a_3 - 2a_5 + \frac{1}{2}(a_9 - a_7 - a_{10}) + (a_6 - \frac{1}{2}a_8)R_3'\left(1 - \frac{f_{\eta'}^u}{f_{\eta'}^s}\right)\right. \\
&\quad \left.\left. +(a_3 - a_5 + a_9 - a_7)\frac{f_{\eta'}^c}{f_{\eta'}^u} + \left(a_3 - a_5 - \frac{1}{2}(a_9 - a_7)\right)\frac{f_{\eta'}^s}{f_{\eta'}^u}\right]\right\}.
\end{aligned}
$$

The matrix elements for $M(\bar{B}^0 \to \eta\eta)$ are the same with the above equation with $\eta' \to \eta$.

(2) $b \to s$ processes:

$$
\begin{aligned}
M(\bar{B}^0 \to K^-\pi^+) &= -i\frac{G_F}{\sqrt{2}} f_K F_0^{B\to\pi}(m_K^2)(m_B^2 - m_\pi^2) \\
&\times \quad \{V_{ub}V_{us}^* a_1 - V_{tb}V_{ts}^*[a_4 + a_{10} + (a_6 + a_8)R_4]\}, \qquad (91)
\end{aligned}
$$

with $R_4 = \frac{2m_K^2}{(m_b-m_u)(m_u+m_s)}$.

$$\begin{aligned} M(\bar{B}^0 \to \bar{K}^0\pi^0) &= -i\frac{G_F}{2} f_K F_0^{B\to\pi}(m_K^2)(m_B^2-m_\pi^2) V_{tb}V_{ts}^* \left[a_4 - \frac{1}{2}a_{10} + (a_6 - \frac{1}{2}a_8)R_5\right] \\ &- i\frac{G_F}{2} f_\pi F_0^{B\to K}(m_\pi^2)(m_B^2-m_K^2)\left\{V_{ub}V_{us}^* a_2 - V_{tb}V_{ts}^* \times \frac{3}{2}(a_9-a_7)\right\}, \end{aligned} \tag{92}$$

with $R_5 = \frac{2m_{K^0}^2}{(m_b-m_d)(m_d+m_s)}$.

$$\begin{aligned} M(B^- \to K^-\pi^0) &= -i\frac{G_F}{2} f_K F_0^{B\to\pi}(m_K^2)(m_B^2-m_\pi^2)\{V_{ub}V_{us}^* a_1 \\ &\quad -V_{tb}V_{ts}^*[a_4 + a_{10} + (a_6+a_8)R_4]\} \\ &- i\frac{G_F}{2} f_\pi F_0^{B\to K}(m_\pi^2)(m_B^2-m_K^2)\left\{V_{ub}V_{us}^* a_2 - V_{tb}V_{ts}^* \times \frac{3}{2}(a_9-a_7)\right\}. \end{aligned} \tag{93}$$

$$\begin{aligned} M(B^- \to K^-\eta^{(\prime)}) &= -i\frac{G_F}{\sqrt{2}} f_K F_0^{B\to\eta^{(\prime)}}(m_K^2)(m_B^2-m_{\eta^{(\prime)}}^2)\{V_{ub}V_{us}^* a_1 \\ &\quad -V_{tb}V_{ts}^*[a_4 + a_{10} + (a_6+a_8)R_4]\} \\ &- i\frac{G_F}{\sqrt{2}} f_{\eta^{(\prime)}}^u F_0^{B\to K}(m_{\eta^{(\prime)}}^2)(m_B^2-m_K^2)\left\{V_{ub}V_{us}^* a_2 + V_{cb}V_{cs}^* a_2 \frac{f_{\eta^{(\prime)}}^c}{f_{\eta^{(\prime)}}^u}\right. \\ &\quad -V_{tb}V_{ts}^*\left[2a_3 - 2a_5 + \frac{1}{2}(a_9-a_7) - (a_6-\frac{1}{2}a_8)R_6^{(\prime)}\right. \\ &\quad + (a_3 - a_5 + a_9 - a_7)\frac{f_{\eta^{(\prime)}}^c}{f_{\eta^{(\prime)}}^u} + \\ &\quad \left.\left.\left(a_3 - a_5 + a_4 + \frac{1}{2}(a_7 - a_9 - a_{10}) + (a_6 - \frac{1}{2}a_8)R_6^{(\prime)}\right)\frac{f_{\eta^{(\prime)}}^s}{f_{\eta^{(\prime)}}^u}\right]\right\}, \end{aligned} \tag{94}$$

with $R_6^{(\prime)} = \frac{2m_{\eta^{(\prime)}}^2}{(m_b-m_s)(m_s+m_s)}$.

$$\begin{aligned} M(\bar{B}^0 \to \bar{K}^0\eta^{(\prime)}) &= i\frac{G_F}{\sqrt{2}} f_K F_0^{B\to\eta^{(\prime)}}(m_K^2)(m_B^2-m_{\eta^{(\prime)}}^2) V_{tb}V_{ts}^*\left[a_4 - \frac{1}{2}a_{10} + (a_6-\frac{1}{2}a_8)R_5\right] \\ &- i\frac{G_F}{\sqrt{2}} f_{\eta^{(\prime)}}^u F_0^{B\to K}(m_{\eta^{(\prime)}}^2)(m_B^2-m_K^2)\left\{V_{ub}V_{us}^* a_2 + V_{cb}V_{cs}^* a_2 \frac{f_{\eta^{(\prime)}}^c}{f_{\eta^{(\prime)}}^u}\right. \\ &\quad -V_{tb}V_{ts}^*\left[2a_3 - 2a_5 + \frac{1}{2}(a_9-a_7) - (a_6-\frac{1}{2}a_8)R_6^{(\prime)}\right. \\ &\quad + (a_3 - a_5 + a_9 - a_7)\frac{f_{\eta^{(\prime)}}^c}{f_{\eta^{(\prime)}}^u} + \\ &\quad \left.\left.\left(a_3 - a_5 + a_4 + \frac{1}{2}(a_7 - a_9 - a_{10}) + (a_6 - \frac{1}{2}a_8)R_6^{(\prime)}\right)\frac{f_{\eta^{(\prime)}}^s}{f_{\eta^{(\prime)}}^u}\right]\right\}. \end{aligned} \tag{95}$$

(3) Pure penguin processes:

$$M(B^- \to \pi^- \bar{K}^0) = i\frac{G_F}{\sqrt{2}} f_K F_0^{B\to\pi}(m_K^2)(m_B^2 - m_\pi^2) V_{tb}V_{ts}^* \left\{ a_4 - \frac{1}{2}a_{10} + (a_6 - \frac{1}{2}a_8)R_5 \right\}. \quad (96)$$

$$M(B^- \to K^- K^0) = i\frac{G_F}{\sqrt{2}} f_K F_0^{B\to K}(m_{K^0}^2)(m_B^2 - m_K^2) V_{tb}V_{td}^* \left\{ a_4 - \frac{1}{2}a_{10} + (a_6 - \frac{1}{2}a_8)R_7 \right\}, \quad (97)$$

with $R_7 = \frac{2m_{K^0}^2}{(m_b - m_s)(m_d + m_s)}$.

$$M(\bar{B}^0 \to K^0 \bar{K}^0) = i\frac{G_F}{\sqrt{2}} f_K F_0^{B\to K}(m_{K^0}^2)(m_B^2 - m_{K^0}^2) V_{tb}V_{td}^* \left\{ a_4 - \frac{1}{2}a_{10} + (a_6 - \frac{1}{2}a_8)R_7 \right\}. \quad (98)$$

B Matrix elements for B decays to a vector and a pseudoscalar meson

(1) $b \to d$ processes:

$$M(\bar{B}^0 \to \rho^- \pi^+) = \sqrt{2} G_F f_\rho F_1^{B\to\pi}(m_\rho^2) m_\rho (\epsilon \cdot p_\pi) \left\{ V_{ub}V_{ud}^* a_1 - V_{tb}V_{td}^* [a_4 + a_{10}] \right\}. \quad (99)$$

$$\begin{aligned} M(\bar{B}^0 \to \rho^+ \pi^-) &= \sqrt{2} G_F f_\pi A_0^{B\to\rho}(m_\pi^2) m_\rho (\epsilon \cdot p_\pi) \left\{ V_{ub}V_{ud}^* a_1 \right. \\ &\quad \left. - V_{tb}V_{td}^* [a_4 + a_{10} + (a_6 + a_8)Q_1] \right\}, \end{aligned} \quad (100)$$

with $Q_1 = \frac{-2m_\pi^2}{(m_b + m_u)(m_u + m_d)}$.

$$\begin{aligned} M(\bar{B}^0 \to \pi^0 \rho^0) &= -\frac{G_F}{\sqrt{2}} m_\rho (\epsilon \cdot p_\pi) \left(f_\pi A_0^{B\to\rho}(m_\pi^2) \left\{ V_{ub}V_{ud}^* a_2 \right. \right. \\ &\quad \left. + V_{tb}V_{td}^* \left[a_4 - \frac{1}{2}a_{10} + (a_6 - \frac{1}{2}a_8)Q_2 + \frac{3}{2}(a_7 - a_9) \right] \right\} \\ &\quad \left. + f_\rho F_1^{B\to\pi}(m_\rho^2) \left\{ V_{ub}V_{ud}^* a_2 + V_{tb}V_{td}^* [a_4 - \frac{1}{2}a_{10} - \frac{3}{2}(a_7 + a_9)] \right\} \right), \end{aligned} \quad (101)$$

with $Q_2 = \frac{-2m_{\pi^0}^2}{(m_b + m_d)(m_d + m_d)}$.

$$\begin{aligned} M(B^- \to \pi^- \rho^0) &= G_F m_\rho (\epsilon \cdot p_\pi) \left(f_\pi A_0^{B\to\rho}(m_\pi^2) \left\{ V_{ub}V_{ud}^* a_1 - V_{tb}V_{td}^* [a_4 + a_{10} + (a_6 + a_8)Q_1] \right\} \right. \\ &\quad \left. + f_\rho F_1^{B\to\pi}(m_\rho^2) \left\{ V_{ub}V_{ud}^* a_2 - V_{tb}V_{td}^* [-a_4 + \frac{1}{2}a_{10} + \frac{3}{2}(a_7 + a_9)] \right\} \right). \end{aligned} \quad (102)$$

$$\begin{aligned} M(B^- \to \rho^- \pi^0) &= G_F m_\rho (\epsilon \cdot p_\pi) \left(f_\pi A_0^{B\to\rho}(m_\pi^2) \left\{ V_{ub}V_{ud}^* a_2 - V_{tb}V_{td}^* \left[-a_4 + \frac{1}{2}a_{10} \right. \right. \right. \\ &\quad \left. \left. + (-a_6 + \frac{1}{2}a_8)Q_2 + \frac{3}{2}(a_9 - a_7) \right] \right\} \\ &\quad \left. + f_\rho F_1^{B\to\pi}(m_\rho^2) \left\{ V_{ub}V_{ud}^* a_1 - V_{tb}V_{td}^* [a_4 + a_{10}] \right\} \right). \end{aligned} \quad (103)$$

$$
\begin{aligned}
M(\bar{B}^0 \to \pi^0\omega) &= \frac{G_F}{\sqrt{2}} m_\omega (\epsilon\cdot p_\pi)\left(f_\pi A_0^{B\to\omega}(m_\pi^2)\left\{ V_{ub}V_{ud}^* a_2 \right.\right. \\
&\qquad \left. -V_{tb}V_{td}^*\left[-a_4 + \frac{1}{2}a_{10} + (\frac{1}{2}a_8 - a_6)Q_2 + \frac{3}{2}(a_9 - a_7)\right]\right\} \\
&- f_\omega F_1^{B\to\pi}(m_\omega^2)\left\{ V_{ub}V_{ud}^* a_2 \right. \\
&\qquad \left.\left. -V_{tb}V_{td}^*\left[a_4 + 2(a_3 + a_5) + \frac{1}{2}(a_7 + a_9 - a_{10})\right]\right\}\right). \qquad (104)
\end{aligned}
$$

$$
\begin{aligned}
M(B^- \to \pi^-\omega) &= G_F m_\omega (\epsilon\cdot p_\pi)\left(f_\pi A_0^{B\to\omega}(m_\pi^2)\left\{ V_{ub}V_{ud}^* a_1 - V_{tb}V_{td}^*[a_4 + a_{10} + (a_6 + a_8)Q_1]\right\}\right. \\
&+ f_\omega F_1^{B\to\pi}(m_\omega^2)\left\{ V_{ub}V_{ud}^* a_2 \right. \\
&\qquad \left.\left. -V_{tb}V_{td}^*\left[a_4 + 2(a_3 + a_5) + \frac{1}{2}(a_7 + a_9 - a_{10})\right]\right\}\right). \qquad (105)
\end{aligned}
$$

$$
\begin{aligned}
M(B^- \to \rho^-\eta^{(\prime)}) &= \sqrt{2} G_F m_\rho (\epsilon\cdot p_{\eta^{(\prime)}})\left(f_\rho F_1^{B\to\eta^{(\prime)}}(m_\rho^2)\left\{ V_{ub}V_{ud}^* a_1 - V_{tb}V_{td}^*[a_4 + a_{10}]\right\}\right. \\
&+ f_{\eta^{(\prime)}}^u A_0^{B\to\rho}(m_{\eta^{(\prime)}}^2)\left\{ V_{ub}V_{ud}^* a_2 + V_{cb}V_{cd}^* a_2 \frac{f_{\eta^{(\prime)}}^c}{f_{\eta^{(\prime)}}^u} \right. \\
&\qquad -V_{tb}V_{td}^*\left[a_4 + 2a_3 - 2a_5 + \frac{1}{2}(a_9 - a_7 - a_{10}) + (a_6 - \frac{1}{2}a_8)Q_3^{(\prime)}\left(1 - \frac{f_{\eta^{(\prime)}}^u}{f_{\eta^{(\prime)}}^s}\right)\right. \\
&\qquad\left.\left.\left. +(a_3 - a_5 + a_9 - a_7)\frac{f_{\eta^{(\prime)}}^c}{f_{\eta^{(\prime)}}^u} + \left(a_3 - a_5 - \frac{1}{2}(a_9 - a_7)\right)\frac{f_{\eta^{(\prime)}}^s}{f_{\eta^{(\prime)}}^u}\right]\right\}\right), \qquad (106)
\end{aligned}
$$

where $Q_3^{(\prime)} = -\frac{m_{\eta^{(\prime)}}^2}{m_s(m_b+m_d)}$.

$$
\begin{aligned}
M(\bar{B}^0 \to \rho^0\eta^{(\prime)}) &= G_F m_\rho (\epsilon\cdot p_{\eta^{(\prime)}})\left(f_\rho F_1^{B\to\eta^{(\prime)}}(m_\rho^2)\left\{ V_{ub}V_{ud}^* a_2 \right.\right. \\
&\qquad \left. -V_{tb}V_{td}^*\left[-a_4 + \frac{1}{2}a_{10} + \frac{3}{2}(a_9 + a_7)\right]\right\} \\
&- f_{\eta^{(\prime)}}^u A_0^{B\to\rho}(m_{\eta^{(\prime)}}^2)\left\{ V_{ub}V_{ud}^* a_2 + V_{cb}V_{cd}^* a_2 \frac{f_{\eta^{(\prime)}}^c}{f_{\eta^{(\prime)}}^u} \right. \\
&\qquad -V_{tb}V_{td}^*\left[a_4 + 2a_3 - 2a_5 + \frac{1}{2}(a_9 - a_7 - a_{10}) + (a_6 - \frac{1}{2}a_8)Q_3^{(\prime)}\left(1 - \frac{f_{\eta^{(\prime)}}^u}{f_{\eta^{(\prime)}}^s}\right)\right. \\
&\qquad\left.\left.\left. +(a_3 - a_5 + a_9 - a_7)\frac{f_{\eta^{(\prime)}}^c}{f_{\eta^{(\prime)}}^u} + \left(a_3 - a_5 - \frac{1}{2}(a_9 - a_7)\right)\frac{f_{\eta^{(\prime)}}^s}{f_{\eta^{(\prime)}}^u}\right]\right\}\right). \qquad (107)
\end{aligned}
$$

$$
M(\bar{B}^0 \to \omega\eta^{(\prime)}) = G_F m_\omega (\epsilon\cdot p_{\eta^{(\prime)}})\left(f_\omega F_1^{B\to\eta^{(\prime)}}(m_\omega^2)\left\{ V_{ub}V_{ud}^* a_2 \right.\right.
$$

$$
\begin{aligned}
& -V_{tb}V_{td}^*\left[a_4+2(a_3+a_5)+\frac{1}{2}(a_7+a_9-a_{10})\right]\Big\} \\
+ \quad & f_{\eta^{(\prime)}}^u A_0^{B\to\omega}(m_{\eta^{(\prime)}}^2)\Bigg\{V_{ub}V_{ud}^* a_2+V_{cb}V_{cd}^* a_2\frac{f_{\eta^{(\prime)}}^c}{f_{\eta^{(\prime)}}^u} \\
& -V_{tb}V_{td}^*\Bigg[a_4+2a_3-2a_5+\frac{1}{2}(a_9-a_7-a_{10})+(a_6-\frac{1}{2}a_8)Q_3^{(\prime)}\left(1-\frac{f_{\eta^{(\prime)}}^u}{f_{\eta^{(\prime)}}^s}\right) \\
& +(a_3-a_5+a_9-a_7)\frac{f_{\eta^{(\prime)}}^c}{f_{\eta^{(\prime)}}^u}+\left(a_3-a_5-\frac{1}{2}(a_9-a_7)\right)\frac{f_{\eta^{(\prime)}}^s}{f_{\eta^{(\prime)}}^u}\Bigg]\Bigg\}\Bigg). \qquad (108)
\end{aligned}
$$

(2) $b\to s$ processes:

$$
M(\bar{B}^0\to K^{*-}\pi^+)=\sqrt{2}G_F f_{K^*}F_1^{B\to\pi}(m_{K^*}^2)m_{K^*}(\epsilon\cdot p_\pi)\left\{V_{ub}V_{us}^* a_1-V_{tb}V_{ts}^*[a_4+a_{10}]\right\}. \qquad (109)
$$

$$
\begin{aligned}
M(\bar{B}^0\to K^-\rho^+) \quad = \quad & \sqrt{2}G_F f_K A_0^{B\to\rho}(m_K^2)m_\rho(\epsilon\cdot p_K)\left\{V_{ub}V_{us}^* a_1\right. \\
& \left.-V_{tb}V_{ts}^*[a_4+a_{10}+(a_6+a_8)Q_4]\right\}, \qquad (110)
\end{aligned}
$$

with $Q_4=\frac{-2m_K^2}{(m_b+m_u)(m_u+m_s)}$.

$$
\begin{aligned}
M(\bar{B}^0\to\bar{K}^{*0}\pi^0) \quad = \quad & G_F m_{K^{*0}}(\epsilon\cdot p_\pi)\Bigg\{f_\pi A_0^{B\to K^*}(m_\pi^2)\left[V_{ub}V_{us}^* a_2-V_{tb}V_{ts}^*\frac{3}{2}(a_9-a_7)\right] \\
+ \quad & f_{K^*}F_1^{B\to\pi}(m_{K^{*0}}^2)V_{tb}V_{ts}^*\left[a_4-\frac{1}{2}a_{10}\right]\Bigg\}. \qquad (111)
\end{aligned}
$$

$$
\begin{aligned}
M(\bar{B}^0\to\bar{K}^0\rho^0) \quad = \quad & G_F m_\rho(\epsilon\cdot p_K)\Bigg\{f_K A_0^{B\to\rho}(m_{K^0}^2)V_{tb}V_{ts}^*\left[a_4-\frac{1}{2}a_{10}+(a_6-\frac{1}{2}a_8)Q_5\right] \\
& +f_\rho F_1^{B\to K}(m_\rho^2)\left[V_{ub}V_{us}^* a_2-V_{tb}V_{ts}^*\times\frac{3}{2}(a_9+a_7)\right]\Bigg\}, \qquad (112)
\end{aligned}
$$

with $Q_5=\frac{-2m_{K^0}^2}{(m_b+m_d)(m_d+m_s)}$.

$$
\begin{aligned}
M(B^-\to K^{*-}\pi^0) \quad = \quad & G_F m_{K^*}(\epsilon\cdot p_\pi)\left[f_\pi A_0^{B\to K^*}(m_\pi^2)\left\{V_{ub}V_{us}^* a_2-V_{tb}V_{ts}^*\times\frac{3}{2}(a_9-a_7)\right\}\right. \\
+ \quad & \left.f_{K^*}F_1^{B\to\pi}(m_{K^*}^2)\left\{V_{ub}V_{us}^* a_1-V_{tb}V_{ts}^*(a_4+a_{10})\right\}\right]. \qquad (113)
\end{aligned}
$$

$$
\begin{aligned}
M(B^-\to K^-\rho^0) \quad = \quad & G_F m_\rho(\epsilon\cdot p_K)\left[f_K A_0^{B\to\rho}(m_K^2)\left\{V_{ub}V_{us}^* a_1\right.\right. \\
& \left.\left.-V_{tb}V_{ts}^*[a_4+a_{10}+(a_6+a_8)Q_4]\right\}\right. \qquad (114) \\
+ \quad & \left.f_\rho F_1^{B\to K}(m_\rho^2)\left\{V_{ub}V_{us}^* a_2-V_{tb}V_{ts}^*\times\frac{3}{2}(a_9+a_7)\right\}\right].
\end{aligned}
$$

$$
\begin{aligned}
M(\bar{B}^0 \to \bar{K}^0\omega) &= G_F m_\omega(\epsilon\cdot p_K)\left(-f_K A_0^{B\to\omega}(m_{K^0}^2)V_{tb}V_{ts}^*\left[a_4-\frac{1}{2}a_{10}+(a_6-\frac{1}{2}a_8)Q_5\right]\right.\\
&+ f_\omega F_1^{B\to K}(m_\omega^2)\{V_{ub}V_{us}^* a_2\\
&\left.\left. -V_{tb}V_{ts}^*\left[2(a_3+a_5)+\frac{1}{2}(a_9+a_7)\right]\right\}\right). \qquad (115)
\end{aligned}
$$

$$
\begin{aligned}
M(B^- \to K^-\omega) &= G_F m_\omega(\epsilon\cdot p_K)\left[f_K A_0^{B\to\omega}(m_K^2)\{V_{ub}V_{us}^* a_1\right.\\
&\quad -V_{tb}V_{ts}^*(a_4+a_{10}+(a_6+a_8)Q_4)\} \qquad (116)\\
&\left.+ f_\omega F_1^{B\to K}(m_\omega^2)\left\{V_{ub}V_{us}^* a_2 - V_{tb}V_{ts}^*\left(2(a_3+a_5)+\frac{1}{2}(a_9+a_7)\right)\right\}\right].
\end{aligned}
$$

$$
\begin{aligned}
M(B^- \to K^{*-}\eta^{(\prime)}) &= \sqrt{2}G_F m_{K^*}(\epsilon\cdot p_B)\left(f_{K^*}F_1^{B\to\eta^{(\prime)}}(m_K^2)\{V_{ub}V_{us}^* a_1 - V_{tb}V_{ts}^*(a_4+a_{10})\}\right.\\
&+ f_{\eta^{(\prime)}}^u A_0^{B\to K^*}(m_{\eta^{(\prime)}}^2)\left\{V_{ub}V_{us}^* a_2 + V_{cb}V_{cs}^* a_2\frac{f_{\eta^{(\prime)}}^c}{f_{\eta^{(\prime)}}^u}\right.\\
&\quad -V_{tb}V_{ts}^*\left[2(a_3-a_5)+\frac{1}{2}(a_9-a_7)-(a_6-\frac{1}{2}a_8)Q_6^{(\prime)}\right. \qquad (117)\\
&\quad\quad +(a_3-a_5+a_9-a_7)\frac{f_{\eta^{(\prime)}}^c}{f_{\eta^{(\prime)}}^u}+\\
&\quad\quad \left.\left.\left.\left(a_3-a_5-\frac{1}{2}(a_9-a_7)+a_4-\frac{1}{2}a_{10}+(a_6-\frac{1}{2}a_8)Q_6^{(\prime)}\right)\frac{f_{\eta^{(\prime)}}^s}{f_{\eta^{(\prime)}}^u}\right]\right\}\right),
\end{aligned}
$$

with $Q_6^{(\prime)} = -\frac{2m_{\eta^{(\prime)}}^2}{(m_b+m_s)(m_s+m_s)}$.

$$
\begin{aligned}
M(\bar{B}^0 \to \bar{K}^{*0}\eta^{(\prime)}) &= \sqrt{2}G_F m_{K^*}(\epsilon\cdot p_B)\left(-f_{K^*}F_1^{B\to\eta^{(\prime)}}(m_K^2)V_{tb}V_{ts}^*\left[a_4-\frac{1}{2}a_{10}\right]\right.\\
&+ f_{\eta^{(\prime)}}^u A_0^{B\to K^*}(m_{\eta^{(\prime)}}^2)\left\{V_{ub}V_{us}^* a_2 + V_{cb}V_{cs}^* a_2\frac{f_{\eta^{(\prime)}}^c}{f_{\eta^{(\prime)}}^u}\right.\\
&\quad -V_{tb}V_{ts}^*\left[2(a_3-a_5)+\frac{1}{2}(a_9-a_7)-(a_6-\frac{1}{2}a_8)Q_6^{(\prime)}+\right. \qquad (118)\\
&\quad\quad +(a_3-a_5+a_9-a_7)\frac{f_{\eta^{(\prime)}}^c}{f_{\eta^{(\prime)}}^u}+\\
&\quad\quad \left.\left.\left.\left(a_3-a_5-\frac{1}{2}(a_9-a_7)+a_4-\frac{1}{2}a_{10}+(a_6-\frac{1}{2}a_8)Q_6^{(\prime)}\right)\frac{f_{\eta^{(\prime)}}^s}{f_{\eta^{(\prime)}}^u}\right]\right\}\right).
\end{aligned}
$$

(3) Pure penguin processes:

$$
M(B^- \to \pi^-\bar{K}^{*0}) = -\sqrt{2}G_F f_{K^*}F_1^{B\to\pi}(m_{K^*}^2)m_{K^*}(\epsilon\cdot p_\pi)V_{tb}V_{ts}^*\left[a_4-\frac{1}{2}a_{10}\right]. \qquad (119)
$$

$$M(B^- \to \rho^- \bar{K}^0) = -\sqrt{2} G_F f_K A_0^{B\to\rho}(m_{K^0}^2) m_\rho (\epsilon \cdot p_K) V_{tb} V_{ts}^* \left[a_4 - \frac{1}{2} a_{10} + (a_6 - \frac{1}{2} a_8) Q_5 \right]. \quad (120)$$

$$\begin{aligned} M(B^- \to K^- K^{*0}) &= \\ M(\bar{B}^0 \to \bar{K}^0 K^{*0}) &= -\sqrt{2} G_F f_{K^*} F_1^{B\to K}(m_{K^*}^2) m_{K^*} (\epsilon \cdot p_K) V_{tb} V_{td}^* \left[a_4 - \frac{1}{2} a_{10} \right]. \end{aligned} \quad (121)$$

$$\begin{aligned} M(B^- \to K^{*-} K^0) &= \\ M(\bar{B}^0 \to \bar{K}^{*0} K^0) &= -\sqrt{2} G_F f_K A_0^{B\to K^*}(m_{K^0}^2) m_{K^*} (\epsilon \cdot p_K) \\ &\times V_{tb} V_{td}^* \left[a_4 - \frac{1}{2} a_{10} + (a_6 - \frac{1}{2} a_8) Q_7 \right], \end{aligned} \quad (122)$$

with $Q_7 = \frac{-2m_{K^0}^2}{(m_b+m_s)(m_d+m_s)}$.

$$M(\bar{B}^0 \to \pi^0 \phi) = G_F f_\phi F_1^{B\to\pi}(m_\phi^2) m_\phi (\epsilon \cdot p_\pi) V_{tb} V_{td}^* \left\{ a_3 + a_5 - \frac{1}{2}(a_7 + a_9) \right\}. \quad (123)$$

$$M(B^- \to \pi^- \phi) = -\sqrt{2} M(\bar{B}^0 \to \pi^0 \phi). \quad (124)$$

$$M(\bar{B}^0 \to \eta^{(\prime)} \phi) = -\sqrt{2} G_F f_\phi F_1^{B\to\eta^{(\prime)}}(m_\phi^2) m_\phi (\epsilon \cdot p_\eta^{(\prime)}) V_{tb} V_{td}^* \left\{ a_3 + a_5 - \frac{1}{2}(a_7 + a_9) \right\}. \quad (125)$$

$$\begin{aligned} M(B^- \to K^- \phi) &= \\ M(\bar{B}^0 \to \bar{K}^0 \phi) &= -\sqrt{2} G_F f_\phi F_1^{B\to K}(m_\phi^2) m_\phi (\epsilon \cdot p_K) V_{tb} V_{ts}^* \\ &\times \left\{ a_3 + a_4 + a_5 - \frac{1}{2}(a_7 + a_9 + a_{10}) \right\}. \end{aligned} \quad (126)$$

C Matrix elements for B decays to two vector mesons

(1) $b \to d$ processes:

$$\begin{aligned} M(\bar{B}^0 \to \rho^- \rho^+) &= -i \frac{G_F}{\sqrt{2}} f_\rho m_\rho \left\{ (\epsilon_+ \cdot \epsilon_-)(m_B + m_\rho) A_1^{B\to\rho}(m_\rho^2) \right. \\ &\left. -(\epsilon_+ \cdot p_B)(\epsilon_- \cdot p_B) \frac{2A_2^{B\to\rho}(m_\rho^2)}{(m_B + m_\rho)} - i\epsilon_{\mu\nu\alpha\beta} \epsilon_-^\mu \epsilon_+^\nu p_B^\alpha p_+^\beta \frac{2V^{B\to\rho}(m_\rho^2)}{(m_B + m_\rho)} \right\} \\ &\times \left\{ V_{ub} V_{ud}^* a_1 - V_{tb} V_{td}^* [a_4 + a_{10}] \right\}. \end{aligned} \quad (127)$$

$$
\begin{aligned}
M(\bar{B}^0 \to \rho^0\rho^0) &= i\frac{G_F}{\sqrt{2}} f_\rho m_\rho \Big\{(\epsilon_1\cdot\epsilon_2)(m_B+m_\rho)A_1^{B\to\rho}(m_\rho^2) \\
&\quad -(\epsilon_1\cdot p_B)(\epsilon_2\cdot p_B)\frac{2A_2^{B\to\rho}(m_\rho^2)}{(m_B+m_\rho)} - i\epsilon_{\mu\nu\alpha\beta}\epsilon_1^\mu\epsilon_2^\nu p_B^\alpha p_2^\beta \frac{2V^{B\to\rho}(m_\rho^2)}{(m_B+m_\rho)}\Big\} \\
&\times \Big\{V_{ub}V_{ud}^* a_2 + V_{tb}V_{td}^*[a_4 - \frac{1}{2}a_{10} - \frac{3}{2}a_7 - \frac{3}{2}a_9]\Big\}. \qquad (128)
\end{aligned}
$$

$$
\begin{aligned}
M(B^- \to \rho^-\rho^0) &= -i\frac{G_F}{2} f_\rho m_\rho \Big[(\epsilon_0\cdot\epsilon_-)(m_B+m_\rho)A_1^{B\to\rho}(m_\rho^2) \\
&\quad -(\epsilon_0\cdot p_B)(\epsilon_-\cdot p_B)\frac{2A_2^{B\to\rho}(m_\rho^2)}{(m_B+m_\rho)} - i\epsilon_{\mu\nu\alpha\beta}\epsilon_-^\mu\epsilon_0^\nu p_B^\alpha p_0^\beta \frac{2V^{B\to\rho}(m_\rho^2)}{(m_B+m_\rho)}\Big] \\
&\times \Big\{V_{ub}V_{ud}^*(a_1+a_2) - V_{tb}V_{td}^* \times \frac{3}{2}[a_7+a_9+a_{10}]\Big\}. \qquad (129)
\end{aligned}
$$

$$
\begin{aligned}
M(\bar{B}^0 \to \omega\omega) &= -i\frac{G_F}{\sqrt{2}} f_\omega m_\omega \Big\{(\epsilon_1\cdot\epsilon_2)(m_B+m_\omega)A_1^{B\to\omega}(m_\omega^2) \\
&\quad -(\epsilon_1\cdot p_B)(\epsilon_2\cdot p_B)\frac{2A_2^{B\to\omega}(m_\omega^2)}{(m_B+m_\omega)} - i\epsilon_{\mu\nu\alpha\beta}\epsilon_1^\mu\epsilon_2^\nu p_B^\alpha p_2^\beta \frac{2V^{B\to\omega}(m_\omega^2)}{(m_B+m_\omega)}\Big\} \\
&\times \Big\{V_{ub}V_{ud}^* a_2 - V_{tb}V_{td}^*[a_4 + 2(a_3+a_5) + \frac{1}{2}(a_7+a_9-a_{10})]\Big\}. \qquad (130)
\end{aligned}
$$

$$
\begin{aligned}
M(\bar{B}^0 \to \rho^0\omega) &= -i\frac{G_F}{2\sqrt{2}} f_\rho m_\rho \Big\{(\epsilon_0\cdot\epsilon_\omega)(m_B+m_\omega)A_1^{B\to\omega}(m_\rho^2) \\
&\quad -(\epsilon_0\cdot p_B)(\epsilon_\omega\cdot p_B)\frac{2A_2^{B\to\omega}(m_\rho^2)}{(m_B+m_\omega)} - i\epsilon_{\mu\nu\alpha\beta}\epsilon_0^\mu\epsilon_\omega^\nu p_B^\alpha p_\omega^\beta \frac{2V^{B\to\omega}(m_\rho^2)}{(m_B+m_\omega)}\Big\} \\
&\times \Big\{V_{ub}V_{ud}^* a_2 - V_{tb}V_{td}^*[-a_4 + \frac{1}{2}a_{10} + \frac{3}{2}(a_7+a_9)]\Big\} \\
&+ i\frac{G_F}{2\sqrt{2}} f_\omega m_\omega \Big\{(\epsilon_0\cdot\epsilon_\omega)(m_B+m_\rho)A_1^{B\to\rho}(m_\omega^2) \\
&\quad -(\epsilon_0\cdot p_B)(\epsilon_\omega\cdot p_B)\frac{2A_2^{B\to\rho}(m_\omega^2)}{(m_B+m_\rho)} - i\epsilon_{\mu\nu\alpha\beta}\epsilon_\omega^\mu\epsilon_0^\nu p_B^\alpha p_-^\beta \frac{2V^{B\to\rho}(m_\omega^2)}{(m_B+m_\rho)}\Big\} \\
&\times \Big\{V_{ub}V_{ud}^* a_2 - V_{tb}V_{td}^*[a_4 + 2(a_3+a_5) + \frac{1}{2}[a_7+a_9-a_{10}]\Big\}. \qquad (131)
\end{aligned}
$$

$$
\begin{aligned}
M(B^- \to \rho^-\omega) &= -i\frac{G_F}{2} f_\rho m_\rho \Big\{(\epsilon_0\cdot\epsilon_-)(m_B+m_\omega)A_1^{B\to\omega}(m_\rho^2) \\
&\quad -(\epsilon_0\cdot p_B)(\epsilon_-\cdot p_B)\frac{2A_2^{B\to\omega}(m_\rho^2)}{(m_B+m_\omega)} - i\epsilon_{\mu\nu\alpha\beta}\epsilon_-^\mu\epsilon_0^\nu p_B^\alpha p_\omega^\beta \frac{2V^{B\to\omega}(m_\rho^2)}{(m_B+m_\omega)}\Big\}
\end{aligned}
$$

$$
\begin{aligned}
&\times \quad \{V_{ub}V_{ud}^* a_1 - V_{tb}V_{td}^*[a_4 + a_{10}]\} \\
&- \quad i\frac{G_F}{2} f_\omega m_\omega \Big\{(\epsilon_0 \cdot \epsilon_-)(m_B + m_\rho) A_1^{B\to\rho}(m_\omega^2) \\
&\qquad -(\epsilon_0 \cdot p_B)(\epsilon_- \cdot p_B)\frac{2A_2^{B\to\rho}(m_\omega^2)}{(m_B + m_\rho)} - i\epsilon_{\mu\nu\alpha\beta}\epsilon_0^\mu \epsilon_-^\nu p_B^\alpha p_-^\beta \frac{2V^{B\to\rho}(m_\omega^2)}{(m_B + m_\rho)}\Big\} \\
&\times \quad \left\{V_{ub}V_{ud}^* a_2 - V_{tb}V_{td}^*\left[a_4 + 2(a_3 + a_5) + \frac{1}{2}(a_7 + a_9 - a_{10})\right]\right\}. \qquad (132)
\end{aligned}
$$

(2) $b \to s$ processes:

$$
\begin{aligned}
M(\bar{B}^0 \to K^{*-}\rho^+) \;&=\; -i\frac{G_F}{\sqrt{2}} f_{K^*} m_{K^*} \Big\{(\epsilon_+ \cdot \epsilon_-)(m_B + m_\rho) A_1^{B\to\rho}(m_{K^*}^2) \\
&\qquad -(\epsilon_+ \cdot p_B)(\epsilon_- \cdot p_B)\frac{2A_2^{B\to\rho}(m_{K^*}^2)}{(m_B + m_\rho)} \\
&\qquad -i\epsilon_{\mu\nu\alpha\beta}\epsilon_-^\mu \epsilon_+^\nu p_B^\alpha p_+^\beta \frac{2V^{B\to\rho}(m_{K^*}^2)}{(m_B + m_\rho)}\Big\} \\
&\times \quad \{V_{ub}V_{us}^* a_1 - V_{tb}V_{ts}^*[a_4 + a_{10}]\}. \qquad (133)
\end{aligned}
$$

$$
\begin{aligned}
M(\bar{B}^0 \to \bar{K}^{*0}\rho^0) \;&=\; -i\frac{G_F}{2} f_\rho m_\rho \Big\{(\epsilon_\rho \cdot \epsilon_K)(m_B + m_{K^*}) A_1^{B\to K^*}(m_\rho^2) \\
&\qquad -(\epsilon_\rho \cdot p_B)(\epsilon_K \cdot p_B)\frac{2A_2^{B\to K^*}(m_\rho^2)}{(m_B + m_{K^*})} - i\epsilon_{\mu\nu\alpha\beta}\epsilon_\rho^\mu \epsilon_K^\nu p_B^\alpha p_K^\beta \frac{2V^{B\to K^*}(m_\rho^2)}{(m_B + m_{K^*})}\Big\} \\
&\times \quad \left\{V_{ub}V_{us}^* a_2 - V_{tb}V_{ts}^* \times \frac{3}{2}(a_9 + a_7)\right\} \\
&- \quad i\frac{G_F}{2} f_{K^*} m_{K^*} \Big\{(\epsilon_\rho \cdot \epsilon_K)(m_B + m_\rho) A_1^{B\to\rho}(m_{K^*}^2) \\
&\qquad -(\epsilon_\rho \cdot p_B)(\epsilon_K \cdot p_B)\frac{2A_2^{B\to\rho}(m_{K^*}^2)}{(m_B + m_\rho)} - i\epsilon_{\mu\nu\alpha\beta}\epsilon_K^\mu \epsilon_\rho^\nu p_B^\alpha p_\rho^\beta \frac{2V^{B\to\rho}(m_{K^*}^2)}{(m_B + m_\rho)}\Big\} \\
&\times \quad V_{tb}V_{ts}^*\left[a_4 - \frac{1}{2}a_{10}\right]. \qquad (134)
\end{aligned}
$$

$$
\begin{aligned}
M(B^- \to K^{*-}\rho^0) \;&=\; -i\frac{G_F}{2} f_\rho m_\rho \Big\{(\epsilon_0 \cdot \epsilon_-)(m_B + m_{K^*}) A_1^{B\to K^*}(m_\rho^2) \\
&\qquad -(\epsilon_0 \cdot p_B)(\epsilon_- \cdot p_B)\frac{2A_2^{B\to K^*}(m_\rho^2)}{(m_B + m_{K^*})} - i\epsilon_{\mu\nu\alpha\beta}\epsilon_0^\mu \epsilon_-^\nu p_B^\alpha p_-^\beta \frac{2V^{B\to K^*}(m_\rho^2)}{(m_B + m_{K^*})}\Big\} \\
&\times \quad \left\{V_{ub}V_{us}^* a_2 - V_{tb}V_{ts}^* \times \frac{3}{2}(a_9 + a_7)\right\} \qquad (135) \\
&- \quad i\frac{G_F}{2} f_{K^*} m_{K^*} \Big\{(\epsilon_0 \cdot \epsilon_-)(m_B + m_\rho) A_1^{B\to\rho}(m_{K^*}^2) \\
&\qquad -(\epsilon_0 \cdot p_B)(\epsilon_- \cdot p_B)\frac{2A_2^{B\to\rho}(m_{K^*}^2)}{(m_B + m_\rho)} - i\epsilon_{\mu\nu\alpha\beta}\epsilon_-^\mu \epsilon_0^\nu p_B^\alpha p_0^\beta \frac{2V^{B\to\rho}(m_{K^*}^2)}{(m_B + m_\rho)}\Big\} \\
&\times \quad \{V_{ub}V_{us}^* a_1 - V_{tb}V_{ts}^*[a_4 + a_{10}]\}.
\end{aligned}
$$

$$
\begin{aligned}
M(\bar{B}^0 \to \bar{K}^{*0}\omega) &= -i\frac{G_F}{2} f_{K^*} m_{K^{*0}} \Big\{ (\epsilon_0 \cdot \epsilon_\omega)(m_B + m_\omega) A_1^{B\to\omega}(m^2_{K^{*0}}) \\
&\quad -(\epsilon_0 \cdot p_B)(\epsilon_\omega \cdot p_B) \frac{2A_2^{B\to\omega}(m^2_{K^*})}{(m_B + m_\omega)} - i\epsilon_{\mu\nu\alpha\beta}\epsilon_0^\mu \epsilon_\omega^\nu p_B^\alpha p_0^\beta \frac{2V^{B\to\omega}(m^2_{K^*})}{(m_B + m_\omega)} \Big\} \\
&\times \quad V_{tb}V_{ts}^* [-a_4 + \frac{1}{2}a_{10}] \\
&- \quad i\frac{G_F}{2} f_\omega m_\omega \Big\{ (\epsilon_0 \cdot \epsilon_\omega)(m_B + m_{K^*}) A_1^{B\to K^*}(m^2_\omega) \\
&\quad -(\epsilon_0 \cdot p_B)(\epsilon_\omega \cdot p_B) \frac{2A_2^{B\to K^*}(m^2_\omega)}{(m_B + m_{K^*})} - i\epsilon_{\mu\nu\alpha\beta}\epsilon_\omega^\mu \epsilon_0^\nu p_B^\alpha p_-^\beta \frac{2V^{B\to K^*}(m^2_\omega)}{(m_B + m_{K^*})} \Big\} \\
&\times \quad \Big\{ V_{ub}V_{us}^* a_2 - V_{tb}V_{ts}^* [2(a_3 + a_5) + \frac{1}{2}(a_9 + a_7) \Big\} . \qquad (136)
\end{aligned}
$$

$$
\begin{aligned}
M(B^- \to K^{*-}\omega) &= -i\frac{G_F}{2} f_{K^*} m_{K^*} \Big\{ (\epsilon_0 \cdot \epsilon_-)(m_B + m_\omega) A_1^{B\to\omega}(m^2_{K^*}) \\
&\quad -(\epsilon_0 \cdot p_B)(\epsilon_- \cdot p_B) \frac{2A_2^{B\to\omega}(m^2_{K^*})}{(m_B + m_\omega)} - i\epsilon_{\mu\nu\alpha\beta}\epsilon_-^\mu \epsilon_0^\nu p_B^\alpha p_0^\beta \frac{2V^{B\to\omega}(m^2_{K^*})}{(m_B + m_\omega)} \Big\} \\
&\times \quad \{ V_{ub}V_{us}^* a_1 - V_{tb}V_{ts}^* [a_4 + a_{10}] \} \\
&- \quad i\frac{G_F}{2} f_\omega m_\omega \Big\{ (\epsilon_0 \cdot \epsilon_-)(m_B + m_{K^*}) A_1^{B\to K^*}(m^2_\omega) \\
&\quad -(\epsilon_0 \cdot p_B)(\epsilon_- \cdot p_B) \frac{2A_2^{B\to K^*}(m^2_\omega)}{(m_B + m_{K^*})} - i\epsilon_{\mu\nu\alpha\beta}\epsilon_0^\mu \epsilon_-^\nu p_B^\alpha p_-^\beta \frac{2V^{B\to K^*}(m^2_\omega)}{(m_B + m_{K^*})} \Big\} \\
&\times \quad \Big\{ V_{ub}V_{us}^* a_2 - V_{tb}V_{ts}^* [2(a_3 + a_5) + \frac{1}{2}(a_9 + a_7) \Big\} . \qquad (137)
\end{aligned}
$$

(3) Pure penguin processes:

$$
\begin{aligned}
M(B^- \to \rho^- \bar{K}^{*0}) &= i\frac{G_F}{\sqrt{2}} f_{K^*} m_{K^*} \Big\{ (\epsilon_\rho \cdot \epsilon_K)(m_B + m_\rho) A_1^{B\to\rho}(m^2_{K^*}) \\
&\quad -(\epsilon_\rho \cdot p_B)(\epsilon_K \cdot p_B) \frac{2A_2^{B\to\rho}(m^2_{K^*})}{(m_B + m_\rho)} \\
&\quad -i\epsilon_{\mu\nu\alpha\beta}\epsilon_K^\mu \epsilon_\rho^\nu p_B^\alpha p_\rho^\beta \frac{2V^{B\to\rho}(m^2_{K^*})}{(m_B + m_\rho)} \Big\} V_{tb}V_{ts}^* \Big\{ a_4 - \frac{1}{2}a_{10} \Big\} . \qquad (138)
\end{aligned}
$$

$$
\begin{aligned}
M(\bar{B}^0 \to \omega\phi) &= i\frac{G_F}{2} f_\phi m_\phi \Big\{ (\epsilon_\phi \cdot \epsilon_\omega)(m_B + m_\omega) A_1^{B\to\omega}(m^2_\phi) \\
&\quad -(\epsilon_\phi \cdot p_B)(\epsilon_\omega \cdot p_B) \frac{2A_2^{B\to\omega}(m^2_\phi)}{(m_B + m_\omega)} \\
&\quad -i\epsilon_{\mu\nu\alpha\beta}\epsilon_\phi^\mu \epsilon_\omega^\nu p_B^\alpha p_\omega^\beta \frac{2V^{B\to\omega}(m^2_\phi)}{(m_B + m_\omega)} \Big\} \\
&\times \quad V_{tb}V_{td}^* \Big\{ a_3 + a_5 - \frac{1}{2}(a_7 + a_9) \Big\} . \qquad (139)
\end{aligned}
$$

$$
\begin{aligned}
M(\bar{B}^0 \to \rho^0 \phi) &= -i\frac{G_F}{2} f_\phi m_\phi \Big\{ (\epsilon_\phi \cdot \epsilon_\rho)(m_B + m_\rho) A_1^{B\to\rho}(m_\phi^2) \\
&\quad -(\epsilon_\phi \cdot p_B)(\epsilon_\rho \cdot p_B) \frac{2A_2^{B\to\rho}(m_\phi^2)}{(m_B + m_\rho)} \\
&\quad -i\epsilon_{\mu\nu\alpha\beta} \epsilon_\phi^\mu \epsilon_\rho^\nu p_B^\alpha p_\rho^\beta \frac{2V^{B\to\rho}(m_\phi^2)}{(m_B + m_\rho)} \Big\} \\
&\times \quad V_{tb} V_{td}^* \left\{ a_3 + a_5 - \frac{1}{2}(a_7 + a_9) \right\}. \qquad (140)
\end{aligned}
$$

$$
M(B^- \to \rho^- \phi) = -\sqrt{2} M(\bar{B}^0 \to \rho^0 \phi). \qquad (141)
$$

$$
\begin{aligned}
M(B^- \to K^{*-} \phi) &= \\
M(\bar{B}^0 \to \bar{K}^{*0} \phi) &= i\frac{G_F}{\sqrt{2}} f_\phi m_\phi \Big\{ (\epsilon_\phi \cdot \epsilon_K)(m_B + m_{K^*}) A_1^{B\to K^*}(m_\phi^2) \\
&\quad -(\epsilon_\phi \cdot p_B)(\epsilon_K \cdot p_B) \frac{2A_2^{B\to K^*}(m_\phi^2)}{(m_B + m_{K^*})} \\
&\quad -i\epsilon_{\mu\nu\alpha\beta} \epsilon_\phi^\mu \epsilon_K^\nu p_B^\alpha p_K^\beta \frac{2V^{B\to K^*}(m_\phi^2)}{(m_B + m_{K^*})} \Big\} \\
&\times \quad V_{tb} V_{ts}^* \left\{ a_3 + a_4 + a_5 - \frac{1}{2}(a_7 + a_9 + a_{10}) \right\}. \qquad (142)
\end{aligned}
$$

$$
\begin{aligned}
M(B^- \to K^{*-} K^{*0}) &= \\
M(\bar{B}^0 \to K^{*0} \bar{K}^{*0}) &= i\frac{G_F}{\sqrt{2}} f_{K^*} m_{K^*} \Big\{ (\epsilon_1 \cdot \epsilon_2)(m_B + m_{K^*}) A_1^{B\to K^*}(m_{K^*}^2) \\
&\quad -(\epsilon_1 \cdot p_B)(\epsilon_2 \cdot p_B) \frac{2A_2^{B\to K^*}(m_{K^*}^2)}{(m_B + m_{K^*})} \\
&\quad -i\epsilon_{\mu\nu\alpha\beta} \epsilon_1^\mu \epsilon_2^\nu p_B^\alpha p_2^\beta \frac{2V^{B\to K^*}(m_{K^*}^2)}{(m_B + m_{K^*})} \Big\} V_{tb} V_{td}^* \left\{ a_4 - \frac{1}{2} a_{10} \right\}. \qquad (143)
\end{aligned}
$$

References

[1] R. Anastassov et al. (CLEO Collaboration), CLEO CONF 97-24, EPS-334; paper submitted to the EPS Conference, Jerusalem, Israel, 1997;
R. Godang et al. (CLEO Collaboration), preprint CLNS 97-1522, CLEO 97-27;
B.H. Behrens et al. (CLEO Collaboration), preprint CLNS 97/1536, CLEO 97-31, hep-ex/9801012;
J.G. Smith, preprint COLO-HEP-395 (1998); to appear in Proc. of the Seventh Int. Symp. on Heavy Flavor Physics, Santa Barbara, CA, July 7 - 11, 1997.

[2] T. Bergfeld et al. (CLEO Collaboration), preprint CLNS 97/1537, CLEO 97-32, hep-ex/9803018.

[3] K.G. Wilson, Phys. Rev. **179**, 1499 (1969).

[4] G. Altarelli and L. Maiani, Phys. Lett. **B52**, 351 (1974);
M.K. Gaillard and B.W. Lee, Phys. Rev. Lett. **33**, 108 (1974);
G. Altarelli, G. Curci, G. Martinelli and S. Petrarca, Phys. Lett. **B99**, 141 (1981); Nucl. Phys. **B187**, 461 (1981).

[5] For a review, see: G. Buchalla, A.J. Buras and M.E. Lautenbacher, Rev. Mod. Phys. **68**, 1125 (1996).

[6] R.P. Feynman in *Symmetries in Particle Physics*, ed. A. Zichichi (Acad. Press, 1965) 167;
O. Haan and B. Stech, Nucl. Phys. **B22**, 448 (1970).

[7] J. Ellis, M.K. Gaillard and D.V. Nanopoulos, Nucl. Phys. **B100**, 313 (1975);
D. Fakirov and B. Stech, Nucl. Phys. **B133**, 315 (1978);
A. Ali, J. Körner, G. Kramer and J. Willrodt, Z. Phys. **C1**, 203 (1979).

[8] M. Bauer and B. Stech, Phys. Lett. **B152**, 380 (1985);
M. Bauer, B. Stech and M. Wirbel, Z. Phys. **C34**, 103 (1987).

[9] A. Abada et al. (APE Collaboration), Phys. Lett. **B365**, 275 (1996).

[10] J.M. Flynn and C.T. Sachrajda, preprint SHEP-97-20, hep-lat/9710057.

[11] J.M. Flynn et al. (UKQCD Collaboration), Nucl. Phys. **B461**, 327 (1996);
L. Del Debbio et al. (UKQCD Collaboration), Phys. Lett. **B416**, 392 (1998).

[12] A. Ali, V.M. Braun and H. Simma, Z. Phys. **C63**, 437 (1994).

[13] P. Ball and V.M. Braun, Phys. Rev. **D55**, 5561 (1997).

[14] A. Khodjamirian et al., Phys. Lett. **B410**, 275 (1997);
A. Khodjamirian and R. Rückl, preprint WUE-ITP-97-049, hep-ph/9801443.

[15] P. Ball, preprint FERMILAB-PUB-98/067-T, hep-ph/9802394.

[16] N. Isgur, D. Scora, B. Grinstein and M.B. Wise, Phys. Rev. **D39**, 799 (1989).

[17] D. Ebert, R.N. Faustov and V.O. Galkin, Phys. Rev. **D56**, 312 (1997).

[18] M. Neubert and B. Stech, preprint CERN-TH/97-99 [hep-ph 9705292], to appear in *Heavy Flavors*, Second Edition, ed. A.J. Buras and M. Lindner (World Scientific, Singapore).

[19] R.M. Barnett et al. (Particle Data Group), Phys. Rev. **D54**, 1 (1996).

[20] J.D. Bjorken, Nucl. Phys. B(Proc. Suppl.) **11**, 325 (1989).

[21] T.E. Browder, K.Honscheid and D. Pedrini, Ann. Rev. Nucl. Part. Sci. **46**, 395 (1996).

[22] I.I. Bigi et al., in *CP Violation*, Editor: C. Jarlskog, Advanced series on Directions in High Energy Physics, Vol. 3, World Scientific, Singapore, New Jersey, London, Hong Kong, 1989, and the earlier literature quoted therein.

[23] L.-L. Chau, in *CP Violation*, Editor: C. Jarlskog, Advanced series on Directions in High Energy Physics, Vol. 3, World Scientific, Singapore, New Jersey, London, Hong Kong, 1989, and the earlier literature quoted therein.

[24] L.L. Chau et al., Phys. Rev. **D43**, 2176 (1991).

[25] D. Du and Z. Xing, Phys. Lett. **B312**, 199 (1993).

[26] A. Deandrea et al., Phys. Lett. **B318**, 549 (1993); *ibid* **B320**, 170 (1994).

[27] A. Ali, C. Greub, Phys. Rev **D57**, 2996 (1998).

[28] A. Ali, J. Chay, C. Greub and P. Ko, preprint DESY 97-235, hep-ph/9712372 (to appear in Phys. Lett. B).

[29] N.G. Deshpande, B. Dutta, Sechul Oh, preprint OITS-641, hep-ph/9710354 ;
preprint OTIS-644, hep-ph/9712445.

[30] H.Y. Cheng, hep-ph/9712244 and references quoted therein.

[31] H.-Y. Cheng and B. Tseng, preprint IP-ASTP-01-98, hep-ph/9803457.

[32] G. Kramer, W. F. Palmer and H. Simma, Nucl. Phys. **B428**, 77 (1994);
Z. Phys. **C66**, 429 (1995).

[33] G. Kramer, W. F. Palmer, Phys. Rev. **D52**, 6411 (1995); Phys. Rev. **D45**, 132 (1992);
Phys. Lett. **B279**, 181 (1992).

[34] M. Ciuchini, E. Franco, G. Martinelli and L. Silvestrini, Nucl. Phys. **B501**, 271 (1997);
M. Ciuchini et al., Nucl. Phys. **B512**, 3 (1998).

[35] M.B. Voloshin, Phys. Let. **B397**, 275 (1997).

[36] A. Khodjamirian et al., Phys. Lett. **B402**, 167 (1997);
Z. Ligeti, L. Randall and M.B. Wise, Phys. Lett. **B402**, 178 (1997);
A.K. Grant et al., Phys. Rev. **D56**, 3151 (1997).

[37] G. Buchalla, G. Isidori and S.J. Rey, Nucl. Phys. **B511**, 594 (1998).

[38] A.F. Falk, A.L. Kagan, Y. Nir and A.A. Petrov, preprint JHU-TIPAC-97018, hep-ph/9712225.

[39] M. Neubert, preprint CERN-TH/97-342, hep-ph/9712224.

[40] R. Fleischer, preprint CERN-TH/98-60, hep-ph/9802433.

[41] H.J. Lipkin, preprint hep-ph/9802205.

[42] D. Delepine, J.-M. Gérard, J. Pestieau and J. Wyers, preprint UCL-IPT-98-01, hep-ph/9802361.

[43] Z.Z. Xing, Phys. Rev. **D53**, 2847 (1996);
D.S. Du, L.B. Guo and D.X. Zhang, Phys. Lett. **B406**, 110 (1997);
C.D. Lü and D.X. Zhang, Phys. Lett. **B400**, 188 (1997).

[44] N. Cabibbo, Phys. Rev. Lett. **10**, 531 (1963);
M. Kobayashi and T. Maskawa, Prog. Theor. Phys. **49**, 652 (1973).

[45] R. Fleischer and T. Mannel, Phys. Rev. **D57**, 2752 (1998);
preprint TTP-97-22 [hep-ph/9706261].

[46] R. Fleischer, Phys. Lett. **B365**, 399 (1996);
A.J. Buras, R. Fleischer, T. Mannel, hep-ph/9711262.

[47] A. Ali, DESY Report 97-256, hep-ph/9801270; to be published in Proc. of the First APCTP Workshop, Pacific Particle Physics Phenomenology, Seoul, South Korea. For further details, see A. Ali and D. London, Nucl. Phys. B (Proc. Suppl.) **54A**, 297 (1997).

[48] F. Parodi, P. Roudeau and A. Stocchi, preprint hep-ph/9802289.

[49] L. Wolfenstein, Phys. Rev. Lett. **51**, 1945 (1983).

[50] M. Gronau, J.L. Rosner, Phys. Lett. **B376**, 205 (1996).

[51] A. Ali, H. Asatrian and C. Greub, preprint DESY 97-255, hep-ph/9803314 (submitted to Phys. Lett. B).

[52] A. J. Buras, M. Jamin, M. E. Lautenbacher and P.H. Weisz, Nucl. Phys. **B370**, 69 (1992); *ibid* **B375**, 501 (1992).

[53] M.A. Shifman, A.I. Vainshtein and V.I. Zakharov, Nucl. Phys. **B120** (1977) 316; Sov. Phys. JETP **45**, 670 (1977);
F. Gilman and M. Wise, Phys. Rev. **D20**, 2392 (1979);
W. Ponce, Phys. Rev. **D23**, 1134 (1981).

[54] A.J. Buras et al., Nucl. Phys. **B370**, 69 (1992);
M. Ciuchini, E. Franco, G. Martinelli and L. Reina, Nucl. Phys. **B415**, 403 (1994).

[55] H. Simma and D. Wyler, Phys. Lett. **B272**, 395 (1991).

[56] N.G. Deshpande and J. Trampetic, Phys. Rev. **D41**, 2926 (1990).

[57] M. Schmelling, preprint hep-ex/9701002.

[58] M. Gremm, A. Kapustin, Z. Ligeti and M.B. Wise, Phys. Rev. Lett. **77**, 20 (1996).

[59] M. Neubert, preprint CERN-TH/97-24, hep-ph/9702375.

[60] J. Gasser and H. Leutwyler, Nucl. Phys. **B250**, 465 (1985).

[61] H. Leutwyler, preprint hep-ph/9609467.

[62] J. Bijnens, J. Prades and E. de Rafael, Phys. Lett. **B348**, 226 (1995).

[63] K.G. Chetyrkin, D. Pirjol and K. Schilcher, Phys. Lett. **B404**, 337 (1997).

[64] P. Colangelo et al., Phys. Lett. **B408**, 340 (1997).

[65] M. Jamin, preprint HD-THEP-97-51, hep-ph/9709484.

[66] K. Kanaya et al. (CP-PACS Collaboration), preprint UTCCP-P-26, hep-lat/9709139.

[67] V. Gimenez, L. Giusti, F. Rapuano and M. Talevi, preprint Edinburgh 97-15, hep-lat/9801028.

[68] R. Gupta, preprint LAUR-98-271, hep-ph/9801412.

[69] H. Leutwyler, preprint hep-ph/9709408.

[70] P. Herrera-Sikoldy, J.I. Latorre, P. Pascual and J. Taron, preprint hep-ph/9710268.

[71] T. Feldmann and P. Kroll, preprint WU-B 97-28, hep-ph/9711231.

[72] T. Feldmann, P. Kroll and B. Stech, preprint WU-B 98-2, hep-ph/9802409.

[73] F. Araki, M. Musakhanov and H. Toki, preprint hep-ph/9803356.

[74] M. Neubert and C. Sachrajda, Nucl. Phys. **B483**, 339 (1997).

[75] A. Ali, G. Kramer and C.-D. Lü, DESY report (to be pulished).

[76] P. Ball, J.M. Frère, M. Tytgat, Phys. Lett. **B365**, 367 (1996).

[77] R. Akhoury, J.M. Frère, Phys. Lett. **B220**, 258 (1989).